

An Analysis of Global Positioning System (GPS) Standard Positioning System (SPS) Performance for 2014

TR-SGL-17-02

March 2017

Space and Geophysics Laboratory
Applied Research Laboratories
The University of Texas at Austin
P.O. Box 8029
Austin, TX 78713-8029

Brent A. Renfro,
Audric Terry,
Nicholas Boeker

Contract: NAVSEA Contract N00024-01-D-6200
Task Order: 5101147

Distribution A: Approved for public release; Distribution is unlimited.

This Page Intentionally Left Blank

Executive Summary

Applied Research Laboratories, The University of Texas at Austin (ARL:UT) examined the performance of the Global Positioning System (GPS) throughout 2014 for the Global Positioning Systems Directorate (SMC/GP). This report details the results of that performance analysis. This material is based upon work supported by the US Air Force Space & Missile Systems Center Global Positioning Systems Directorate through Naval Sea Systems Command Contract N00024-01-D-6200, task order 5101147, “FY15 GPS Signal and Performance Analysis”.

Performance is characterized in terms of the 2008 Standard Positioning Service (SPS) Performance Standard (SPS PS). The performance standards provide the U.S. government’s assertions regarding the expected performance of GPS. This report does not address each of the assertions in the performance standards. The emphasis is on those assertions which can be verified by anyone with knowledge of standard GPS data analysis practices, familiarity with the relevant signal specification, and access to a data archive.

The assertions evaluated include those associated with the accuracy, integrity, continuity, and availability of the GPS signal-in-space (SIS) and the position performance standards. Section 2 of the report includes a tabular summary of the assertions that were evaluated and a summary of the results. The remaining sections present details on the analysis associated with each assertion.

All the SPS PS and metrics examined in the report were met in 2014 with one exception. The exception is the reporting notification requirement for scheduled interruptions. This was met in 29 of 30 cases (97%).

Contents

1	Introduction	1
2	Summary of Results	4
3	Discussion of Performance Standard Metrics and Results	6
3.1	SIS Accuracy	6
3.1.1	URE Over All AOD	8
3.1.1.1	An Alternate Approach	12
3.1.2	URE at Any AOD	12
3.1.3	URE at Zero AOD	20
3.1.4	URE Bounding	20
3.1.5	SIS URE at 14 Days	21
3.2	SIS Integrity	23
3.3	SIS Continuity	23
3.3.1	Unscheduled Failure Interruptions	23
3.3.2	Status and Problem Reporting Standards	28
3.3.2.1	Scheduled Events	28
3.3.2.2	Unscheduled Outage	30
3.4	SIS Availability	31
3.4.1	Per-slot Availability	31
3.4.2	Constellation Availability	33
3.4.3	Operational Satellite Counts	34
3.5	Position/Time Availability	35
3.5.1	PDOP Availability	35
3.5.2	Additional DOP Analysis	37
3.5.3	Position Service Availability	47

3.5.4	Position Accuracy	47
3.5.4.1	Results for Daily Average	50
3.5.4.2	Results for Worst Site 95 th Percentile	55
4	Additional Results of Interest	58
4.1	Frequency of Different SV Health States	58
4.2	Age of Data	58
4.3	User Range Accuracy Index Trends	62
4.4	Extended Mode Operations	62
A	URE as a Function of Age-of-Data	66
A.1	Notes	66
A.2	Block IIA SVs	68
A.3	Block IIR SVs	70
A.4	Block IIR-M SVs	73
A.5	Block IIF SVs	75
B	URE Analysis Implementation Details	77
B.1	Introduction	77
B.2	Clock and Position Values for Broadcast and Truth	77
B.3	95 th Percentile Global Average As Per the SPS PS	78
B.4	An Alternate Approach	79
B.5	Limitations of URE Analysis	81
C	SVN to PRN Mapping for 2014	82
D	NANU Activity in 2014	84
E	SVN to Plane-Slot Mapping for 2014	86
F	Translation of URE Statistics Between Signals	89
F.1	Group Delay Differential	89
F.2	Intersignal Bias	90
F.3	Adjusting PPS Dual-Frequency Results for SPS	91
G	Acronyms and Abbreviations	92

List of Figures

1.1	Maps of the Network of Stations Used as Part of this Report	3
3.1	Range of the Monthly 95 th Percentile Values for all SVs	11
3.2	Range of the Monthly 95 th Percentile Values for all SVs (via Alternate Method)	14
3.3	Range of Differences in Monthly Values for all SVs	14
3.4	Worst Performing Block IIA SV in Terms of Any AOD (SVN 38/PRN 08)	17
3.5	Worst Performing Block IIR/IIR-M SV in Terms of Any AOD (SVN 44/PRN 28)	17
3.6	Worst Performing Block IIF SV in Terms of Any AOD (SVN 65/PRN 24)	18
3.7	Best Performing Block IIA SV in Terms of Any AOD (SVN 26/PRN 26)	18
3.8	Best Performing Block IIR/IIR-M SV in Terms of Any AOD (SVN 61/PRN 02)	19
3.9	Best Performing Block IIF SV in Terms of Any AOD (SVN 63/PRN 01)	19
3.10	SIS RMS URE for SVN 64 During Extended Operations	22
3.10	Daily Average Number of Occupied Slots	34
3.11	Count of Operational SVs by Day	36
3.12	Daily PDOP Metrics Using all SVs, 2014	40
3.13	GPS Visibility on Day 045 at 14:25 Relative to 40S, 325.31E	43
3.14	GPS Visibility on Day 275 at 19:00 Relative to 28N, 160.75E	44
3.15	Time History of SV Visibility at DOP Spike Location	45
3.16	Daily averaged position residuals computed using a RAIM solution . . .	53
3.17	Daily averaged autonomous position residuals using no data editing . . .	53
3.18	Pseudorange residuals for RAIM solution, enlarged to show variation in average residual	54
3.19	The non-edited pseudorange solution, enlarged to show variation in average residual.	54

3.20	Worst site 95 th percentile horizontal and vertical residuals for the RAIM Solution	56
3.21	Worst site 95 th percentile horizontal and vertical residuals with no data editing	56
4.1	Constellation Age of Data for 2014	60
B.1	Global Average URE as defined in SPS PS	78
B.2	Illustration of the 577 Point Grid	80
C.1	PRN to SVN Mapping for 2014	83
D.1	Plot of NANU activity in 2014	85
E.1	Time History of Satellite Plane/Slots for 2014	88

List of Tables

2.1	Summary of SPS PS Metrics Examined for 2014	5
3.1	Characteristics of SIS URE Methods	7
3.2	Monthly 95 th Percentile Values of SIS RMS URE for all SVs	10
3.3	Monthly 95 th Percentile Values of SIS Instantaneous URE for all SVs (via Alternate Method)	13
3.4	Probability Over Any Hour of Not Losing Availability Due to Unscheduled Interruption.	27
3.5	Scheduled Events Covered in NANUs for 2014	29
3.6	Decommissioning Notice Times	29
3.7	Unscheduled Events Covered in NANUs for 2014	30
3.8	Per-Slot Availability in 2014 for Baseline 24 Slots	32
3.9	Summary of PDOP Availability	37
3.10	Additional DOP Annually-Averaged Visibility Statistics for 2011 through 2014	39
3.11	Additional PDOP Statistics.	39
3.12	Organization of Positioning Results	50
3.13	Mean of Daily Average Position Errors for 2014	52
3.14	Median of Daily Average Position Errors for 2014	52
3.15	Maximum of Daily Average Position Errors for 2014	52
3.16	Standard Deviation of Daily Average Position Errors for 2014	52
3.17	Mean of Daily Worst Site 95 th Percentile Position Errors for 2014	57
3.18	Median of Daily Worst Site 95 th Percentile Position Errors for 2014	57
3.19	Maximum of Daily Worst Site 95 th Percential Position Errors for 2014	57
3.20	Standard Deviation of Daily Worst Site 95 th Percentile Position Errors for 2014	57

4.1	Frequency of Health Codes	59
4.2	Age of Data of the Navigation Message by SV Type	60
4.3	Distribution of URA Index Values	63
4.4	Distribution of URA Index Values (As a Percentage of All Collected) . .	64
4.5	Summary of Occurrences of Extended Mode Operations	65
E.1	Summary of SV-Slot Relationships for 2014	87
G.1	List of Acronyms and Abbreviations	92

Chapter 1

Introduction

Applied Research Laboratories, The University of Texas at Austin (ARL:UT)¹ examined the performance of the Global Positioning System (GPS) throughout 2014 for the Global Positioning Systems Directorate (SMC/GP). This report details the results of our performance analysis. This material is based upon work supported by the US Air Force Space & Missile Systems Center Global Positioning Systems Directorate through Naval Sea Systems Command Contract N00024-01-D-6200, task order 5101147, “FY15 GPS Signal and Performance Analysis”.

Performance is assessed relative to selected commitments in the 2008 Standard Positioning Service (SPS) Performance Standard (SPS PS) [1]. (Hereafter the term SPS PS, or SPSPS08, are used when referring to the 2008 SPS PS.) Section 2 contains a tabular summary of performance stated in terms of the metrics stated in performance standards. Section 3 contains explanations and amplifications regarding the summary values. Section 4 details additional findings of the performance analysis.

The performance standards define the services delivered through the L1 C/A code signal. The metrics are limited to characterizing the signal in space (SIS) and do not address error sources such as atmospheric errors, receiver errors, or error due to the user environment (e.g. multipath errors, terrain masking, and foliage). This report addresses assertions in the SPS PS that can be verified by anyone with knowledge of standard GPS data analysis practices, familiarity with the relevant signal specification [2], and access to a data archive (such as that available via the International Global Navigation Satellite System (GNSS) Service (IGS)) [3]. The assertions examined include those related to URE, availability of service, and position domain standards (specifics can be found in Table 2.1).

The majority of the assertions related to URE values are evaluated through comparison of the space vehicle (SV) clock and position representations as computed from the broadcast Legacy Navigation (LNAV) message data against the SV truth clock and position data as provided by a precise orbit calculated after the time of interest. The broadcast clock and position data is denoted in this report by BCP and the truth clock

¹*A list of abbreviations is provided in Appendix G*

and position data by TCP. The process by which the URE values are calculated is described in Appendix B of this report.

Observation data from tracking stations are used to cross-check the URE values and to evaluate non-URE assertions. Examples of the latter application include the areas of Continuity (3.3), Availability (3.4), and Position/Time Availability (3.5). In these cases, data from two networks are used. The two networks considered are the National Geospatial-Intelligence Agency (NGA) Monitor Station Network (MSN) [4] and a subset of the tracking stations that contribute to the IGS. The distribution of these stations is shown in Figure 1.1. These sets of stations ensure continuous observation of all space vehicles by multiple stations.

Several metrics in the performance standards are stated in terms of the Base 24 constellation of six planes and four slots/plane or the Expandable 24 constellation in which three of the 24 slots may be occupied by two SVs. Currently, there are more than 32 GPS SVs on-orbit. Of these, 31 or 32 SVs may be broadcasting at any time. Of the SVs on-orbit, 27 are located in the expandable 24 constellation. The SVs in excess of those located in defined slots are assigned to locations in various planes in accordance with operational considerations.

The majority of the metrics in this report are evaluated on either a per-SV basis or for the full constellation. The metrics associated with continuity and availability are defined with respect to the slot definitions.

The GPS SVs are referred to by pseudo-random noise ID and by space vehicle number (referred to hereafter as PRN and SVN, respectively). As the number of active PRNs has increased to nearly the total available number, PRNs are now being used by multiple SVs within a given year. Therefore, the SVN represents a unique identifier for the vehicle under discussion. In general, we list the SVN first and the PRN second since the SVN is the unique identifier of the two. As an unintended side effect, this arrangement makes some of the tabular information appear in satellite Block order, which in turn makes some time-history comparisons more straightforward. The PRN-to-SVN relationships were provided by the Master Control Station (MCS), however another useful summary of this information may be found through the U.S. Naval Observatory (USNO) website [5].

The authors acknowledge and appreciate the effort of several ARL:UT staff members who reviewed these results. For 2014 this included Shannon Kolensky, Johnathan York, and David Munton.

Karl Kovach of Aerospace provided valuable assistance in interpreting the SPSPS08 metrics. John Lavrakas of Advanced Research Corporation and P.J. Mendicki of Aerospace Corporation have long been interested in GPS performance metrics and provided comments on the final draft. These inputs were very valuable, however, the results presented in this report are derived by ARL:UT and any errors are the responsibility of ARL:UT.

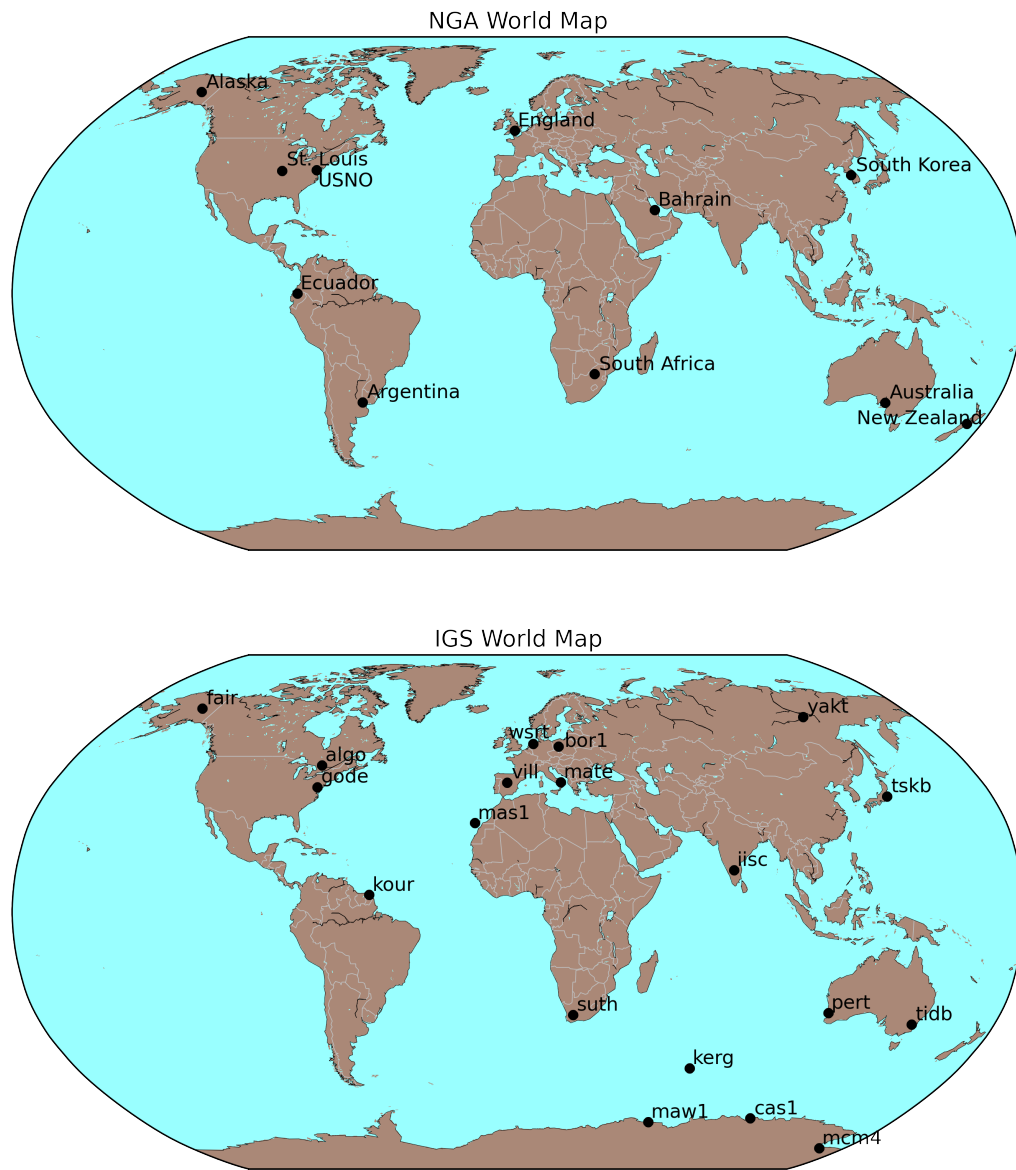


Figure 1.1: Maps of the Network of Stations Used as Part of this Report

Chapter 2

Summary of Results

Table 2.1 is a summary of the assertions defined in the performance standards. The table is annotated to show which assertions are evaluated in this report and the status of each assertion that was evaluated.

Of the assertions evaluated, only one was not met in 2014. The exception is associated with the notification time for scheduled interruptions. This assertion that at least 48 hours notice will be provided for scheduled interruptions was met in 29 of 30 cases (97%). In the case of the exception, only 17 hours notice was provided.

Details regarding each result may be found in Chapter 3.

Table 2.1: Summary of SPS PS Metrics Examined for 2014

SPSPS08 Section	SPS PS Metric	2014 Status
3.4.1 SIS URE Accuracy	≤ 7.8 m 95% Global average URE during normal operations over all AODs	✓
	≤ 6.0 m 95% Global average URE during normal operations at zero AOD	✓
	≤ 12.8 m 95% Global average URE during normal operations at any AOD	✓
	≤ 30 m 99.94% Global average URE during normal operations	✓
	≤ 30 m 99.79% Worst case single point average URE during normal operations	✓
	≤ 388 m 95% Global average URE after 14 days without upload	✓*
3.4.2 SIS URRE Accuracy	≤ 0.006 m/s 95% Global average at any AOD	not eval.
3.4.3 SIS URAE Accuracy	≤ 0.002 m/s ² 95% Global average at any AOD	not eval.
3.4.4 SIS UTCOE Accuracy	≤ 40 nsec 95% Global average at any AOD	not eval.
3.5.1 SIS Instantaneous URE Integrity	$\leq 1 \times 10^{-5}$ Probability over any hour of exceeding the NTE tolerance without a timely alert	✓
3.5.4 SIS Instantaneous UTCOE Integrity	$\leq 1 \times 10^{-5}$ Probability over any hour of exceeding the NTE tolerance without a timely alert	not eval.
3.6.1 SIS Continuity - Unscheduled Failure Interruptions	≥ 0.9998 Probability over any hour of not losing the SPS SIS availability from the slot due to unscheduled interruption	✓
3.6.3 Status and Problem Reporting	Appropriate NANU issue at least 48 hours prior to a scheduled event	not met
3.7.1 SIS Per-Slot Availability	≥ 0.957 Probability that (a.) a slot in the baseline 24-slot will be occupied by a satellite broadcasting a healthy SPS SIS, or (b.) a slot in the expanded configuration will be occupied by a pair of satellites each broadcasting a healthy SIS	✓
3.7.2 SIS Constellation Availability	≥ 0.98 Probability that at least 21 slots out of the 24 slots will be occupied by a satellite (or pair of satellites for expanded slots) broadcasting a healthy SIS	✓
	≥ 0.99999 Probability that at least 20 slots out of the 24 slots will be occupied by a satellite (or pair of satellites for expanded slots) broadcasting a healthy SIS	✓
3.7.3 Operational Satellite Counts	≥ 0.95 Probability that the constellation will have at least 24 operational satellites regardless of whether those operational satellites are located in slots or not	✓
3.8.1 PDOP Availability	$\geq 98\%$ Global PDOP of 6 or less	✓
	$\geq 88\%$ Worst site PDOP of 6 or less	✓
3.8.2 Position Service Availability	$\geq 99\%$ Horizontal, average location	✓
	$\geq 99\%$ Vertical, average location	
	$\geq 90\%$ Horizontal, worst-case location	
	$\geq 90\%$ Vertical, worst-case location	
3.8.3 Position Accuracy	≤ 9 m 95% Horizontal, global average	✓
	≤ 15 m 95% Vertical, global average	
	≤ 17 m 95% Horizontal, worst site	
	≤ 37 m 95% Vertical, worst site	
	≤ 40 nsec time transfer error 95% of the time	

✓ - Met

* - One instance in 2014

Chapter 3

Discussion of Performance Standard Metrics and Results

While Chapter 2 notes the SPSPS08 specifications that were met for 2014, the statistics and trends reported in this chapter provide both additional information and support for these conclusions.

3.1 SIS Accuracy

SIS URE accuracy is asserted in Section 3.4 of the SPSPS08. The following standards (from Table 3.4-1) are considered in this report:

- “ ≤ 7.8 m 95% Global Average URE during Normal Operations over all AODs”
- “ ≤ 6.0 m 95% Global Average URE during Normal Operations at Zero AOD”
- “ ≤ 12.8 m 95% Global Average URE during Normal Operations at any AOD”
- “ ≤ 30 m 99.94% Global Average URE during Normal Operations”
- “ ≤ 30 m 99.79% Worst Case Single Point Average URE during Normal Operations”
- “ ≤ 40 nsec 95% Global Average UTCOE during Normal Operations at Any AOD”

The remaining standard associated with operations after extended periods without an upload are not relevant in 2014 as periods of extended operations were very limited. (This is discussed in Section 4.4)

The URE statistics presented in this report are based on a comparison of the BCP against the TCP. (Refer to Appendix B for further details on the process by which the URE are computed.) This is a useful approach, but one that has specific limitations,

the most significant of which is that the TCP may not reflect the effect of individual discontinuities or large effects over a short time (such as a frequency step or clock runoff). Nonetheless, this approach is appropriate given the long period of averaging implemented in determining URE, namely 30 days. Briefly, this approach allows the computation of URE without direct reference to observations from any particular ground sites, though the TCP carries an implicit network dependency based on the set of ground stations used to derive the precise orbits from which the TCP is derived.

In the case of this report, the BCP and TCP are both referenced to the L1/L2 P(Y)-code signal. As a result the resulting URE values are best characterized as PPS dual-frequency URE values. The SPS results are derived from the PPS dual-frequency results by a process described in Appendix F.

Throughout this section and the next, there are references to several different SIS URE expressions. Each of these SIS URE expressions means something slightly different. It is important to pay careful attention to the particular SIS URE expression being used in each case to avoid misinterpreting the associated URE numbers. Appendix C of the PPSPS07 and SPSPS08 provide definitions for the two ways SIS URE are computed, *Instantaneous SIS URE*, which expresses URE on an instantaneous basis and *root mean square (RMS) SIS URE*, which expresses URE on a statistical basis. When the BCP and TCP are used to estimate the range residual along a specific satellite-to-receiver line-of-sight vector at a given instant in time, then that is an “Instantaneous SIS URE”. Some of the primary differences between Instantaneous basis SIS UREs and statistical basis SIS UREs are given below.

Table 3.1: Characteristics of SIS URE Methods

Instantaneous Basis SIS URE	Statistical Basis SIS URE
Always algebraically signed (\pm) number	Never an algebraic sign
Never a statistical qualifier	Always a statistical qualifier (RMS, 95%, etc.)
Specific to a particular time and place	Statistic over span of times, or places, or both
Next section of this report (Section 3.2)	This section of this report (Section 3.1)

Throughout this section, there are references to the “Instantaneous RMS SIS URE.” This is a statistical basis SIS URE (note the “RMS” statistical qualifier), where the measurement quantity is the Instantaneous SIS URE, and the span of the statistic covers that one particular point (“instant”) in time across a large range of spatial points. This is effectively the evaluation of the Instantaneous SIS URE across every spatial point in the area of the service volume visible to the SV at that particular instant in time. Put another way; consider the signal from a given SV at a given point in time. That signal intersects the surface of the Earth over an area, and at each location there is a unique Instantaneous SIS URE value based on geometric relationship between the SV and the location of interest. In the name “Instantaneous RMS SIS URE,” the “Instantaneous” means that no time averaging occurs. The “RMS” refers to taking the RMS of all the individual Instantaneous SIS URE values across the area visible to the SV. This concept is explained in SPSPS08 Section A.4.11, and the relevant equation is presented in Appendix B of this report.

3.1.1 URE Over All AOD

The performance standard URE metric that most closely matches a user's observations is the calculation of URE over all AODs. This is associated with the SPSPS08 Section 3-4 metric:

- “ ≤ 7.8 m 95% Global Average URE during Normal Operations over all AODs”

These metrics can be decomposed into several pieces in order to better understand the process. For example, the first metric may be decomposed as follows:

- 7.8 m - This is the limit against which to test. The value is unique to the signal under evaluation.
- 95th Percentile - This is the statistical measure applied to the data to determine the actual URE. In this case, there are a sufficiently large number of samples to allow direct sorting of the results across time and selection of the 95th percentile.
- Global Average URE - This is another term for the Instantaneous RMS SIS URE, a statistical quantity representing the average URE across the area of the service volume visible to the SV at a given point in time. The expression used to compute this quantity is provided in Appendix B.
- Normal Operations - This is a constraint related to normal vs. extended mode operations. See IS-GPS-200 20.3.4.4 [2].
- over all AODs - This constraint means that the Global Average URE will be considered at each evaluation time regardless of the age of data (AOD) at the evaluation time. A more detailed explanation of the AOD and how this quantity is computed can be found in Section 4.2.

In addition, there are three general statements in Section 3.4 that have a bearing on this calculation:

- These statistics only include data from periods when each SV was healthy.
- These statistics are “per SV” - That is, they apply to the signal from each satellite, not for averages across the constellation.
- “The ergodic period contains the minimum number of samples such that the sample statistic is representative of the population statistic. Under a one-upload-per-day scenario, for example, the traditional approximation of the URE ergodic period is 30 days” (SPSPS08 Section 3.4, Note 1) Therefore the statistics will be computed over a monthly period and not daily. Since outages do occur, we have computed the statistic for each month, regardless of the number of days of availability, but identified these values when displayed.

Based on this set of assumptions and constraints, the monthly 95th percentile values of the RMS SIS URE were computed for each SV as provided in Table 3.2. Values computed for incomplete months are shown with shaded cells. For each SVN we show the worst of these values across the year in red. The gaps in URE indicate that the satellite was decommissioned (SVN 33, 36, 38, 39), or not yet launched (SVN 64, 67, 68, 69). Note that none of the values in this table exceed the threshold of 7.8 m. In all cases, no values exceed 7.8 m and so this requirement is met for 2014.

Figure 3.1 provides a summary of these results for the entire constellation. For each SVN, shown along the x-axis, the median value of the monthly 95th percentile SIS URE is computed and displayed as a point. The full range of the annual monthly 95th percentile SIS URE is shown by the vertical bars. Color distinguishes between the Block II/IIA, Block IIR, Block IIR-M, and Block IIF SVs. The red horizontal line at 7.8 m indicates the upper bound given by the SPSPS08 Section 3-4 performance metric.

A number of points are evident from Figure 3.1:

1. All SVs meet the performance specification of the SPSPS08, even when only the worst performing month is considered. Even the worst value for each SV (indicated by the upper extent of the range bars) is a factor of 2 or more smaller than the threshold.
2. As a general rule, the newer satellites outperform the older Block IIA satellites in terms of the 95th Percentile SIS URE metric. The average performance of the Block IIA SVs nearly a meter higher than that of the Block IIR, IIR-M, and IIF SVs if SVN 65/PRN 24 is omitted (see Table 3.2).
3. For most of the SVs, the value of the 95th Percentile SIS URE metric is relatively stable over the course of the year, as indicated by relatively small range bars.
4. For some SVs there are large range extents for the bars. This includes SVNs 54 and 64, which both have spreads of URE values of greater than 1.0 m. In both cases, the maximum value was from a single month of out-of-family performance.
5. The “best” SVs appear to be the Block IIR, Block IIR-M, and Block IIF which cluster near the 1.0 m level, and whose range variation is small. This includes SVNs 48, 50, 51, 55, 56, 58, 59, 60, 61, and 62.
6. The values for SVN 65 are noticeably different than the other Block IIF SVs. It is also the only Block IIF SV operating on a Cesium frequency standard.
7. Four new SVs were launched in 2014: SVN 64, 67, 68, and 69. The RMS SIS URE values for new SVs are sometimes slightly worse for the first few months of operation. See the June value for SVN 64 in Table 3.2 for an example.

Table 3.2: Monthly 95th Percentile Values of SIS RMS URE for all SVs in Meters

SVN	PRN	Block	Jan.	Feb.	Mar.	Apr.	May	Jun.	Jul.	Aug.	Sept.	Oct.	Nov.	Dec.	2014
23	32	IIA	1.40	1.51	1.82	1.34	1.54	1.31	1.41	1.26	1.30	1.59	1.34	1.50	1.43
26	26	IIA	1.29	1.44	1.28	1.09	1.66	1.32	1.17	1.07	1.50	1.01	1.29	1.30	1.28
33	3	IIA	2.59	2.69	2.60	2.60	2.71	2.65	2.59	2.37					2.63
34	4	IIA	2.23	2.24	2.03	1.70	2.54	2.18	1.80	1.93	1.84	1.93	1.71	1.68	2.01
36	6	IIA	1.73	1.53											1.66
38	8	IIA	2.63	2.70	2.60	2.69	2.85	2.73	2.84	2.82	2.89	2.85			2.77
39	9	IIA	2.64	2.67	2.78	2.69	2.81								2.72
40	10	IIA	2.56	2.73	2.69	2.42	2.59	2.69	2.64	2.46	2.58	2.57	2.56	2.31	2.58
41	14	IIR	1.41	1.07	1.07	1.03	1.17	1.15	1.13	1.00	1.08	1.12	1.09	1.01	1.10
43	13	IIR	1.10	1.44	1.07	1.34	1.09	1.15	1.12	1.17	1.24	1.17	1.35	1.33	1.21
44	28	IIR	2.41	2.50	2.60	2.28	2.64	2.65	2.65	2.49	2.61	2.51	2.49	2.38	2.54
45	21	IIR	1.09	1.37	1.03	1.00	0.98	1.03	0.96	0.96	1.07	1.00	0.94	1.13	1.03
46	11	IIR	1.21	1.36	1.41	1.26	1.12	1.40	1.60	1.42	1.35	1.55	1.18	1.58	1.40
47	22	IIR	2.02	1.92	1.91	1.97	2.14	1.75	1.84	1.80	1.97	1.61	1.87	2.22	1.92
48	7	IIR-M	1.16	1.24	1.15	1.12	1.18	1.07	1.04	1.06	1.12	1.06	1.12	1.21	1.12
50	5	IIR-M	0.93	0.97	0.91	0.94	0.95	0.96	0.94	0.96	0.91	1.06	0.97	0.94	0.95
51	20	IIR	0.91	0.97	0.95	0.95	0.95	0.91	0.95	0.91	0.93	0.98	0.95	0.96	0.95
52	31	IIR-M	1.28	1.26	1.33	1.38	1.36	1.28	1.41	1.41	1.26	1.34	1.23	1.26	1.31
53	17	IIR-M	1.62	1.53	1.82	1.34	1.72	1.29	1.18	1.59	1.33	1.41	1.40	1.82	1.52
54	18	IIR	1.20	1.01	1.55	1.06	1.00	2.23	1.26	1.03	1.30	1.35	1.03	0.97	1.22
55	15	IIR-M	0.93	0.92	0.96	0.92	0.94	0.95	0.92	0.92	0.89	0.94	0.98	1.06	0.94
56	16	IIR	0.91	0.92	0.93	0.97	0.95	0.91	0.91	0.91	0.94	0.98	0.93	0.93	0.94
57	29	IIR-M	1.24	1.53	1.52	1.50	1.30	1.26	1.33	1.30	1.44	1.40	1.70	1.30	1.40
58	12	IIR-M	0.97	1.00	0.99	0.99	0.98	0.94	1.00	0.96	0.94	1.13	0.95	0.96	0.98
59	19	IIR	1.02	0.98	1.04	0.97	0.97	0.97	0.99	0.98	1.00	0.99	0.96	1.01	0.99
60	23	IIR	0.94	0.92	0.92	0.92	1.03	0.98	0.95	0.92	0.90	0.92	0.97	0.99	0.94
61	2	IIR	0.99	1.01	1.02	0.99	0.93	0.94	0.98	0.97	1.00	0.94	0.94	0.96	0.98
62	25	IIF	0.95	0.93	0.95	0.96	0.96	0.99	0.96	0.98	1.03	1.02	0.97	1.02	0.98
63	1	IIF	1.22	1.03	0.98	0.96	0.87	0.92	0.97	0.96	0.95	0.97	0.92	0.90	0.99
64	30	IIF					0.90	2.23	1.10	1.12	1.02	1.19	0.97	0.98	1.15
65	24	IIF	1.96	2.59	2.41	2.61	2.22	2.49	2.51	2.50	2.12	2.43	2.46	2.56	2.42
66	27	IIF	1.08	0.95	0.93	0.96	0.94	1.03	1.20	1.14	0.94	0.94	0.98	1.07	1.01
67	6	IIF						1.43	1.35	1.20	1.07	0.93	0.91	0.97	1.15
68	9	IIF									1.28	1.28	1.46	1.14	1.30
69	3	IIF												1.28	1.28
Block IIA			2.37	2.42	2.41	2.32	2.56	2.43	2.43	2.29	2.30	2.21	1.89	1.82	2.35
Block IIR/IIR-M			1.27	1.34	1.35	1.24	1.28	1.29	1.29	1.22	1.30	1.31	1.25	1.30	1.29
Block IIF			1.55	1.73	1.62	1.67	1.50	1.80	1.58	1.56	1.32	1.35	1.43	1.38	1.52
All SVs			1.76	1.80	1.82	1.70	1.86	1.77	1.72	1.56	1.57	1.54	1.41	1.41	1.67

Notes: Values not present indicate that the satellite was unavailable during this period. Months during which an SV was available for less than 25 days are shown shaded. Months with the highest SIS RMS URE for a given SV are colored red. The column labeled “2014” is the 95th Percentile over the year. The four rows at the bottom are the monthly 95th Percentile values over various sets of SVs.

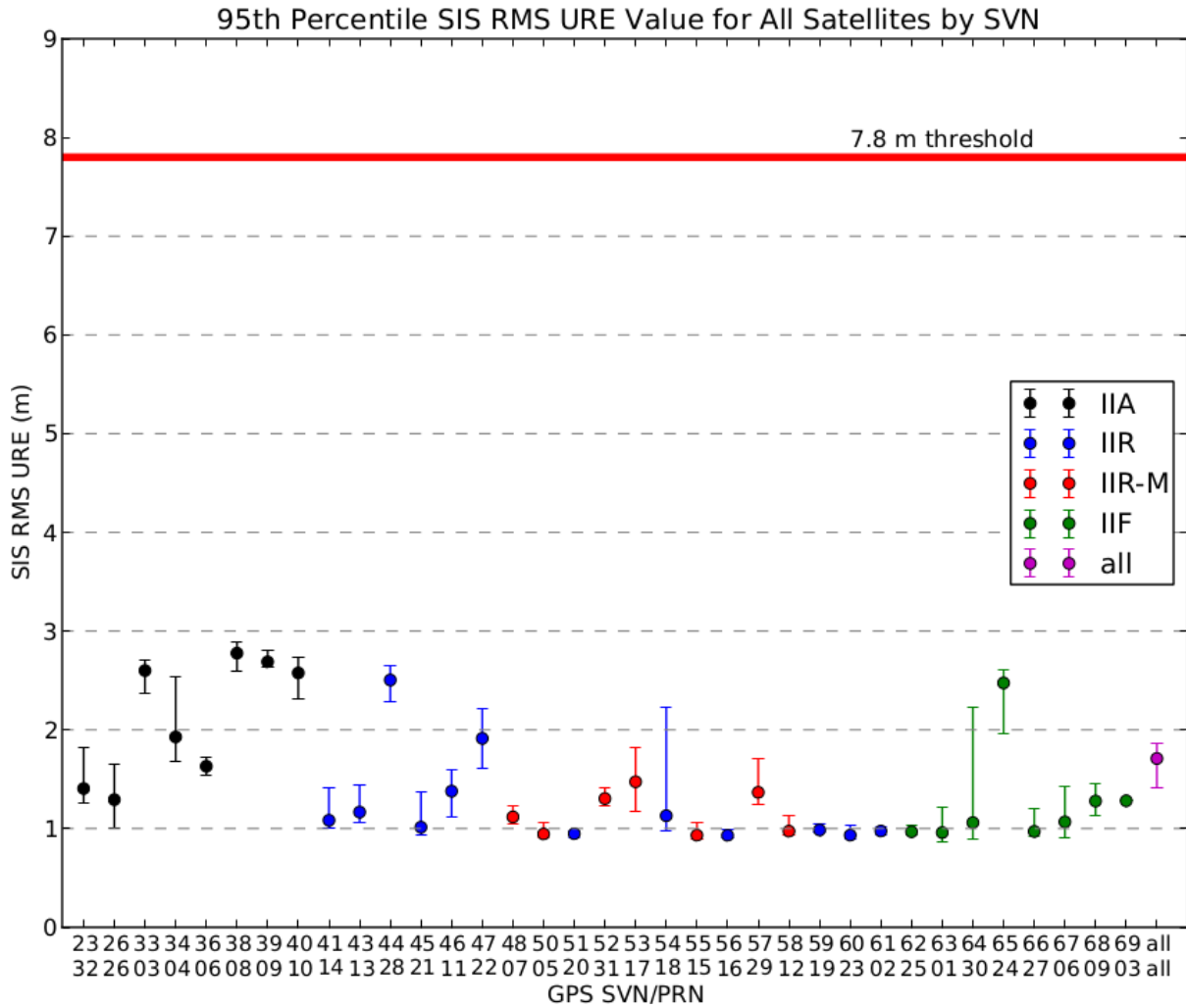


Figure 3.1: Range of the Monthly 95th Percentile Values for all SVs

Notes: Each SVN with valid data is shown sequentially along the x-axis. The median value of the monthly 95th Percentile SIS URE displayed as a point along the vertical axis. The full range of the monthly 95th Percentile SIS URE for 2014 is shown by the vertical bars. Color distinguishes between the Block II/IIA, Block IIR, Block IIR-M, and Block IIF SVs. The red horizontal line at 7.8 m indicates the upper bound given by the SPSPS08 Section 3-4 performance metric. The markers for “all” represent the monthly 95th Percentile values across all satellites.

3.1.1.1 An Alternate Approach

As described toward the end of Section 3.1, the 95th percentile Global Average URE values are formed by first deriving the Instantaneous RMS SIS URE at a succession of time points, then picking the 95th percentile value over that set of results. This has the computational advantage that the Instantaneous RMS SIS URE is derived from a single equation in radial, along-track, cross-track, and time errors at a given instant in time (as explained in Appendix B.3). However, it leads to a two-step implementation under which we first derive an RMS over a spatial area at a series of time points, then derive a 95th percentile statistic over time.

Given current computation and storage capability, it is practical to derive a set of 95th percentile URE values in which the Instantaneous SIS URE values are derived over a reasonably dense grid at a uniform cadence throughout the period of interest. The 95th percentile value is then selected from the entire set of Instantaneous SIS URE values. This was done in parallel to the process that produced the results shown in Section 3.1.1. A five-degree uniform grid was used along with a 5 minute cadence. Further details on the implementation are provided in Appendix B.4.

Table 3.3 presents a summary of the results obtained by this alternate method. This table is in the same format as Table 3.2. Figure 3.2 (which is in the same format as Figure 3.1) presents the values in Table 3.3 in a graphical manner. The values in Table 3.3 are larger than the values in Table 3.2 by an average of 0.02 m. The maximum difference (alternate - original) for a given SV-month is 0.13 m; the minimum difference is -0.04 m.

Figure 3.3 is an illustration of the differences between the Monthly 95th percentile SIS URE values calculated by the two different methods. Each pair of monthly values for a given SV found in Table 3.2 and Table 3.3 were taken and the difference computed as the quantity [alternate - original]. The median, maximum, and minimum differences were then selected from each set and plotted in Figure 3.3. Figure 3.3 illustrates that the two methods agree to within 20 cm and generally a good deal less with the alternate method typically being a few cm larger.

None of the values in Table 3.3 exceed the threshold of 7.8 m. Therefore, the threshold is met for 2014 even under this alternate interpretation of the metric.

3.1.2 URE at Any AOD

The next URE metric considered is the calculation of URE at any AOD. This is associated with the following SPSPS08 Section 3-4 metrics:

- “ ≤ 12.8 m 95% Global Average URE during Normal Operations at Any AOD”

This metric may be decomposed in a manner similar to the previous metric. The key difference is the term “at any AOD” and the change in the threshold values. The

Table 3.3: Monthly 95th Percentile Values of SIS Instantaneous URE for all SVs in Meters (via Alternate Method)

SVN	PRN	Block	Jan.	Feb.	Mar.	Apr.	May	Jun.	Jul.	Aug.	Sept.	Oct.	Nov.	Dec.	2014
23	32	IIA	1.43	1.51	1.81	1.37	1.56	1.33	1.42	1.28	1.32	1.57	1.42	1.53	1.46
26	26	IIA	1.32	1.45	1.28	1.11	1.68	1.37	1.20	1.09	1.51	1.03	1.35	1.28	1.30
33	3	IIA	2.64	2.70	2.63	2.62	2.74	2.69	2.61	2.35					2.66
34	4	IIA	2.22	2.30	2.05	1.71	2.55	2.22	1.82	1.93	1.84	1.92	1.74	1.71	2.02
36	6	IIA	1.81	1.58											1.74
38	8	IIA	2.69	2.75	2.62	2.72	2.89	2.77	2.86	2.87	2.94	2.89			2.81
39	9	IIA	2.72	2.72	2.81	2.72	2.82								2.76
40	10	IIA	2.57	2.76	2.69	2.44	2.60	2.70	2.67	2.46	2.61	2.57	2.57	2.31	2.60
41	14	IIR	1.44	1.10	1.09	1.04	1.18	1.18	1.16	1.03	1.09	1.15	1.10	1.05	1.12
43	13	IIR	1.12	1.42	1.09	1.35	1.10	1.17	1.16	1.20	1.25	1.18	1.38	1.31	1.24
44	28	IIR	2.42	2.48	2.60	2.31	2.65	2.67	2.65	2.54	2.65	2.56	2.51	2.41	2.54
45	21	IIR	1.12	1.37	1.06	1.03	1.01	1.06	0.98	0.99	1.09	1.03	0.99	1.14	1.06
46	11	IIR	1.27	1.43	1.42	1.29	1.15	1.42	1.62	1.46	1.38	1.59	1.21	1.55	1.42
47	22	IIR	2.01	1.92	1.92	1.99	2.17	1.76	1.87	1.81	2.00	1.67	1.90	2.17	1.93
48	7	IIR-M	1.18	1.26	1.19	1.14	1.20	1.10	1.06	1.08	1.13	1.09	1.15	1.19	1.14
50	5	IIR-M	0.95	0.99	0.92	0.96	0.97	0.98	0.95	0.97	0.93	1.08	0.99	0.96	0.97
51	20	IIR	0.91	1.01	0.96	0.95	0.99	0.93	0.96	0.94	0.95	1.01	0.98	0.99	0.97
52	31	IIR-M	1.27	1.25	1.34	1.40	1.36	1.29	1.44	1.40	1.28	1.35	1.26	1.29	1.33
53	17	IIR-M	1.64	1.54	1.86	1.38	1.73	1.31	1.21	1.60	1.35	1.48	1.45	1.81	1.54
54	18	IIR	1.25	1.03	1.55	1.09	1.02	2.21	1.28	1.07	1.31	1.40	1.07	1.01	1.26
55	15	IIR-M	0.96	0.96	1.01	0.95	0.98	0.99	0.96	0.94	0.91	0.96	1.00	1.09	0.98
56	16	IIR	0.93	0.94	0.96	1.00	0.97	0.94	0.94	0.94	0.96	0.99	0.95	0.96	0.96
57	29	IIR-M	1.25	1.66	1.53	1.53	1.39	1.30	1.38	1.30	1.40	1.45	1.71	1.35	1.44
58	12	IIR-M	0.98	1.04	1.02	1.02	1.00	0.97	1.04	1.00	0.97	1.12	0.99	0.97	1.01
59	19	IIR	1.02	1.00	1.05	0.99	1.00	0.98	1.00	0.99	1.03	1.04	0.99	1.01	1.01
60	23	IIR	0.96	0.95	0.96	0.95	1.04	1.02	0.98	0.94	0.92	0.93	0.98	1.00	0.97
61	2	IIR	1.02	1.06	1.04	1.01	0.95	0.97	1.00	1.00	1.04	0.98	0.97	0.98	1.00
62	25	IIF	0.96	0.95	0.97	0.98	0.98	1.02	0.97	1.00	1.05	1.04	1.00	1.05	1.00
63	1	IIF	1.29	1.07	0.99	0.98	0.89	0.95	0.97	0.98	0.97	1.01	0.94	0.92	1.01
64	30	IIF					0.93	2.24	1.11	1.11	1.04	1.20	0.99	1.01	1.16
65	24	IIF	2.02	2.59	2.40	2.58	2.24	2.51	2.52	2.52	2.12	2.43	2.46	2.57	2.44
66	27	IIF	1.10	0.97	0.94	0.97	0.98	1.07	1.23	1.17	0.99	0.96	1.00	1.10	1.04
67	6	IIF						1.43	1.36	1.25	1.10	0.97	0.93	0.98	1.17
68	9	IIF									1.30	1.30	1.48	1.15	1.32
69	3	IIF												1.37	1.37
Block IIA			2.39	2.44	2.43	2.34	2.58	2.44	2.43	2.29	2.32	2.24	1.93	1.83	2.36
Block IIR/IIR-M			1.29	1.35	1.37	1.26	1.29	1.31	1.30	1.25	1.31	1.32	1.27	1.30	1.30
Block IIF			1.53	1.73	1.62	1.68	1.51	1.81	1.60	1.57	1.34	1.37	1.44	1.40	1.53
All SVs			1.77	1.82	1.83	1.71	1.86	1.77	1.73	1.57	1.57	1.55	1.43	1.43	1.68

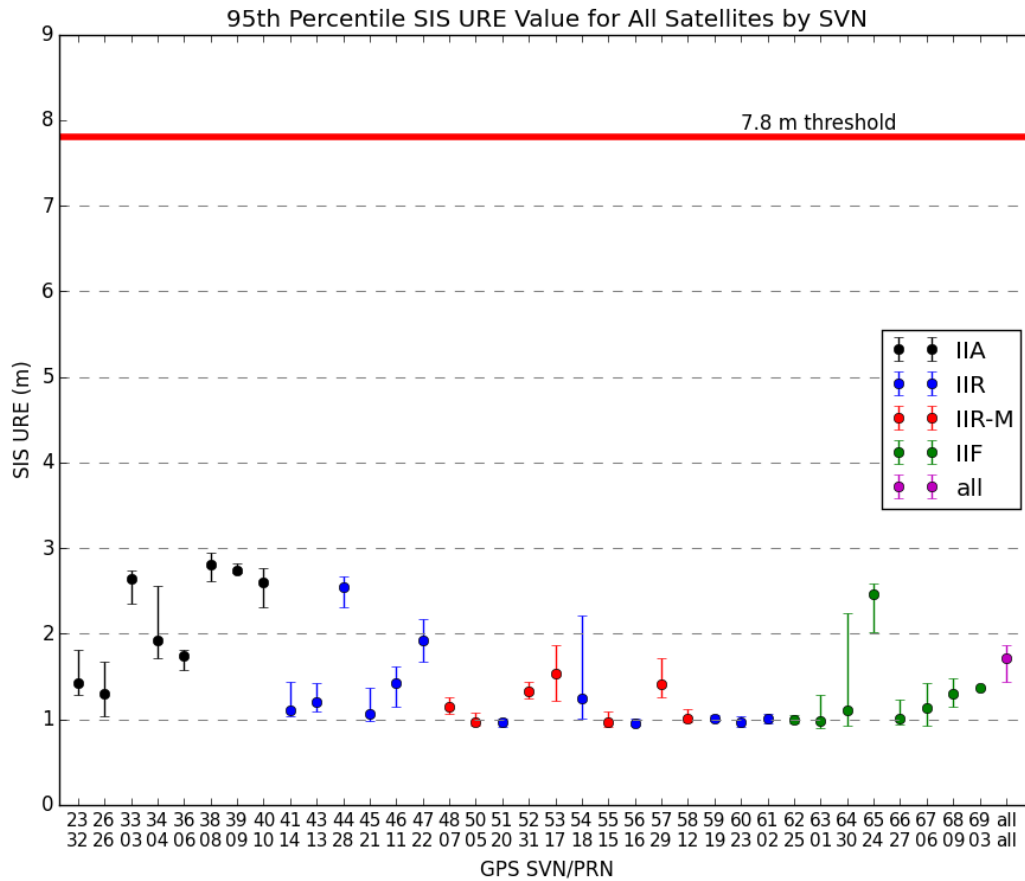


Figure 3.2: Range of the Monthly 95th Percentile Values for all SVs (via Alternate Method)

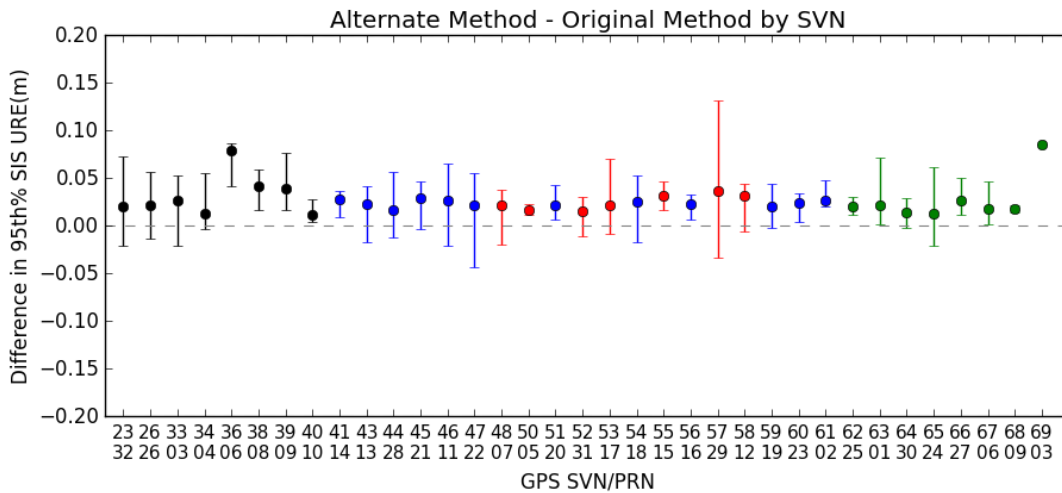


Figure 3.3: Range of Differences in Monthly Values for all SVs

phrase “at any AOD” is interpreted to mean that at any AOD where sufficient data can be collected to constitute a reasonable statistical set, the value of required statistic should be ≤ 12.8 m. See Section 4.2 for a discussion of how the AOD is computed.

To examine this requirement, the same set of 30 s Instantaneous RMS SIS URE values used in Section 3.1.1 was analyzed using a bin approach. The details are covered in Appendix A. In summary, the RMS SIS URE values were divided into bins based on 15 minute intervals of AOD. The 95th percentile values for each bin were selected and the results were plotted as a function of the AOD.¹

Figures 3.4 through Figure 3.9 show two curves: shown in blue is the 95th Percentile URE vs. AOD (in hours), and shown in green the count of points in each bin as a function of AOD. For satellites that are operating on the normal pattern (roughly one upload per day), the count of points in each bin is roughly equal from the time the upload becomes available until about 24 hours AOD. In fact, the nominal number of points can be calculated by multiplying the number of expected 30 s estimates in a 15 minute bin (30) by the number of days in the year (365). The result is 10950, or a little less than 11000. This corresponds well to the plateau area of the green curve for the well-performing satellites (e.g. Figures 3.7, 3.8, and 3.9). For satellites that are uploaded more frequently, the green curve will show a left-hand peak higher than the nominal count declining to the right. This is a result of the fact that there will be fewer points at higher AOD due to the more frequent uploads. The vertical scales on Figure 3.4 through 3.9 and the figures in Appendix A have been constrained to a constant value to aid in comparisons between the charts. This means that satellites that were only operational for part of the year (e.g. SVN 33, 36, 38, 39, 64, 67, 68, 69) will have a lower number of points per bin than the nominal.

The first three plots show the worst performing (i.e. highest URE values) Block IIA, Block IIR/IIR-M, and Block IIF SVs, SVN 38, SVN 44, and SVN 65 respectively. Note that the distribution of AOD samples for SVN 38 is concentrated at shorter values of AOD, which indicates that frequent uploads are occurring. SVN 44 shows similar behavior, but at a much larger AOD, indicating less frequent additional uploads.

The best performers for Block IIA, Block IIR/IIR-M, and Block IIF are shown in Figures 3.7 through 3.9. These figures show a very flat distribution of AODs, and the UREs appear to degrade roughly linearly with time, at least out to the point that the distribution (represented by the green curve) shows a marked reduction in the number of points.

The plots for all satellites are contained in Appendix A. A review of the full set leads to the conclusion that the behaviors described in the previous two paragraphs are not block-specific but are rather characteristic of age or the type of frequency standard. For example, five of the eight Block IIA satellites exhibit evidence of more frequent uploads as indicated by an uneven distribution of observation across the time bins. The

¹*Bins with a small number of points are suppressed from the plots. Such bins tend to occur at the right most end of the plots and the results are sometimes dominated by outliers. To avoid such misleading distractions, we determine the bin with the maximum number of points, then plot bins from left-to-right until a bin is reached with $\leq 10\%$ of the number of points in the bin with the maximum number of points.*

remaining three Block IIA satellites, each of which operate on older Cesium frequency standards, exhibit somewhat faster URE growth than the later satellites operating on Rubidium clocks, but the distribution of points is still roughly even across the day. Among the Block IIF SVs, The rate of URE growth is noticeably higher for the single satellite that uses a Cesium frequency reference. While there are noticeable differences between individual satellites, all the results are well within the assertion for this metric.

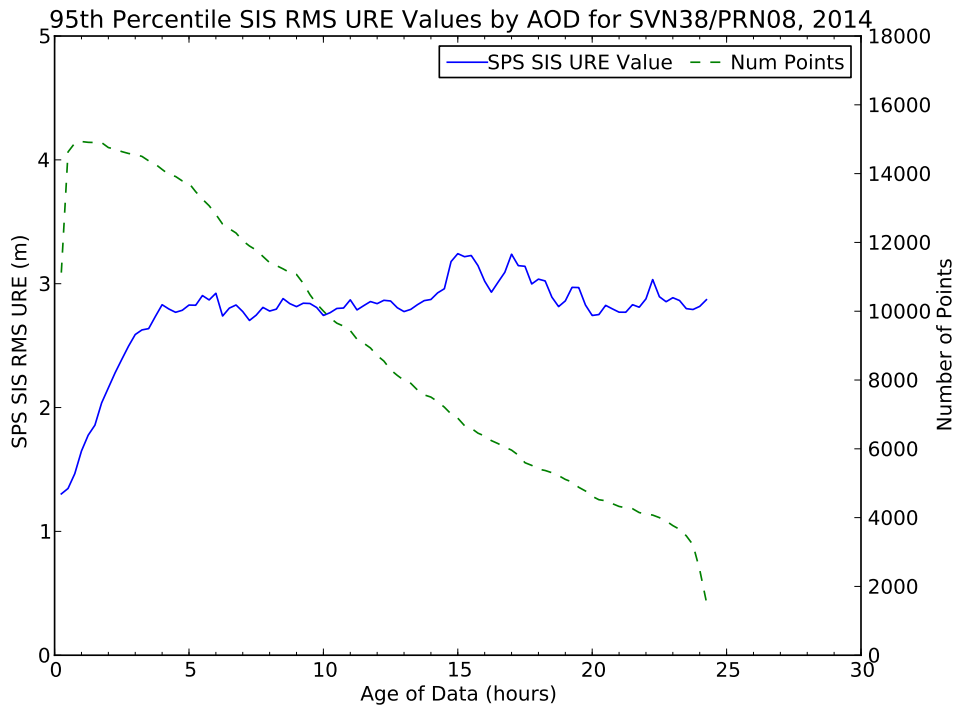


Figure 3.4: Worst Performing Block IIA SV in Terms of Any AOD (SVN 38/PRN 08)

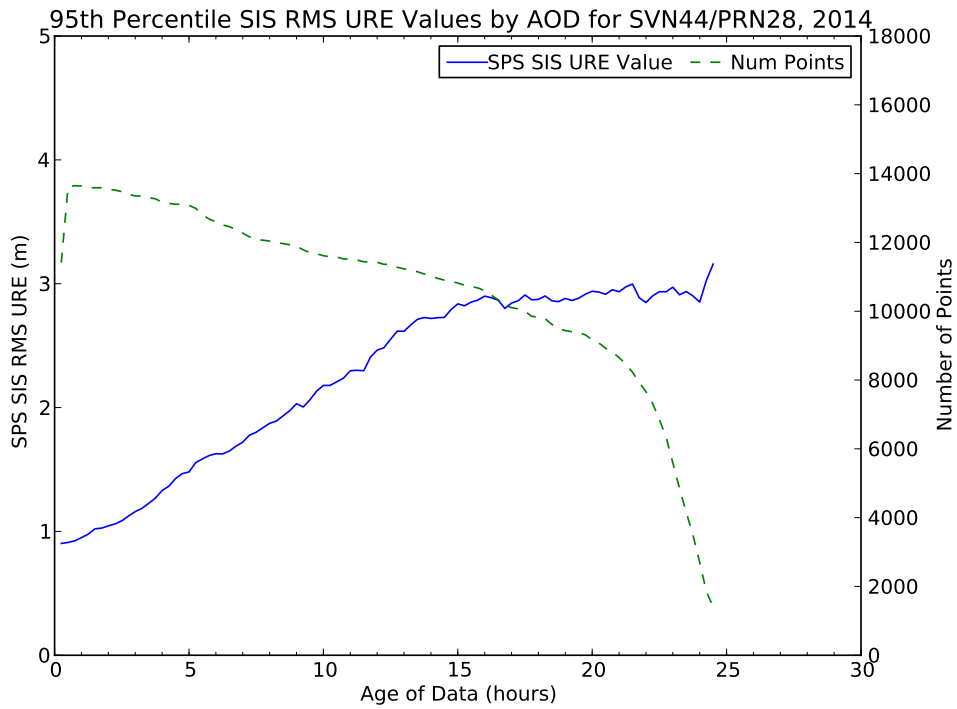


Figure 3.5: Worst Performing Block IIR/IIR-M SV in Terms of Any AOD (SVN 44/PRN 28)

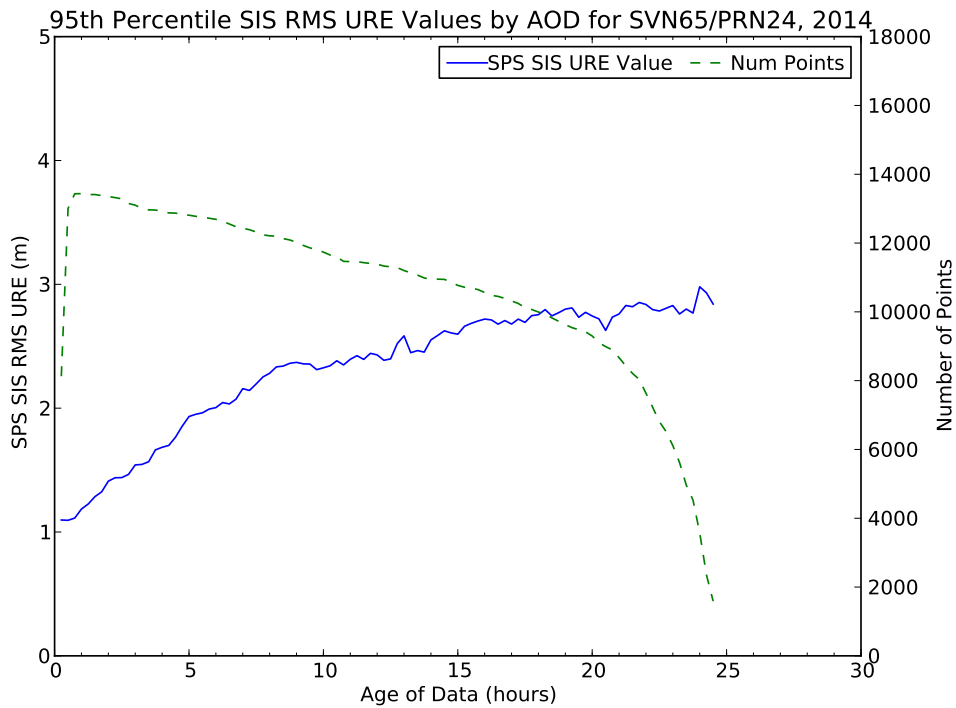


Figure 3.6: Worst Performing Block IIF SV in Terms of Any AOD (SVN 65/PRN 24)

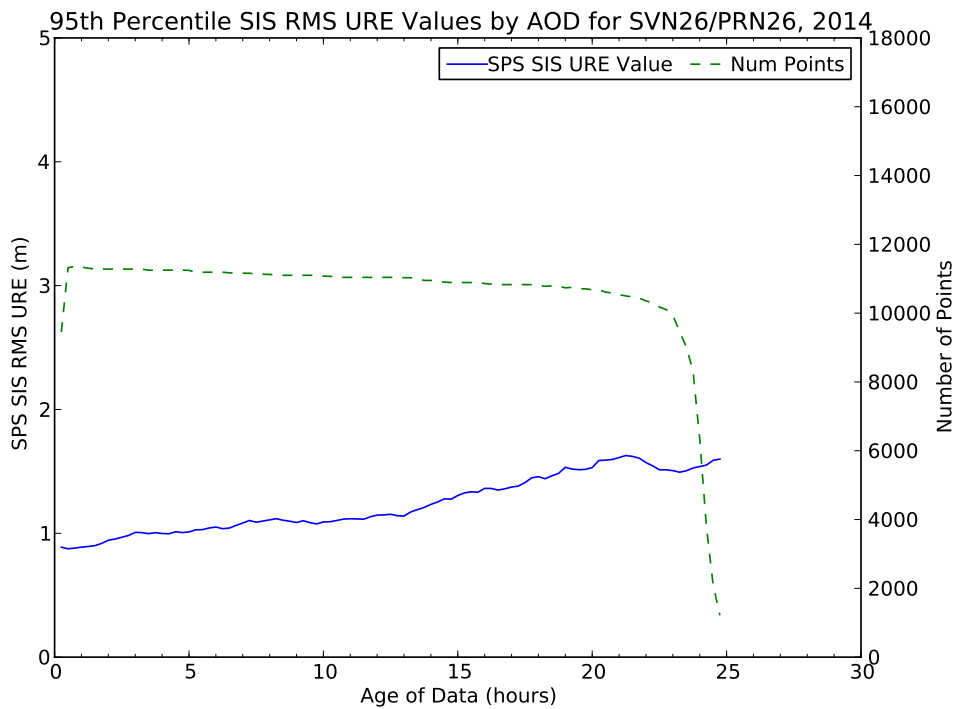


Figure 3.7: Best Performing Block IIA SV in Terms of Any AOD (SVN 26/PRN 26)

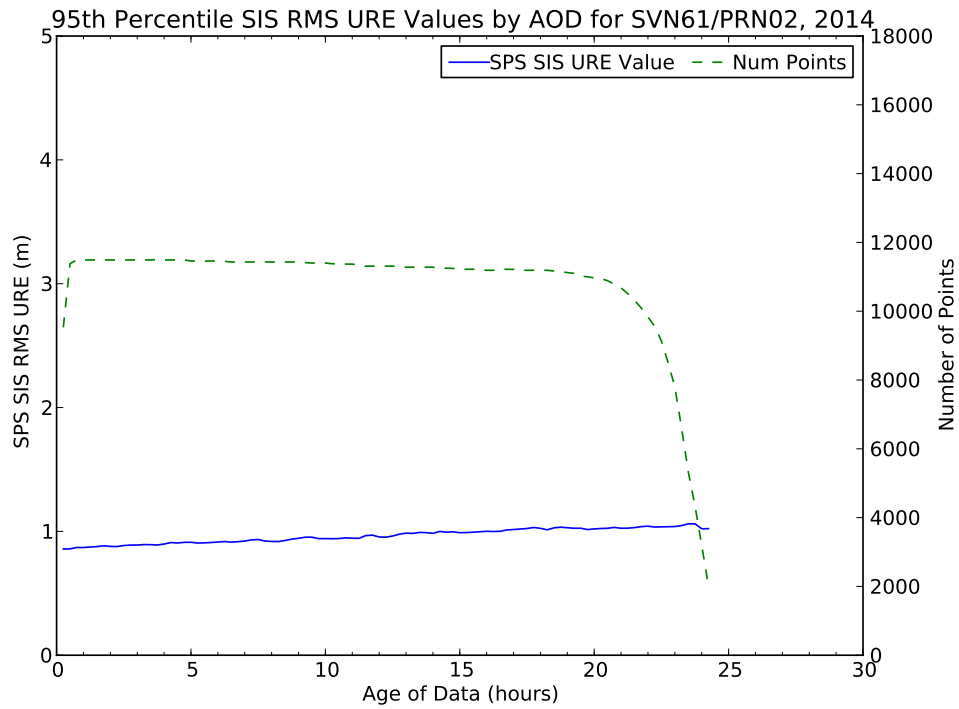


Figure 3.8: Best Performing Block IIR/IIR-M SV in Terms of Any AOD (SVN 61/PRN 02)

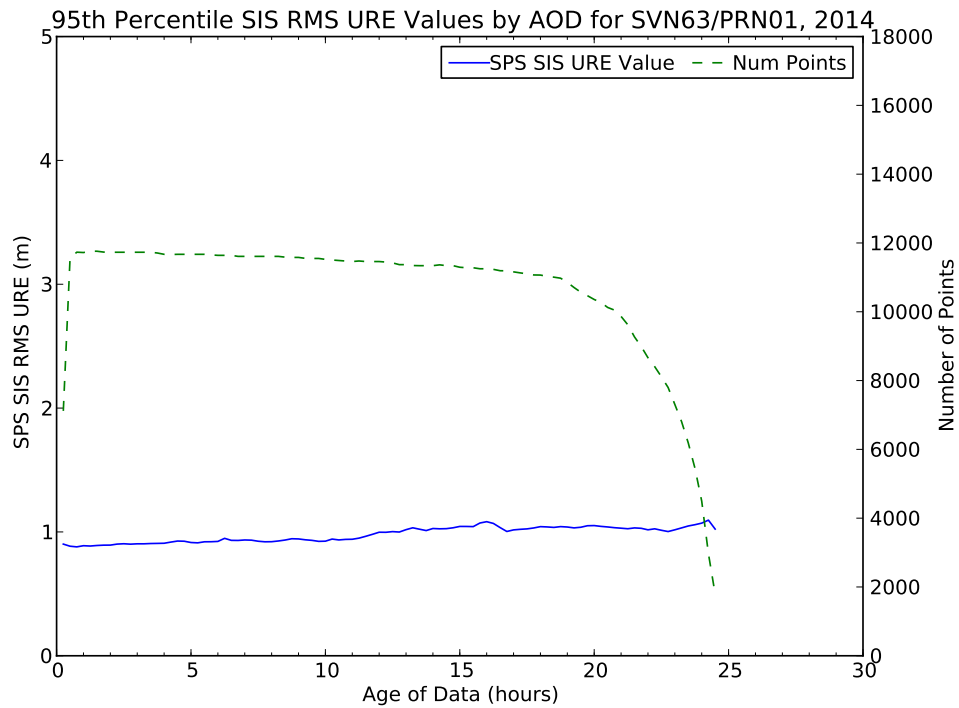


Figure 3.9: Best Performing Block IIF SV in Terms of Any AOD (SVN 63/PRN 01)

3.1.3 URE at Zero AOD

Another URE metric considered is the calculation of URE at Zero Age of Data (ZAOD). This is associated with the SPSPS08 Section 3-4 metric:

- “ ≤ 6.0 m 95% Global Average URE during Normal Operations at Zero AOD”

This metric may be decomposed in a manner similar to the previous two metrics. The key difference is the term “at Zero AOD” and the change in the threshold values.

The broadcast ephemeris is never available to user equipment at Zero AOD simply due to the delays inherent in preparing the broadcast ephemeris and uploading it to the SV. However, we can still make a case that this assertion is met by examining the 95th percentile SIS RMS URE value at 15 minutes AOD. These values are represented by the left-most data point on the red lines shown in Figure 3.4 through Figure 3.9. The ZAOD values should be slightly better than the 15 minute AOD values, or at worst roughly comparable. Inspection of the 15 minute AOD values shows that the values for all SVs are well within the 6.0 m value associated with the assertion. Therefore the assertion is fulfilled.

3.1.4 URE Bounding

The SPSPS08 asserts the following requirements for single frequency C/A code:

- “ ≤ 30 m 99.94% Global Average URE during Normal Operations”
- “ ≤ 30 m 99.79% Worst Case Single Point Average URE during Normal Operations”

As noted earlier the 30 s instantaneous SIS RMS URE values were used to evaluate these requirements. However, there are limitations to our technique of estimating UREs that are worth noting such as fits across orbit/clock discontinuities, thrust events, and clock run-offs. These are discussed in Appendix B.5. As a result of these limitations, the UREs were only used as a screening tool to identify possible violations of this requirement. Possible candidate events were then screened further by examining the observed range deviations (ORDs) to determine actual values during the event.

The ORDs are formed using the observation data collected to support the position accuracy analysis described in Section 3.5.4. In the case of ORDs, the observed range is differenced from the range predicted by subtracting the known station position from the predicted SV location. The selected stations are geographically distributed such that at least two sets of observations are available for each SV at all times. As a result, any actual SV problems that would lead to a violation of this assertion will produce large ORDs from multiple stations.

The 30 s instantaneous SIS RMS URE values and the 30 s ORD values throughout 2014 were examined to determine if any values exceeded 30 m. No such values were found. As a result, these assertions are considered satisfied.

3.1.5 SIS URE at 14 Days

The performance standard asserts the following requirement:

- “ ≤ 388 m 95% Global Average URE during Extended Operations after 14 Days without Upload” (for any satellite marked as healthy in the NAV message)

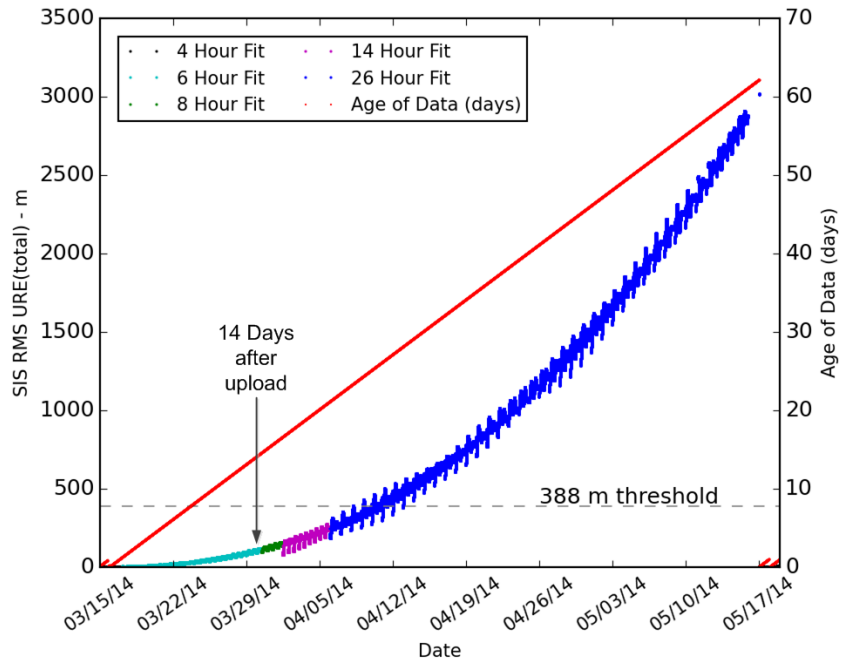
In past years, this requirement could not be evaluated due to lack of relevant information. Short periods of extended operations have been observed (see Section 4.4), but lengthy periods are quite rare.

However, in 2014, SVN 64/PRN 30 was allowed to operate in extended operations mode for over 30 days. The SV was set unhealthy throughout this period, but the NGA MSN tracking data and the NGA precise ephemerides are available. SVN 64 was launched on 21 Feb 2014. After initial checkout, it was allowed to go into an extended operations mode test. The test was conducted and completed prior to the time the SV was declared initially usable.

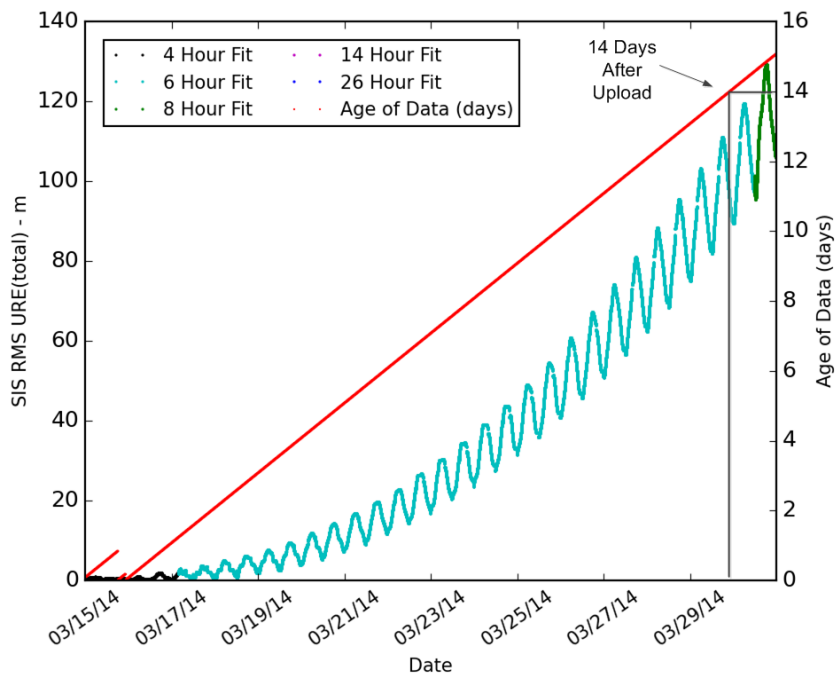
The last upload prior to the test was conducted at 22:26:30Z on 15 March 2014 (Day 74). The next upload occurred at 01:33:30Z on 17 May 2014 (Day 137). The 63 day period is sufficiently long that each of the curve fit intervals defined in Table 20-XII of IS-GPS-200 Section 20.3.4.4 [2] may be observed. The event does not provide sufficient information to validate the metric in a statistical sense (one observation on one SV is a sample size of one), but examining the trend of the SIS RMS URE as the AOD increases provides a useful illustration of such an event.

The SIS RMS URE and AOD during the test are shown in Figure 3.10. Figure 3.10 (a) covers the entire test period. Figure 3.10(b) provides a more detailed view of the first 14 days of the test. The SIS RMS URE are plotted in different colors corresponding to the different curve fit intervals. There are clear differences in the characteristics between the various curve fit intervals. The GPS SVs have a period of approximately 12 hours. Therefore, the 14 hour curve fit interval covers a little more than one orbit while the 26 hour curve fit intervals cover a little more than two orbits. Providing a fit over an entire orbit (or longer) likely explains the large increase in the spread of the SIS RMS URE values and the obvious periodicity in these results. For example, between 6 April and 13 April, there are seven up/down cycles in the URE plot corresponding to the seven days of 26 hour fit intervals.

Returning to the metric, the 14 day AOD value corresponds to a time shortly before the URE trace shown in Figure 3.10(a) transitions to the green line representing the 8 hour curve fit intervals. While recalling that one sample does not constitute a statistic, the fact that the SIS RMS URE is around 100 m at that time provides confidence that the control segment is capable of meeting a metric that only requires 388 m 95th percentile.



(a) URE by Curve Fit and Age of Data, Days 74-138, 2014



(b) URE by Curve Fit and Age of Data, Days 74-89, 2014

Figure 3.10: SIS RMS URE for SVN 64 During Extended Operations.

Notes: The SIS RMS URE and the associated AOD are shown. The red line is the AOD in days. It increases linearly from the last regular upload until the upload at the end of the test.

3.2 SIS Integrity

Under the heading of SIS Integrity, the SPSPS08 makes the following assertion in Section 3.5.1, Table 3.5-1:

- “ $\leq 1 \times 10^{-5}$ Probability Over Any Hour of the SPS SIS Instantaneous URE Exceeding the NTE Tolerance Without a Timely Alert During Normal Operations”

The associated conditions and constraints include a limitation to healthy SIS, a Not to Exceed (NTE) tolerance ± 4.42 times the upper bound on the user range accuracy (URA) currently broadcast, and a worst case for a delayed alert of 6 hours.

The reference to “a Timely Alert” in the assertion refers to any of a number of possible conditions. See SPSPS08 Section A.5.5 for a complete description.

To estimate the worst-case probability of users experiencing misleading signal information (MSI), note that immediately below SPSPS08 Table 3.5-1 is an explanation that for a 32 SV constellation (full broadcast almanac) the corresponding average annual number of SPS SIS instantaneous URE integrity losses is 3. Assuming each of the 3 losses lasts no more than 6 hours, the fraction of time in which MSI will occur is 0.002.

This assertion was verified using two methods:

- The 30 s Instantaneous SIS RMS URE values were examined to determine the number of values that exceed ± 4.42 times the URA.
- Observed Range Deviations (ORDs) from a network of tracking stations were examined to determine the number of values that exceed ± 4.42 times the URA.

Two methods were used due to the fact that each method may result in false positives in rare cases. For example, the URE values may be incorrect near discontinuities in the URE (as described in Appendix B). Similarly, the ORD values may be incorrect due to receiver or reception issues. Therefore, all reported violations are examined manually to determine whether a violation actually occurred, and if so, the extent of the violation.

Screening the 30 s instantaneous SIS RMS URE values and the ORD data did not reveal any events for which this threshold was exceeded. So this requirement is considered satisfied.

3.3 SIS Continuity

3.3.1 Unscheduled Failure Interruptions

The metric is stated in SPSPS08 Table 3.6-1 as follows:

- “ ≥ 0.9998 Probability Over Any Hour of Not Losing the SPS SIS Availability from a Slot Due to Unscheduled Interruption”

The conditions and constraints note the following:

- The empirical estimate of the probability is calculated as an average over all slots in the 24-slot constellation, normalized annually.
- The SPS SIS is available from the slot at the start of the hour.

The notion of SIS continuity is slightly more complex for an expandable slot, because multiple SVs are involved. Following SPSPS08 Section A.6.5, a loss of continuity is considered to occur when,

“The expandable slot is in the expanded configuration, and either one of the pair of satellites occupying the orbital locations defined in Table 3.2-2 for the slot loses continuity.”

Hence, the continuity of signal of the expanded slot will be determined by the logical “and” of the availability of the individual SVs.

Another point is that there is some ambiguity in this metric, which is stated in terms of “a slot” while the associated Conditions and Constraints note that this is an average over all slots. Therefore both the per-slot and 24-slot constellation averages have been computed. As discussed below, while the per-slot values are interesting, the constellation average is the correct value to compare to the SPS PS metric.

Three factors must be considered in looking at this metric:

1. We must establish which SVs were assigned to which slots during the period of the evaluation.
2. We must determine when SVs were not transmitting (or not transmitting a PRN available to users).
3. We must determine which interruptions were scheduled vs. unscheduled.

The derivation of the SV/Slot assignments is described in Appendix E.

For purposes of this report, interruptions were considered to have occurred if one or more of the SV(s) assigned to the given slot is (are) unhealthy in the sense of SPSPS08 Section 2.3.2. The following specific indications were considered:

- If the health bits in navigation message subframe 1 are set to anything other than all zeros.
- If an appropriately distributed worldwide network of stations failed to collect any pseudorange data sets for a given measurement interval.

The latter case (failure to collect any data) indicates that the satellite signal was removed from service (e.g. non-standard code or some other means). The NGA MSN provides at least two-station visibility (and at least 90% three-station visibility) with redundant receivers at each station. Therefore, if no data for a satellite are received for a specific time, it is highly likely that the satellite was not transmitting on the assigned PRN at that time. The 30 s Receiver Independent Exchange format (RINEX) [6] observation files from this network were examined for each measurement interval (i.e. every 30 s) for each SV. If at least one receiver collected a pseudorange data set on L1 C/A, L1 P(Y), and L2 P(Y) with a signal-to-noise level of at least 25 dB-Hz on all frequencies and no loss-of-lock flags, the SV is considered trackable at that moment. In addition, the 30 s IGS data collected to support the position accuracy estimates (Section 3.5.4) were examined in a similar fashion to guard against any MSN control center outages that could have led to missing data across multiple stations simultaneously. This allows us to define an epoch by epoch availability for each satellite. Then, for each slot, each hour in year was examined, and if any SV occupying the slot was not available at the start of the hour, the hour was not considered as part of the evaluation of the metric. If the slot was determined to be available, then the remaining data was examined to determine if an outage occurred during the hour.

The preceding criteria were applied to determine the times and durations of interruptions. Once this was done, the Notice Advisories to Navstar Users (NANUs) effective in 2014 were reviewed to determine which of these interruptions could be considered scheduled interruptions as defined in SPSPS08 Section 3.6. The scheduled interruptions were removed from consideration for purposes of assessing continuity of service. When a slot was available at the start of an hour, but a scheduled interruption occurred during the hour the hour was assessed based on whether data were available prior to the scheduled outage.

Unscheduled interruptions are not always documented with a NANU. A small number of short-duration outages not covered by NANUs were observed. When such outages occurred on satellites that are assigned to one of 24 slots, the outage was counted in evaluating this assertion.

Scheduled interruptions as defined in the ICD-GPS-240 [7] have a nominal notification time of 96 hours prior to the outage. Following the SPSPS08 Section 2.3.5, scheduled interruptions announced 48 hours in advance are not to be considered as contributing to the loss of continuity. So to contribute to a loss of continuity, the notification time for a scheduled interruption must occur less than 48 hours in advance of the interruption. The time from the start of the interruption to the 48 hour after notification time can be considered as a potential unscheduled interruption (for continuity purposes). However, a healthy SIS must exist at the start of any hour for an interruption to be considered to occur.

The following NANU types are considered to represent (or modify) scheduled interruptions (assuming the 48 hour advance notice is met):

- FCSTDV - Forecast Delta-V

- FCSTMX - Forecast Maintenance
- FCSTEXTD - Forecast Extension
- FCSTRESCD - Forecast Rescheduled
- FCSTUUFN - Forecast Unusable Until Further Notice

The FCSTSUMM (Forecast Summary) NANU that occurs after the outage is referenced to confirm the actual beginning and ending time of the outage.

For scheduled interruptions that extend beyond the period covered by a FCSTDV or FCSTMX NANU, the uncovered portion will be considered an unscheduled interruption. However, if a FCSTEXTD NANU extending the length of a scheduled interruption is published 48 hours in advance of the effective time of extension, the interruption will remain categorized as scheduled. It is worth reiterating that, for the computation of the metric, only those hours for which a valid SIS is available from the slot at the start of the hour, are actually considered in the computation of the values.

Table 3.4 is a summary of the results of the assessment of SIS continuity. Interpreting the metric as being averaged over the constellation, the constellation exceeded the goal of 0.9998 probability of not losing the SPS SIS availability due to a unscheduled interruption.

To put this in perspective, there were 8760 hours in 2014. The required probability of not losing SPS SIS availability implies that there be less than $8760 \times (1 - 0.9998) = 1.75$ hours that experience unscheduled interruptions in a year. If this were a per-slot metric, this would mean no slot may experience more than one unscheduled interruption in a year. The maximum number of unscheduled interruptions over the 24 slot constellation is given by $8760 \times 24 \times (1 - 0.9998) = 42$ unscheduled hours that experience interruptions. This is less than two unscheduled interruptions per SV per year, but allows for the possibility that some SVs may have no unscheduled interruptions while others may have more than one.

Slot B1 is considered empty in 2014. The slot has been configured as an expanded slot for some time. However, on 28 March 2013 the satellite occupying the B1F half of slot B1 experienced an unscheduled interruption (SVN 35/PRN 30, see NANU 2013022). It was later decommissioned (NANU 2013027). B1F remained empty until April 2015. As a result, for purposes of this analysis, slot B1 is considered empty for all of 2014. In Table 3.4 the row associated with B1 shows no hours of availability and therefore, no possibility of an unscheduled interruption. (Note that the beginning of the unscheduled interruption was already logged in the 2013 report.) This outage is also addressed in Section 3.4 in terms of the impact on availability.

Returning to Table 3.4, across the constellation slots the total number of hours lost was 12. This is smaller than the maximum number of hours of unscheduled interruptions (42) available to meet the metric (see the previous paragraph), and leads to empirical value for the fraction of hours in which SIS continuity was maintained of 0.99994. Therefore, this assertion is considered fulfilled in 2014.

Table 3.4: Probability Over Any Hour of Not Losing Availability Due to Unscheduled Interruption.

Plane-Slot	# of Hours with the SPS SIS available at the start of the hour	# of Hours with Unscheduled Interruption ^b	Fraction of Hours in Which Availability was Not Lost
A1	8760	0	1.00000
A2	8760	0	1.00000
A3	8652	3	0.99966
A4	8760	0	1.00000
B1 ^a	0	0	0.00000
B2	8760	2	0.99977
B3	8760	0	1.00000
B4	8760	1	0.99989
C1	8760	0	1.00000
C2	8760	0	1.00000
C3	8757	1	0.99989
C4	8760	0	1.00000
D1	8760	0	1.00000
D2 ^a	8759	2	0.99977
D3	8760	0	1.00000
D4	8760	1	0.99989
E1	8760	0	1.00000
E2	8760	0	1.00000
E3	8760	0	1.00000
E4	8760	0	1.00000
F1	8759	1	0.99989
F2 ^a	8760	1	0.99989
F3	8760	0	1.00000
F4	8760	0	1.00000
All Slots	201367	12	0.99994

^aWhen B1, D2, and F2 are configured as expandable slots, both slot locations must be occupied by an available satellite for the slot to be counted as available.

^bNumber of hours in which (1.) an SV transmitted navigation message with subframe 1 health bits set to other than all zeroes without a scheduled outage, (2.) signal lost without a scheduled outage, or (3.) the URE NTE tolerance was violated.

3.3.2 Status and Problem Reporting Standards

3.3.2.1 Scheduled Events

The SPSPS08 makes the following assertion in Section 3.6.3 regarding notification of scheduled events affecting service:

- *“Appropriate NANU issued to Coast Guard and the FAA at least 48 hours prior to the event”*

While beyond the assertion in the performance standards, ICD-GPS-240 [7] states a nominal notification time of 96 hours prior to outage start and an objective of 7 days prior to outage start.

This metric was evaluated by examining the NANUs provided throughout the year and comparing the NANU periods to outages observed in the data. In general, scheduled events are described in a pair of NANUs. The first NANU is a forecast of when the outage will occur. The second NANU is provided after the outage and summarizes the actual start and end times of the outage. (This is described in ICD-GPS-240 Section 10.1.1.)

Table 3.5 summarizes the pairs found for 2014. The two leftmost columns provide the SVN/PRN of the subject SV. The next three columns specify the NANU #, type, and date/time of the NANU for the forecast NANU. These are followed by three columns that specify the NANU #, and date/time of the NANU for the FCSTSUMM NANU provided after the outage along with the date/time of the beginning of the outage. The final column is the time difference between the time the forecast NANU was released and the beginning of the actual outage (in hours). This represents the length of time between the release of the forecast and the actual start of the outage.

To meet the assertion in the performance standard, the number of hours in the rightmost column of Table 3.5 should always be greater than 48.0. The average notice was over 145 hours. However, there was one case in which the forecast was less than the 48 hour assertion. In that case, the notice was only 17.3 hours (see NANU 2014043 in Table 3.5). Given that this event did not meet the 48 hour assertion, it has been treated as an unscheduled interruption for purposes of the evaluation in the previous section and marked as unscheduled in Appendix D.

Four times in 2014 satellites were decommissioned. These were handled as special cases of scheduled outages. A FCSTUUFN (Forecast unusable until further notice) NANU was provided specifying when the satellite would be set unusable. Following this, a DECOM (decommission) NANU was provided following the actual event. The details on the notice provided by these four pairs are provided in Table 3.6. Each of the pairs meets the assertion of the SPS PS and the nominal time of the ICD-GPS-240 for scheduled events. Three of the four meet the objective time of the ICD-GPS-240 for scheduled events.

Table 3.5: Scheduled Events Covered in NANUs for 2014

SVN	PRN	Prediction NANU			Summary NANU (FCSTSUMM)			Notice (hrs)
		NANU #	TYPE	Release Time	NANU #	Release Time	Start Of Outage	
59	19	2014001	FCSTDV	03 Jan 1537Z	2014002	10 Jan 0301Z	09 Jan 2058Z	149.35
47	22	2014003	FCSTDV	10 Jan 1714Z	2014004	16 Jan 2246Z	16 Jan 1741Z	144.45
63	01	2014006	FCSTMX	30 Jan 0842Z	2014009	03 Feb 2136Z	03 Feb 1616Z	103.57
45	21	2014008	FCSTDV	31 Jan 1836Z	2014011	07 Feb 1843Z	07 Feb 1302Z	162.43
61	02	2014012	FCSTDV	07 Feb 2106Z	2014014	14 Feb 1510Z	14 Feb 0941Z	156.58
56	16	2014013	FCSTRESCD	10 Feb 2307Z	2014016	18 Feb 2217Z	18 Feb 1556Z	184.82
38	08	2014017	FCSTDV	20 Feb 2026Z	2014020	27 Feb 0632Z	27 Feb 0101Z	148.58
50	05	2014021	FCSTDV	27 Feb 2118Z	2014023	05 Mar 0759Z	05 Mar 0014Z	122.93
53	17	2014022	FCSTDV	28 Feb 1533Z	2014024	07 Mar 0950Z	07 Mar 0355Z	156.37
65	24	2014029	FCSTDV	17 Mar 2215Z	2014030	20 Mar 0859Z	20 Mar 0314Z	52.98
23	32	2014031	FCSTDV	25 Mar 2226Z	2014033	01 Apr 1352Z	01 Apr 0827Z	154.02
51	20	2014034	FCSTDV	04 Apr 1719Z	2014036	15 Apr 2003Z	10 Apr 1741Z	144.37
52	31	2014035	FCSTDV	10 Apr 2055Z	2014037	15 Apr 2031Z	15 Apr 1443Z	113.80
60	23	2014040	FCSTDV	02 May 1927Z	2014041	08 May 2309Z	08 May 1718Z	141.85
38	08	2014043	FCSTDV	14 May 1628Z	2014044	15 May 1641Z	15 May 0946Z	17.30 [†]
34	04	2014048	FCSTDV	06 Jun 2059Z	2014051	12 Jun 2243Z	12 Jun 1420Z	137.35
40	10	2014053	FCSTDV	03 Jul 1913Z	2014056	10 Jul 1740Z	10 Jul 1152Z	160.65
67	06	2014055	FCSTDV	10 Jul 1654Z	2014057	17 Jul 1508Z	17 Jul 0950Z	160.93
38	08	2014061	FCSTDV	31 Jul 1505Z	2014064	07 Aug 1858Z	07 Aug 1252Z	165.78
34	04	2014065	FCSTMX	07 Aug 2057Z	2014067	12 Aug 2220Z	12 Aug 1647Z	115.83
43	13	2014066	FCSTDV	08 Aug 2041Z	2014068	14 Aug 1330Z	14 Aug 0733Z	130.87
43	13	2014070	FCSTDV	11 Sep 2139Z	2014072	19 Sep 1439Z	19 Sep 0713Z	177.57
62	25	2014073	FCSTDV	26 Sep 1841Z	2014074	02 Oct 2144Z	02 Oct 1600Z	141.32
58	12	2014075	FCSTDV	16 Oct 1545Z	2014077	23 Oct 1802Z	23 Oct 1354Z	166.15
63	01	2014076	FCSTMX	22 Oct 1435Z	2014080	27 Oct 2306Z	27 Oct 1844Z	124.15
58	12	2014079	FCSTDV	24 Oct 2036Z	2014081	28 Oct 1047Z	28 Oct 0444Z	80.13
34	04	2014084	FCSTDV	13 Nov 1628Z	2014085	21 Nov 2358Z	21 Nov 1614Z	191.77
55	15	2014086	FCSTDV	04 Dec 1720Z	2014089	11 Dec 2100Z	11 Dec 1538Z	166.30
51	20	2014087	FCSTDV	04 Dec 1740Z	2014091	16 Dec 2346Z	16 Dec 1719Z	287.65
48	07	2014088	FCSTDV	10 Dec 1856Z	2014092	19 Dec 0703Z	19 Dec 0113Z	198.28
Average Notice Period								145.27

[†]This event counts as an unscheduled outage under the assertions of SPS PS 3.6.3.

Table 3.6: Decommissioning Notice Times

SVN	PRN	FCSTUUFN NANU		DECOM NANU			Notice (hrs)
		NANU #	Release Time	NANU #	Release Time	End of Unusable Period	
36	6	2014015	14 Feb 1612Z	2014019	21 Feb 2208Z	21 Feb 1501Z	166.8
39	9	2014042	12 May 1949Z	2014046	19 May 2222Z	19 May 1435Z	162.8
33	3	2014060	25 Jul 1817Z	2014063	02 Aug 2214Z	02 Aug 1959Z	193.7
38	8	2014078	24 Oct 1347Z	2014083	30 Oct 2254Z	30 Oct 1500Z	145.2
Average Notice Period							167.1

3.3.2.2 Unscheduled Outage

The SPS PS provides the following assertion in Section 3.6.3 regarding notification of unscheduled outages or problems affecting service:

- *“Appropriate NANU issued to Coast Guard and the FAA as soon as possible after the event”*

The ICD-GPS-240 states that the nominal notification times is less than 1 hour after the start of the outage with an objective of 15 minutes.

This metric was evaluated by examining the NANUs provided throughout the year and comparing the NANU periods to outages observed in the data. Unscheduled events may be covered by either a single NANU or a pair of NANUs. In the case of a brief outage, a NANU with type UNUNOREF (unusable with no reference) is provided to detail the period of the outage. In the case of longer outages, a UNUSUFN (unusable until further notice) is provided to inform users of an ongoing outage or problem. This is followed by a NANU with type UNUSABLE after the outage is resolved. (This is described in detail in ICD-GPS-240 Section 10.1.2.)

Table 3.7 provides a list of the unscheduled outages found in the NANU information for 2014. These are all pairs of UNUSUFN/UNUSABLE NANUs as no UNUNOREF NANUs were issued in 2014. The two leftmost columns provide the SVN/PRN of the subject SV. The next three columns provide the NANU #, type, and date/time of the UNUSUFN NANU. These are followed by three columns that specify the NANU #, date/time of the NANU for the UNUSABLE NANU provided after the outage along with the date/time of the beginning of the outage. The final column is the time difference between the time the outage began and the time the UNUSUFN NANU was released (in minutes).

Table 3.7: Unscheduled Events Covered in NANUs for 2014

SVN	PRN	UNUSUFN NANU		UNUSABLE NANU			Lag Time (minutes)
		NANU #	Release Time	NANU #	Release Time	Start Of Event	
39	09	2014025	07 Mar 1453Z	2014026	07 Mar 1511Z	07 Mar 1508Z	-15.00
63	01	2014027	14 Mar 0614Z	2014028	14 Mar 0654Z	14 Mar 0502Z	72.00
64	30	2014052	03 Jul 1220Z	2014054	03 Jul 2246Z	03 Jul 1211Z	9.00
59	19	2014058	21 Jul 1628Z	2014059	21 Jul 1845Z	21 Jul 1612Z	16.00
Average Lag Time							20.50

Since the performance standard only states “as soon as possible after the event”, there is no evaluation to be performed. However, the data are provided for information.

3.4 SIS Availability

3.4.1 Per-slot Availability

The SPSPS08 Section 3.7.1 makes two linked statements in this area:

- “ ≥ 0.957 Probability that a Slot in the Baseline Configuration will be Occupied by a Healthy Navstar Satellite Broadcasting a Useable SPS SIS”
- “ ≥ 0.957 Probability that a Slot in the Expanded Configuration will be Occupied by a pair of Healthy Navstar Satellites Each Broadcasting a Useable SPS SIS”

The constraints include the note that this is to be calculated as an average over all slots in the 24-slot constellation, normalized annually.

The derivation of the SV/Slot assignments is described in Appendix E.

This metric was verified by examining the status of each SV in the Baseline 24- Slot configuration (or pair of SVs in an Expandable Slot) at every 30 s interval throughout the year. The health status was determined from the subframe 1 health bits of the ephemeris being broadcast at the time of interest. In addition, data from monitor station networks were examined to verify that the SV was broadcasting a trackable signal at the time. The results are summarized in Table 3.8.

Slots A3 and B1 presented unusual situations in 2014. Slot A3 was unoccupied for approximately four days after SVN 38 left the slot and prior to SVN 64 being set initially usable. (The gap is illustrated in Appendix E.) This accounts for the large count for slot A3 in Table 3.8.

Slot B1 has been configured as an expanded slot for some time. However, the B1F half of slot B1 was unoccupied throughout 2014. (The events that led to this are described in Section 3.3.) Therefore, B1 is considered empty for all of 2014 as only B1A was occupied. This metric is calculated as an average across the entire constellation. For any given evaluation interval the number of epochs/slot will be the same for each slot and there are 24 slots. Therefore, the effect of a missing slot for an entire year is to lower the maximum value achievable from 1.000 to 0.958. This is barely above the threshold of 0.957.

It should be noted that neither of these two unoccupied slots was likely noticed by users. As will be shown in Section 3.5, the Dilution of Precision (DOP) values were excellent throughout 2014. Therefore, 2 SOPS was managing the constellation, including the excess satellites above the slot definitions, in such a manner as to assure good geometric coverage. In the case of B1, the only other satellite available in the plane at the time was SVN 49 (which has never been set healthy since launch).

Therefore the operator’s possible actions came down to:

Table 3.8: Per-Slot Availability in 2014 for Baseline 24 Slots. For each slot there were 1051200 total 30 second epochs.

Plane-Slot	# Missing Epochs	Available
A1	677	0.999356
A2	673	0.999360
A3	13631	0.987033
A4	679	0.999354
B1 ^a	1051200	0.000000
B2	671	0.999362
B3	0	1.000000
B4	1196	0.998862
C1	0	1.000000
C2	0	1.000000
C3	1042	0.999009
C4	699	0.999335
D1	650	0.999382
D2 ^a	1366	0.998701
D3	637	0.999394
D4	633	0.999398
E1	701	0.999333
E2	606	0.999424
E3	926	0.999119
E4	0	1.000000
F1	4	0.999996
F2 ^a	655	0.999377
F3	711	0.999324
F4	691	0.999343
All Slots	1078048 ^b	0.957269

^aWhen B1, D2, and F2 are configured as expandable slots, both slot locations must be occupied by an available satellite in order for the slot to be counted as available.

^bThe total is comprised of 1051200 missing epochs for B1 and 13,572 missing epochs from all other slots.

- collapse the slot,
- move SVN 49 to B1A and consider it operational, or
- leave the configuration as it was and manage the constellation such that sufficiently low DOP is maintained.

It should be noted that collapsing the slot would mean expending fuel to move the satellite in B1A to B1, and later transition it back.

It is beyond the scope of this report to comment on the operational decisions made in managing the system. However, it is worthwhile to note that this is an excellent example of the practical challenges of managing the system in conformance to a standard. There will be times when the operators are constrained by the resources at hand and need to manage the system to the spirit of the standard as opposed to the letter. In this case, the result was to maintain DOP, minimize on-orbit actions, and allow the availability metric to fall to a lower value than typical.

The average availability for the constellation was 0.9573, meeting the threshold of 0.957. The availability values for all slots were better than the threshold. Therefore the assertions being tested in this section were met.

3.4.2 Constellation Availability

The SPSPS08 makes two linked statements in this area:

- *“ ≥ 0.98 Probability that at least 21 Slots out of the 24 Slots will be Occupied Either by a Satellite Broadcasting a Healthy SPS SIS in the Baseline 24-Slot Configuration or by a Pair of Satellites Each Broadcasting a Healthy SPS SIS in the Expanded Slot Configuration”*
- *“ ≥ 0.99999 Probability that at least 20 Slots out of the 24 Slots will be Occupied Either by a Satellite Broadcasting a Healthy SPS SIS in the Baseline 24-Slot Configuration or by a Pair of Satellites Each Broadcasting a Healthy SPS SIS in the Expanded Slot Configuration”*

To evaluate this metric the subframe 1 health condition and the availability of signal was evaluated for each SV every 30 seconds for all of 2014. Following a literal reading of the requirement, the number of SVs broadcasting a healthy SIS was examined for each measurement interval and assigned to the correct slot. For non-expanded baseline slots, if an SV qualified as being in the slot and was transmitting a healthy signal, the slot was counted as occupied. For expanded slots, the slot was counted as occupied if two healthy SVs were found: one in each of the two portions of the expanded slot. If the count of occupied slots was greater than 20, the measurement interval was counted as a 1; otherwise the measurement interval was assigned a zero. The sum of the 1

values was then divided by the total number of measurement intervals. The value for 2014 is 1.00. Thus, both requirements are satisfied.

While this satisfies the metric, it does not provide much information on exactly how many SVs are typically healthy. To address this, at each 30 s interval the number of SVs broadcasting a healthy SIS was counted. This was both for count of occupied slots and for the number of SVs. The daily averages as a function of time are shown in Figure 3.10. As is clear, the number of occupied slots always exceeds 21.

The Number of Occupied Slots shown in Figure 3.10 shows a maximum of 23 for all of 2014. This is again a result of the decommissioning of SVN 35/PRN 30 in March 2013. SVN 35/PRN 30 was assigned to B1F, an expandable slot. After SVN 35/PRN 30 was no longer available, slot B1F remained unoccupied for all of 2014(Section 3.3). This is neither a violation of Constellation Availability assertions (described above) nor does it present a problem for the user (at least in this case). As shown by the DOP values described in Section 3.5.1, even with this expandable slot only half-filled, the DOP values were excellent throughout 2014.

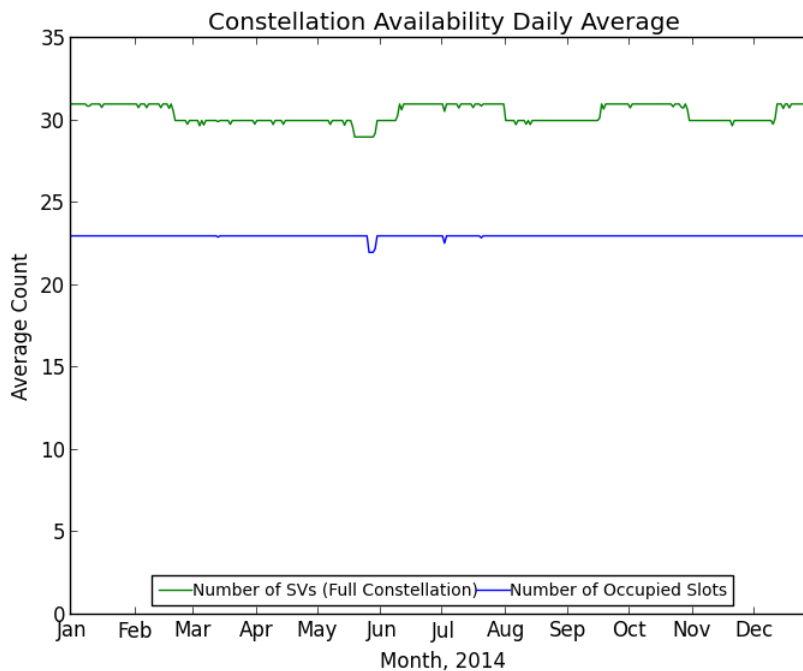


Figure 3.10: Daily Average Number of Occupied Slots

3.4.3 Operational Satellite Counts

In Table 3.7-3, the SPSPS08 states:

- “ ≥ 0.95 Probability that the Constellation will Have at least 24 Operational

Satellites Regardless of Whether Those Operational Satellites are Located in Slots or Not

Under “Conditions and Constraints” the term Operational is defined as

“any satellite which appears in the transmitted navigation message almanac... regardless of whether that satellite is currently broadcasting a healthy SPS SIS or not or whether the broadcast SPS SIS also satisfies the other performance standards in this SPS PS or not.”

Given the information presented in sections 3.4.1 and 3.4.2, we conclude that the probability associated with this metric is 1.00 for 2014. However, the navigation message was examined as a means of checking for consistency in the navigation message. The process selected an almanac for each day in 2014. IS-GPS-200 Section 20.3.3.5.1.3 [2] assigns a special meaning to the SV Health bits in the almanac’s subframe 4 Page 25 and subframe 5 Page 25 (Data ID 51 and 63). When these bits are set to all ones it indicates “the SV which has that ID is not available and there may be no data regarding that SV in that page of subframes 4 and 5...”. Given this definition, the process examines the subframe 4 and 5 health bits for the individual SVs and counts the number of SVs for which the health bits are other than all ones. The results are shown in Figure 3.11. This plot is very similar to the full constellation healthy satellite count shown in Figure 3.10. The almanac health data are not updated as frequently as those in Subframe 1. As a result, the plot in Figure 3.11 contains only integer values. Therefore, on days when it appears the operational SV count is lower than the number of healthy SVs in the constellation, these reflect cases where an SV was set unhealthy for a small portion of the day. In Figure 3.10, such effects are averaged over the day, yielding a higher availability.

3.5 Position/Time Availability

3.5.1 PDOP Availability

Given representative user conditions and considering any 24 hour interval the SPS08 calls for:

- “ $\geq 98\%$ global PDOP of 6 or less”
- “ $\geq 88\%$ worst site PDOP of 6 or less”

Based on the definition of a representative receiver contained in SPS PS Section 3.8, a 5° minimum elevation angle is used for this evaluation.

These assertions were verified empirically throughout 2014 using a regularly spaced grid, containing N_{grid} points, to represent the terrestrial service volume at zero altitude

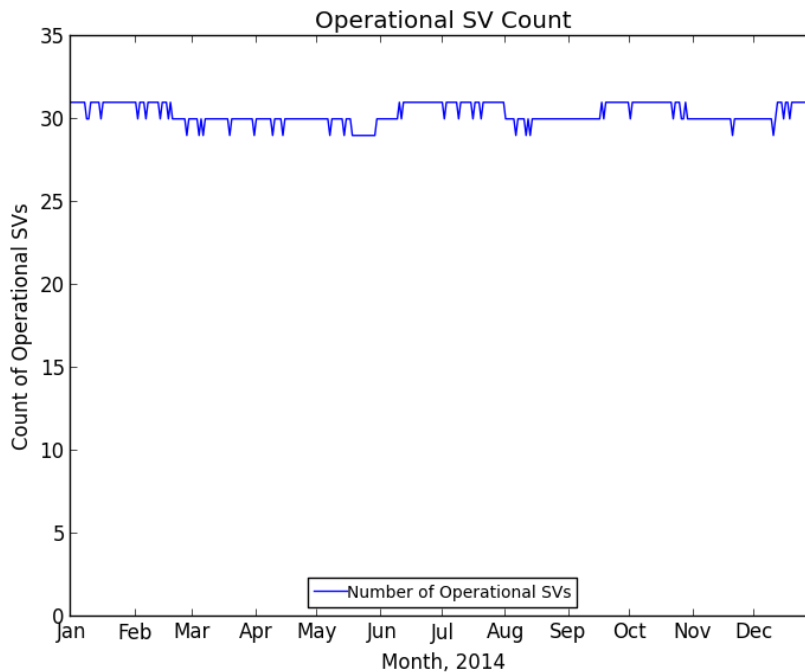


Figure 3.11: Count of Operational SVs by Day

and an archive of the broadcast ephemerides transmitted by the SVs throughout the year. All healthy, transmitting SVs were considered. The grid was $111 \text{ km} \times 111 \text{ km}$ (roughly $1^\circ \times 1^\circ$ at the Equator). The time started at 0000Z each day and stepped through the entire day at five minute intervals (288 points/day, or more generically, N_t). The overall process followed is similar to that defined in Section 5.4.6 of the GPS Civil Monitoring Performance Specification (CMPS) [8].

The Position Dilution of Precision (PDOP) values were formed using the traditional PDOP algorithm, without regard for the impact of terrain. The coordinates of the grid locations provided the ground positions at which the PDOP was computed. The position of each SV was computed from the broadcast ephemeris available to the user at the time of interest. The only filtering performed was to identify and exclude from the calculations any unhealthy SVs (those with subframe 1 health bits set to other than all 0's). The results of each calculation were tested with respect to the threshold of $\text{PDOP} \leq 6$. If the condition was violated, a bad PDOP counter associated with the particular grid point, b_i for $1 \leq i \leq N_{grid}$, was incremented.

At least four SVs must be in view for a valid PDOP computation. This condition was fulfilled for all grid points at all times in 2014.

Once the PDOPs had been computed across all grid points, for each of the 288 time increments during the day, the percentage of time the PDOP was ≤ 6 for the day was computed using the formula:

$$(\%PDOP \leq 6) = 100 \left(1 - \frac{\sum_{i=1}^{N_{grid}} b_i}{N_{grid} N_t} \right)$$

The worst site for a given day was identified from the same set of counters by finding the site with the maximum bad count: $b_{max} = \max_i b_i$. The ratio of b_{max} to N_t is an estimate of the fraction of time the worst site PDOP exceeds the threshold. This value was averaged over the year, and the percentage of time the PDOP is ≤ 6 was computed.

Table 3.9 summarizes the results of this analysis for the configurations all SVs available. The first column (“Average daily % over 2014”) duplicates the values shown in Section 2. The additional column is provided to verify that no single-day value actually dropped below the goal. From this table we conclude that the PDOP availability metrics are met for 2014.

Table 3.9: Summary of PDOP Availability

Metric	Average daily % over 2014	Minimum daily % over 2014
$\geq 98\%$ Global Average PDOP ≤ 6	≥ 99.999	99.978
$\geq 88\%$ Worst site PDOP ≤ 6	99.610	97.917

In addition to verifying the standard, several additional analyses go beyond the direct question and speak to the matter of how well the system is performing on a more granular basis. The remainder of the section describes those analyses and results.

3.5.2 Additional DOP Analysis

There are several ways to look at Dilution of Precision (DOP) values when various averaging techniques are taken into account. Assuming a set of DOP values, each identified by latitude (λ), longitude (θ), and time (t), then each individual value is represented by $DOP_{\lambda,\theta,t}$.

The global average DOP for a day, $\langle DOP \rangle(\text{day})$, is defined to be

$$\langle DOP \rangle(\text{day}) = \frac{\sum_t \sum_\theta \sum_\lambda DOP_{\lambda,\theta,t}}{N_{grid} \times N_t}$$

Another measure of performance is the average DOP over the day at the worst site, $\langle DOP \rangle_{\text{worst site}}$. In this case the average over a day is computed for each unique latitude/longitude combination and the worst average of the day is taken as the result.

$$\langle DOP \rangle_{\text{worst site}}(\text{day}) = \max_{\lambda,\theta} \left(\frac{\sum_t DOP_{\lambda,\theta,t}}{N_t} \right)$$

This statistic is the most closely related to the description of worst site used in Section 3.5.1.

The average of worst site DOP, $\langle DOP_{worst\ site} \rangle$, is obtained by obtaining the worst DOP in the latitude-longitude grid at each time, then averaging these values over the day.

$$\langle DOP_{worst\ site} \rangle(day) = \frac{\sum_t \max_{\lambda, \theta} (DOP_{\lambda, \theta, t})}{N_t}$$

This represents a measure of the worst DOP performance. It is not particularly useful from the user's point of view since the location of the worst site varies throughout the day.

Finally, the absolute worst time-point in a day is given by taking the maximum of the individual DOP values for all locations and all times.

$$DOP_{abs.\ worst}(day) = \max_{\lambda, \theta, t} (DOP_{\lambda, \theta, t})$$

Given that the $\langle DOP \rangle_{worst\ site}(day)$ is most closely related to the worse site definition used in Section 3.5.1, this is the statistic that will be used for "worst site" in the remainder of this section. For 2014, both $\langle DOP \rangle_{worst\ site}(day)$ and $\langle DOP_{worst\ site} \rangle(day)$ satisfy the SPS PS assertions, so the choice is not critical with respect to 2014.

It is worth noting the following mathematical relationship between these quantities:

$$\langle DOP \rangle \leq \langle DOP \rangle_{worst\ site} \leq \langle DOP_{worst\ site} \rangle \leq DOP_{abs.\ worst}$$

This serves as a sanity check on the DOP results in general, and establishes that these metrics are increasingly sensitive to outliers.

In calculating the percentage of the time that the $\langle DOP \rangle$ and $\langle DOP \rangle_{worst\ site}$ are within bounds, several other statistics were calculated which provide insight into the availability of the GPS constellation throughout the world. Included in these statistics are the annual means of the daily globally average DOP and the $\langle DOP \rangle_{worst\ site}$ values. These values are presented in Table 3.10, with values for 2011 through 2013 provided for comparison. The average number of satellites and the fewest satellites visible across the grid are calculated as part of the DOP calculations. Also shown in Table 3.10 are the annual means of the global average number of satellites visible to grid cells on a 111 km \times 111 km (latitude by longitude) global grid and the annual means of the number of satellites in the worst-site grid cell (defined as seeing the fewest number of satellites). It should be noted that the worst site for each of these values was not only determined independently from day-to-day, it was also determined independently for each metric. That is to say, it is not guaranteed that the worst site with respect to HDOP is the same as the worst site with respect to PDOP. For all quantities shown in Table 3.10 the values are very similar across all four years.

There are a few other statistics that can add insight regarding the GPS system availability. The primary availability metric requires that the globally averaged PDOP be in-bounds at least 98% of the time. There are two related values: the number of days for which the PDOP is in bounds and the 98th percentile of the daily globally averaged

Table 3.10: Additional DOP Annually-Averaged Visibility Statistics for 2011 through 2014.

	$\langle DOP \rangle$				$\langle DOP \rangle_{worst\ site}$			
	2014	2013	2012	2011	2014	2013	2012	2011
Horizontal DOP	0.86	0.83	0.84	0.85	0.99	0.96	0.96	0.98
Vertical DOP	1.39	1.35	1.36	1.38	1.73	1.69	1.69	1.72
Time DOP	0.81	0.78	0.79	0.81	0.94	0.91	0.91	0.93
Position DOP	1.64	1.59	1.60	1.62	1.89	1.85	1.85	1.88
Geometry DOP	1.83	1.77	1.79	1.81	2.10	2.05	2.05	2.09
Number of visible SVs	10.30	10.71	10.44	10.24	4.97	5.65	5.94	5.63

PDOP values. Similarly, calculations can be done for $\langle DOP \rangle_{worst\ site}$ criteria of having the PDOP ≤ 6 greater than 88% of the time. Table 3.11 presents these values.

Table 3.11: Additional PDOP Statistics.

	2014	2013	2012	2011
Percentage of Days with the $\langle PDOP \rangle \leq 6$	100	100	100	100
Percentage of Days with the $\langle PDOP \rangle$ at Worst Site ≤ 6	100	100	100	100
98 th Percentile of $\langle PDOP \rangle$	1.67	1.63	1.65	1.68
88 th Percentile of $\langle PDOP \rangle_{worst\ site}$	1.91	1.88	1.87	1.93

Table 3.11 shows that the average DOP values for 2014 are nearly identical to previous years.

Behind the statistics are the day-to-day variations. Figure 3.12 provides a time history of the four PDOP metrics considering all satellites for 2014. Four metrics are plotted.

- Daily Global Average PDOP, $\langle PDOP \rangle$
- Average Worst Site PDOP, $\langle PDOP \rangle_{worst\ site}$
- Average PDOP at Worst Site, $\langle PDOP_{worst\ site} \rangle$
- Absolute Worst PDOP, $PDOP_{abs.\ worst}$

$PDOP_{abs.\ worst}$ is most sensitive to outliers and has features that are idiosyncratic to the particular events in a year, such as SV outages. This is easily understood when it is recognized that this is the only quantity that does not include averaging.

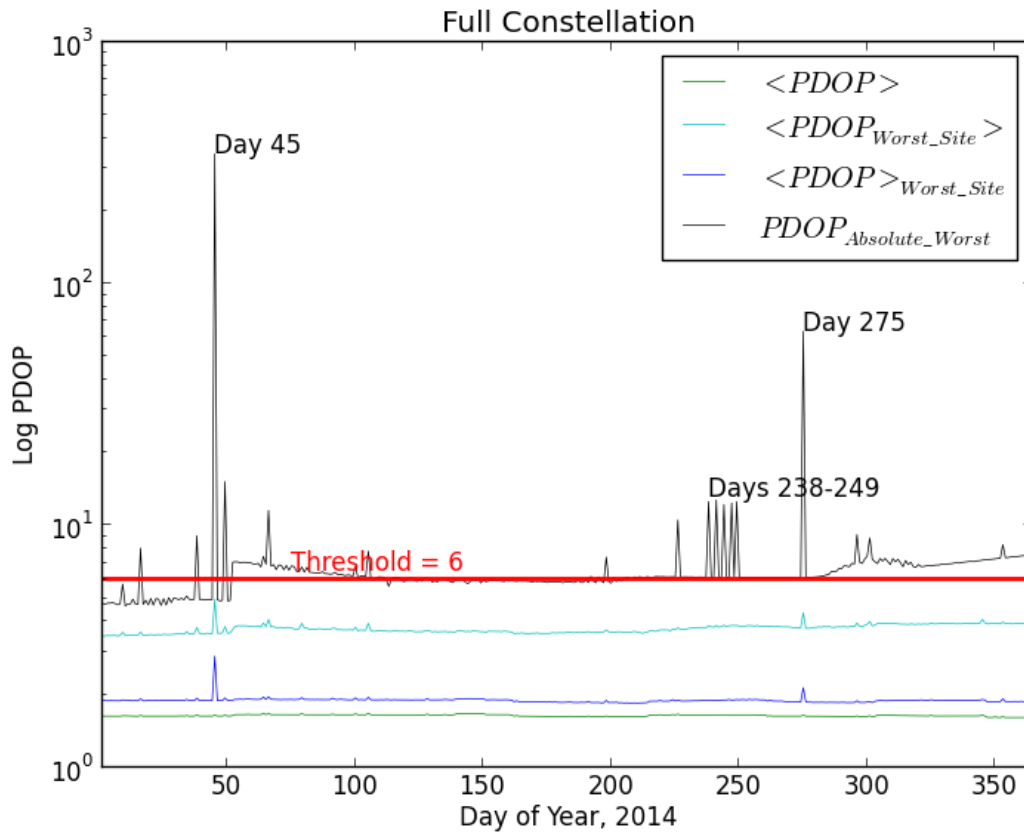


Figure 3.12: Daily PDOP Metrics Using all SVs, 2014

The $PDOP_{abs.worst}$ trace for 2014 shown in Figure 3.12 has several features that were examined in further detail. Four features in particular were selected.

- the sudden rise in $PDOP_{abs.worst}$ on Day 052,
- the spike on Day 045,
- the spike on Day 275, and
- the set of recurring spikes on Days 238-249.

This accounts for all the days on which the $PDOP_{abs.worst}$ rose above 20 and for an interesting pattern that had not been observed in past years.

The trace of $PDOP_{abs.worst}$ begins the year a little below 5 and stays near that value until Day 052 when the trace moves up near 6 and remains there for the remainder of the year. Day 052 corresponds to the decommissioning of SVN 36, so this change is likely related changes in visibility as that satellite is removed from consideration.

The spike on Day 045 was caused by an unhealthy satellite. The maximum PDOP value found was 344. The spike was very limited in both area and time: it occurred for

a single time point and the total number of grid points for which PDOP exceeded 6 was limited to seven (7). The situation is illustrated in Figure 3.13. This plot shows a polar projection looking down at the earth over the time-location at which the $PDOP_{abs. worst}$ occurred. The satellite locations at the time of the $PDOP_{abs. worst}$ are shown as circles labeled with PRN number. The thick green lines illustrate the path of the SV for the preceding 15 minutes. The thin blue lines are the projection of the SV path for the next 15 minutes. The circle and track for PRN 2 are labeled in red to indicate that this SV is transmitting an unhealthy indication during this time.

Since PRN 2 is unhealthy, it is not included in the PDOP analysis. That leaves only four SVs above five degrees elevation at this location. DOP is a measure of geometric diversity. While emphasis is sometimes given to diversity in azimuth, diversity in elevation is also important. In this case, the four lines of sight are all above 30 degrees elevation, leaving no low-elevation lines of sight. PRN 28 and PRN 15 have just left visibility for this location and PRN 10, PRN 14, and PRN 25 will be visible very shortly. Taken together, the health status of PRN 2 and the very transient period with only four SVs visible explain this spike.

The spike on Day 275 was caused by a pair of unhealthy satellites. The maximum PDOP value found was 64. The spike was limited in both time and area: it occurred for a single time point and the total number of grid points for which PDOP exceeded 6 was limited to 38. The situation is illustrated in Figure 3.14. This figure is similar in construction to Figure 3.13. Both PRN 3 and PRN 25 are unhealthy, leaving only four SVs visible at the location that experienced the peak. PRN 12 and PRN 24 had just left visibility and PRN 16 was about to become visible. The health status of two SVs and the very transient period with only four SVs visible explain this spike.

The repeated spikes for the period from Day 238 to Day 249 are an unusual pattern. Examination of the times and locations for these spikes revealed that they were in different locations located 180 degrees apart in longitude and that the characteristic times for the two locations were separated by 12 hours. In addition, the duration of the spikes are limited to something less than a minute.

The fact that the high DOP period lasts less than a minute is the root cause of the pattern. The DOP analysis is conducted on a five minute interval. The GPS satellite ground tracks advance roughly four minutes a day. Therefore, a spike in the plot is seen when the brief high DOP period overlaps a five minute evaluation point. The next day, the ground tracks will have advanced four minutes, and the high DOP period will no longer be aligned with the five minute evaluation period; however, in a few days it will align once more. Put another way, if the high DOP period lasted at least five minutes, the result on Figure 3.12 would have been a “plateau” from Day 238-249. Instead, the figure shows an up/down pattern as the brief high DOP period passes in and out of alignment with the five minute evaluation period.

That subjective description doesn't explain why the effect started and stopped. In order to determine a cause, it was necessary to determine exactly what satellites were involved and how the satellite geometry changed over time. This is illustrated in the time-sequence of plots shown in Figure 3.15. Figure 3.15(a) illustrates the situation on

Day 236 at the location of the spike of Day 238, but with a time 8 minutes later in the day (roughly corresponding to the daily ground track precession). In this geometry, there was no spike. There are 5 satellites visible at or above five degrees elevation: PRN 5, PRN 16, PRN 21, PRN 25, and PRN 29. When the numerical data are examined PRN 25 is at exactly 5.0 degrees and setting.

Figure 3.15(b) illustrates the situation on Day 238 at the location and time of the spike. All the satellites except PRN 25 are in identical locations. However, PRN 25 has shifted slightly and is now at 4.5 degrees elevation, so it is below the threshold to be counted in the DOP calculation.

Figure 3.15(c) and Figure 3.15(d) illustrate two more of the DOP spike cases. Note that near the bottom of the chart PRN 8 is slowly shifting its location. On Day 244 at 17:45 PRN 8 was at 2.8 degrees relative to the location of interest. By Day 249 at 17:25 PRN 8 was at 4.8 degrees relative to the same point. Before the spike recurring again, PRN 8 had drifted just enough to be counted in the DOP calculation. This removed the cause of the pattern that produced the spikes in the range of Day 238-249.

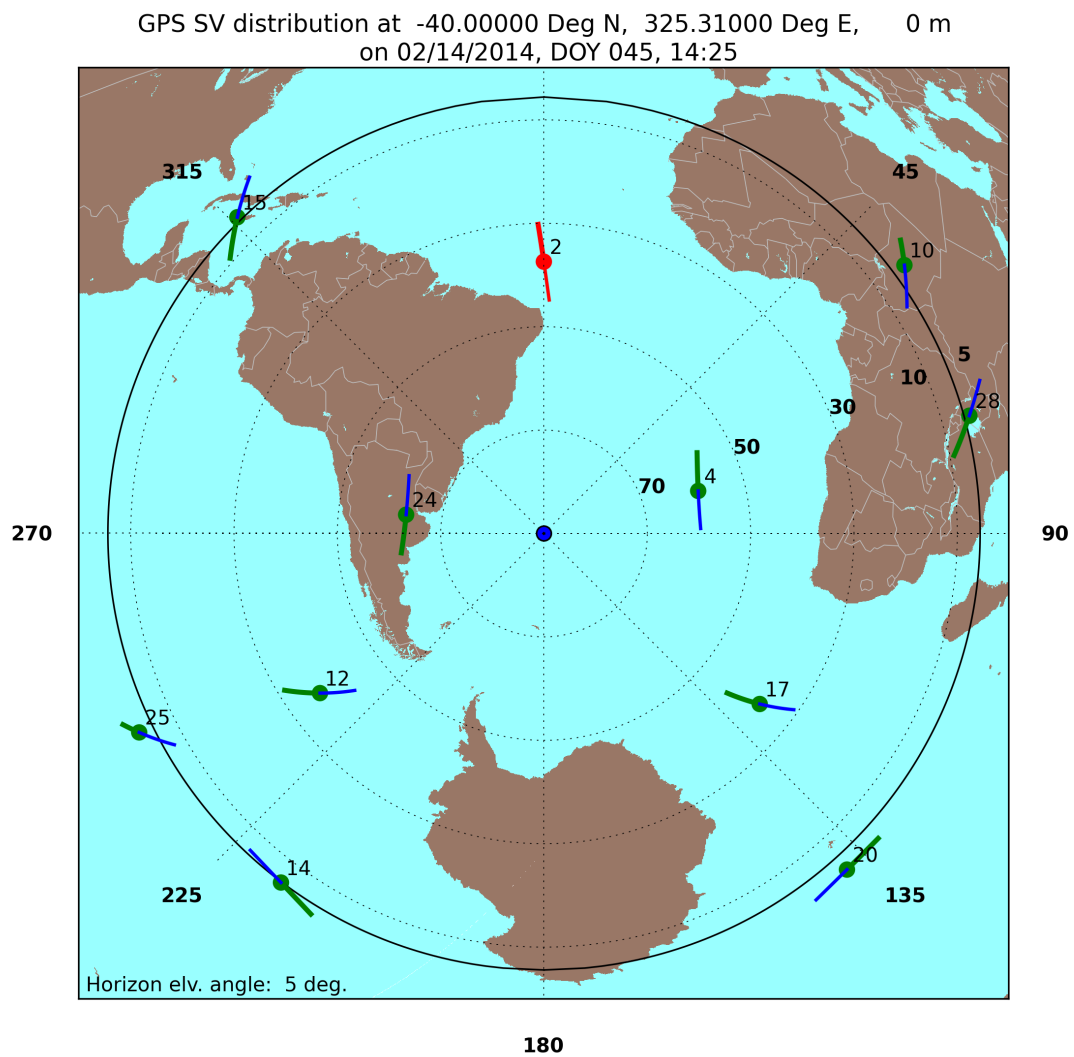


Figure 3.13: GPS Visibility on Day 045 at 14:25 Relative to 40S, 325.31E

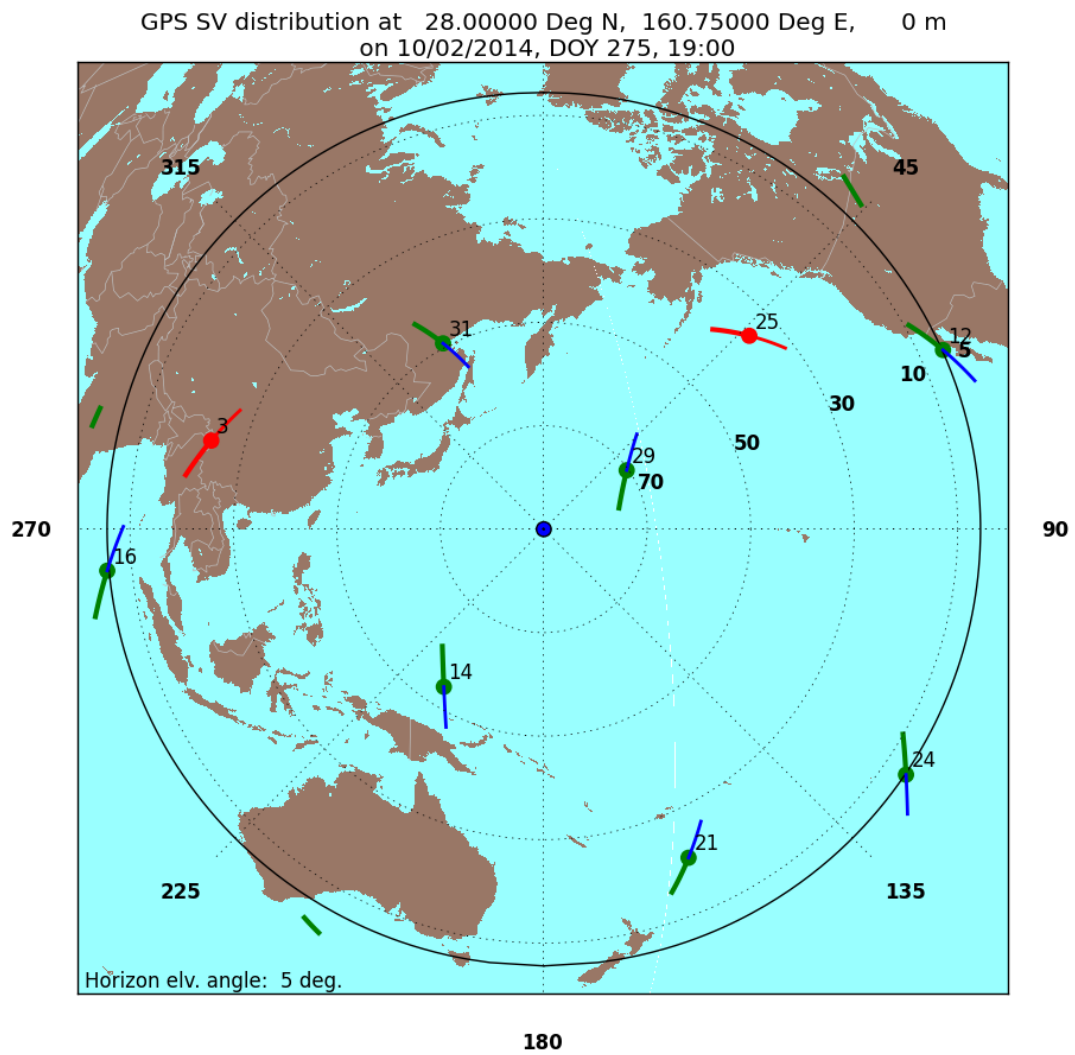
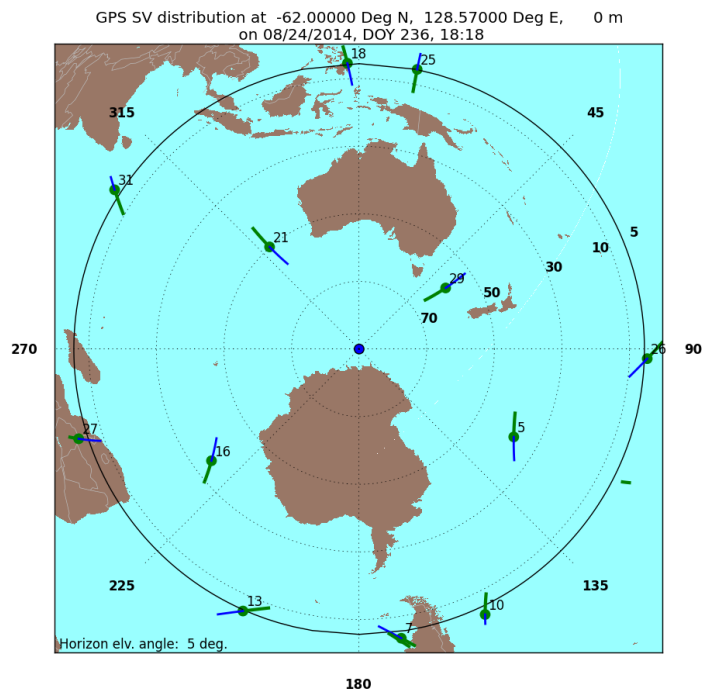
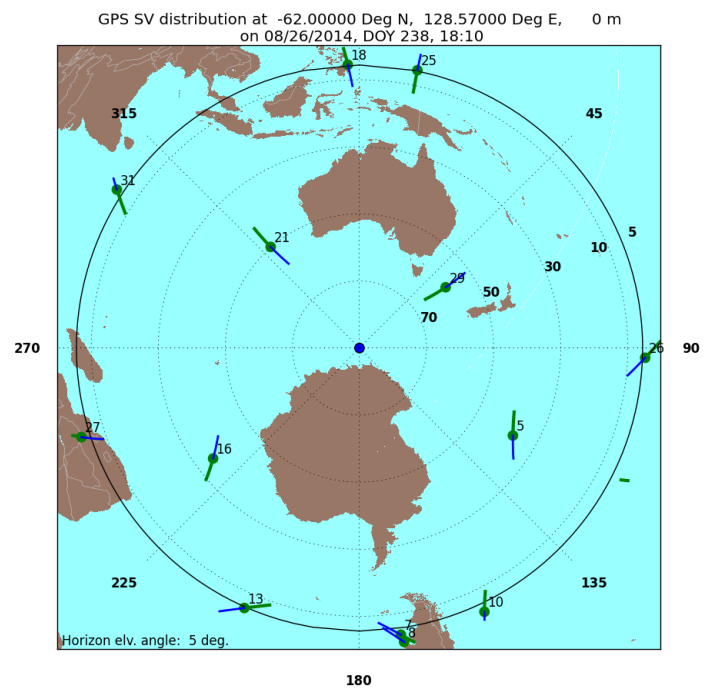


Figure 3.14: GPS Visibility on Day 275 at 19:00 Relative to 28N, 160.75E

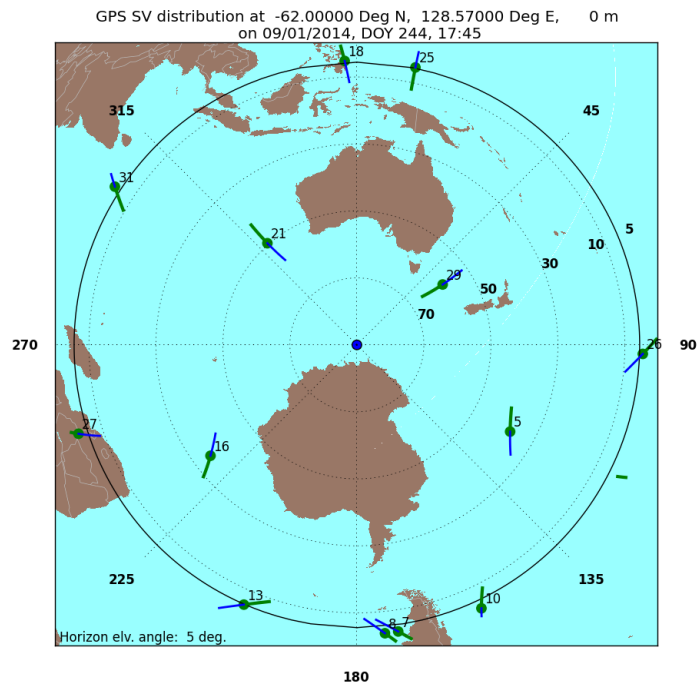


(a) Day 236 at 18:18 Relative to 62S, 128.57E

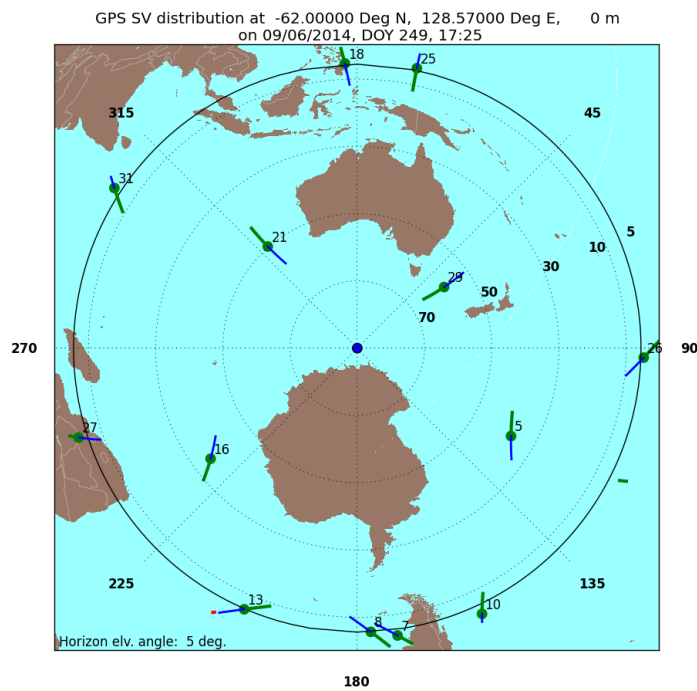


(b) Day 238 at 18:10 Relative to 62S, 128.57E

Figure 3.15: Time History of SV Visibility at DOP Spike Location.



(c) Day 244 at 17:45 Relative to 62S, 128.57E



(d) Day 249 at 17:25 Relative to 62S, 128.57E

Figure 3.15: Time History of SV Visibility at DOP Spike Location.

3.5.3 Position Service Availability

The positioning and timing availability standards are stated in Table 3.8-2 of SPSPS08 as follows:

- “ $\geq 99\%$ Horizontal Service Availability, average location”
- “ $\geq 99\%$ Vertical Service Availability, average location”
- “ $\geq 90\%$ Horizontal Service Availability, worst-case location”
- “ $\geq 90\%$ Vertical Service Availability, worst-case location”

The conditions and constraints associated with the standards include the specification of a 17 m horizontal 95th percentile threshold and a 37 m vertical 95th percentile threshold.

These are derived values as described in the sentence preceding SPSPS08 Table 3.8-2:

“The commitments for maintaining PDOP (Table 3.8-1) and SPS SIS URE accuracy (Table 3.4-1) result in support for position service availability standards as presented in Table 3.8-2.”

Because the commitments for PDOP and constellation SPS SIS URE have not only been met, but exceeded, this assertion in the SPSPS08 implies that the position and timing availability standards have also been fulfilled. A direct assessment of these metrics was not undertaken.

3.5.4 Position Accuracy

The positioning accuracy standards are stated in Table 3.8-3 of SPSPS08 as follows:

- “ ≤ 9 m 95% Horizontal Error Global Average Position Domain Accuracy”
- “ ≤ 15 m 95% Vertical Error Global Average Position Domain Accuracy”
- “ ≤ 17 m 95% Horizontal Error Worst Site Position Domain Accuracy”
- “ ≤ 37 m 95% Vertical Error Worst Site Position Domain Accuracy”

These are derived values as described in the sentence preceding SPSPS08 Table 3.8-3:

“The commitments for maintaining PDOP (Table 3.8-1) and SPS SIS URE accuracy (Table 3.4-1) result in support for position service availability standards as presented in Table 3.8-3.”

Because the commitments for PDOP and constellation SPS SIS URE have been met and exceeded, then the position and timing accuracy standards have also been fulfilled.

While this answer is technically correct, it is not very helpful. Position accuracy is the primary reason that GPS exists. At the same time, position accuracy is a particularly difficult metric to evaluate due to the fact that GPS provides the SIS, but the user is responsible for appropriately processing the SIS to derive a position.

Section 2.4.5 of SPSPS08 provides usage assumptions for the SPS PS and some of the notes in Section 2.4.5 are relevant to the question of position determination. The following is quoted from section 2.4.5:

“The performance standards in Section 3 of this SPS PS do not take into consideration any error source that is not under direct control of the Space Segment or Control Segment. Specifically excluded errors include those due to the effects of:

- *Signal distortions caused by ionospheric and/or tropospheric scintillation*
- *Residual receiver ionospheric delay compensation errors*
- *Residual receiver tropospheric delay compensation errors*
- *Receiver noise (including received signal power and interference power) and resolution*
- *Multipath and receiver multipath mitigation*
- *User antenna effects*
- *Operator (user) error”*

In addition, at the beginning of Section 3.8, the SPSPS08 explains that in addition to the error exclusions listed in 2.4.5, the following assumptions are made regarding the SPS receiver:

“The use of a representative SPS receiver that:

- *is designed in accordance with IS-GPS-200*
- *is tracking the SPS SIS from all satellites in view above a 5° mask angle... It is assumed the receiver is operating in a nominal noise environment...*
- *accomplishes satellite position and geometric range computations in the most current realization of the WGS 84 Earth-Centered, Earth-Fixed (ECEF) coordinate system.*
- *generates a position and time solution from data broadcast by all satellites in view*

- *compensates for dynamic Doppler shift effects on nominal SPS ranging signal carrier phase and C/A code measurements.*
- *processes the health-related information in the SIS and excludes marginal and unhealthy SIS from the position solution.*
- *ensures the use of up-to-date and internally consistent ephemeris and clock data for all satellites it is using in its position solution.*
- *loses track in the event a GPS satellite stops transmitting a trackable SIS.*
- *is operating at a surveyed location (for a time transfer receiver)."*

ARL:UT adopted the following approach for computing a set of accuracy statistics:

1. 30 s GPS observations were collected from the NGA GPS monitor station network and a similar set of 18 IGS stations. This decision addressed the following concerns.
 - (a) All stations selected collect dual-frequency observations. Therefore the first-order ionospheric effects can be eliminated from the results.
 - (b) All stations selected collect weather observations. The program that generates the positions (PRSOLVE) uses the weather data to eliminate first order tropospheric effects.
 - (c) The receiver thermal noise will not be eliminated, but both the NGA and IGS stations are generally using the best available equipment, so effects will be limited.
 - (d) Similarly, multipath cannot be eliminated, but both networks use antennas designed for multipath reduction, and station sites are chosen to avoid the introduction of extraneous multipath.
 - (e) Antenna phase center locations for such stations are very well known. Therefore, position truth is readily available.
2. Process the data using a comprehensive set of broadcast ephemerides that have been checked for consistency. The set of ephemerides used in the URE studies described in Section 3.1 of this report had already been extensively tested and examined. They constitute a complete (or very nearly complete) set of the broadcast ephemeris available for 2014.
3. Process the collected observations using the PRSOLVE program of the ARL:UT-hosted open source GPS Toolkit (GPSTk)[9].
 - (a) PRSOLVE meets the relevant requirements listed above. For example, SV positions are derived in accordance with IS-GPS-200, the elevation mask is configurable, weather data is used to estimate tropospheric effects, and WGS 84 [10] conventions are used. Data from unhealthy SVs was removed from PRSOLVE using an option to exclude specific satellites.

- (b) PRSOLVE is highly configurable. Several of the items in the preceding list of assumptions are configuration parameters to PRSOLVE.
 - (c) Any other organization that wishes to reproduce the results should be able to do so. (Both the algorithm and the IGS data are available.)
4. Process the collected 30 s observations in two ways.
- (a) Use all SVs in view without data editing in an autonomous pseudorange solution to generate 30 s position residuals at all sites.
 - (b) Use a simple receiver autonomous integrity monitoring (RAIM) algorithm (another PRSOLVE option) to remove outlier pseudorange measurements from which a “clean” set of 30 s position residuals is generated at all sites. The RAIM algorithm used by PRSOLVE is dependent on several parameters, the two most important of which are the RMS limit on the post-fit residuals (default: 3.0 m), and the number of SVs that can be eliminated in the RAIM process (default: unlimited). This analysis was conducted using the default values.
5. Compute statistics on each set of data independently.

In contrast to previous years, we conducted the elevation angle processing with a 5° minimum elevation angle for greater agreement with the standard. (Previous years were processed with a 10° minimum elevation angle.)

This process yields four sets of results organized as detailed in Table 3.12.

Table 3.12: Organization of Positioning Results

Case	Constellation Considered	Data Editing Option	Data Source
1	All in View	RAIM	IGS Data
2			NGA Data
3		None	IGS Data
4			NGA Data

Once the solutions are computed, two sets of statistics are developed. The first set is a set of daily average values across all stations. In the second set, the worst site is determined on a day-to-day basis and the worst site 95th percentile values are computed.

These are empirical results and should not be construed to represent a proof that the metrics presented in the standard have been met. Instead, they are presented as a means of corroboration that the standards have been met through the fulfillment of the more basic commitments of PDOP and SPS SIS URE.

3.5.4.1 Results for Daily Average

Using the approach outlined above, position solutions were computed at each 30 s interval for data from both the NGA and IGS stations. In the nominal case in which all

stations are operating for a complete day, this yields 2880 solutions per station per day. Truth positions for the IGS stations were taken from the weekly Station Independent Exchange format (SINEX) files. Truth locations for the NGA stations were taken from station locations defined as part of the latest WGS84 adjustment with corrections for station velocities applied.

Residuals between estimated locations and the truth locations were computed (using PRSOLVE options) in the form of North, East and Up components in meters. The horizontal residual was computed from the North and East components, and the vertical residual was computed from the absolute value of the Up component. As a result, the residuals will have non-zero mean values. The statistics on the residuals were compiled across all stations in a set for a given day. Figure 3.16 through Figure 3.19 show the daily average for the horizontal and vertical residuals corresponding to the options shown in Table 3.12.

The statistics associated with the processing are provided in Table 3.13 through Table 3.16. There is one table each for the mean, median, maximum, and standard deviation of the daily values across 2014. The results are organized in this fashion to facilitate comparison of the same quantity across the various processing options. The results are expressed to the centimeter level. This choice of precision is based on the fact that the truth station positions are known only at the few-centimeter level.

The following general observations may be drawn from the charts and the supporting statistics:

- Outliers - Figure 3.17 shows a number of large outliers for the IGS averages computed with a simple pseudorange solution and no data editing. The outliers are distributed among several stations. These outliers are missing from Figure 3.16. This indicates the importance of conducting at least some level of data editing in the positioning process.
- Mean & Median values - The means and medians of the position residuals given in Table 3.13 and Table 3.14 are nearly identical for the NGA data sets, suggesting that if there are any 30 s position residual outliers, they are few in number and not too large. This also holds true for the RAIM solutions from the IGS data sets. However, the means and medians for the IGS data set solutions with no data editing are very different. This is consistent with the outliers observed in Figure 3.17 and with the maximum and std. dev. values for the IGS data set solutions. This suggest that there are some large 30 s position residuals in the epoch-by-epoch results for these data sets.

The average magnitude of the position residual as reported in Table 3.13 is slightly smaller for the NGA stations than for the IGS stations. There are a number of differences between the two station sets. The NGA station set is more homogeneous in that the same receiver model is used throughout the data processed for this analysis, the data are derived from full-code tracking, and a single organization prepared all the data sets using a single set of algorithms. By

Table 3.13: Mean of Daily Average Position Errors for 2014

Quantity	Data Source	Position Residual Mean (m)	
		RAIM	No Editing
Horizontal	IGS Data	1.35	8.36
	NGA Data	1.09	1.12
Vertical	IGS Data	2.06	9.91
	NGA Data	1.48	1.54

Table 3.14: Median of Daily Average Position Errors for 2014

Quantity	Data Source	Position Residual Median (m)	
		RAIM	No Editing
Horizontal	IGS Data	1.34	1.38
	NGA Data	1.08	1.11
Vertical	IGS Data	2.04	2.09
	NGA Data	1.47	1.52

Table 3.15: Maximum of Daily Average Position Errors for 2014

Quantity	Data Source	Position Residual Maximum (m)	
		RAIM	No Editing
Horizontal	IGS Data	1.61	216.81
	NGA Data	1.46	1.46
Vertical	IGS Data	2.65	159.40
	NGA Data	2.19	2.20

Table 3.16: Standard Deviation of Daily Average Position Errors for 2014

Quantity	Data Source	Position Residual Std. Dev. (m)	
		RAIM	No Editing
Horizontal	IGS Data	0.07	20.43
	NGA Data	0.04	0.06
Vertical	IGS Data	0.11	21.56
	NGA Data	0.07	0.10

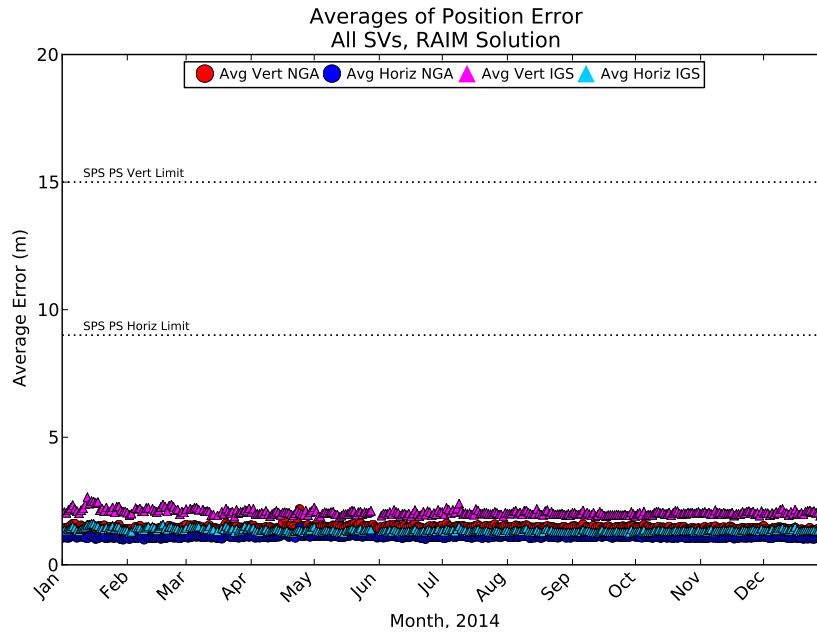


Figure 3.16: Daily averaged position residuals computed using a RAIM solution with default parameters.

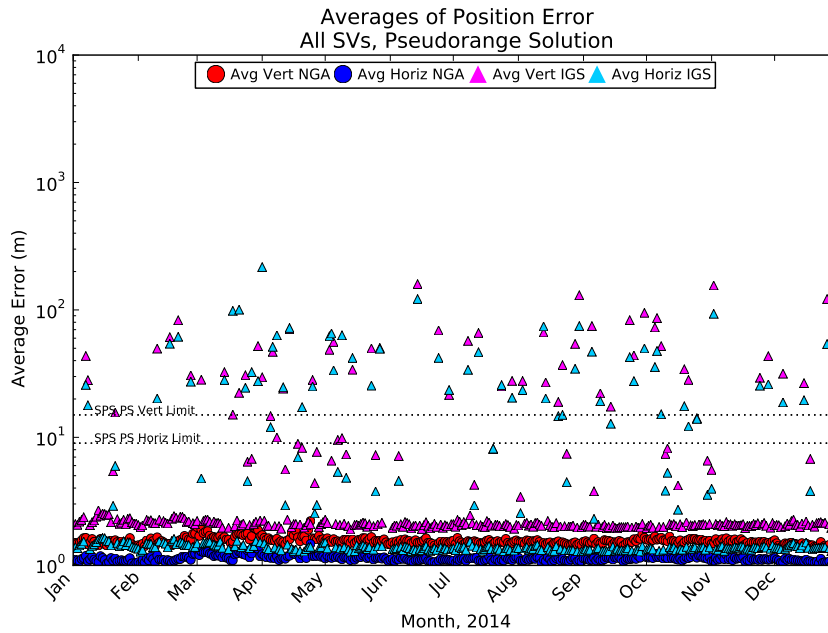


Figure 3.17: Daily averaged autonomous position residuals using no data editing.

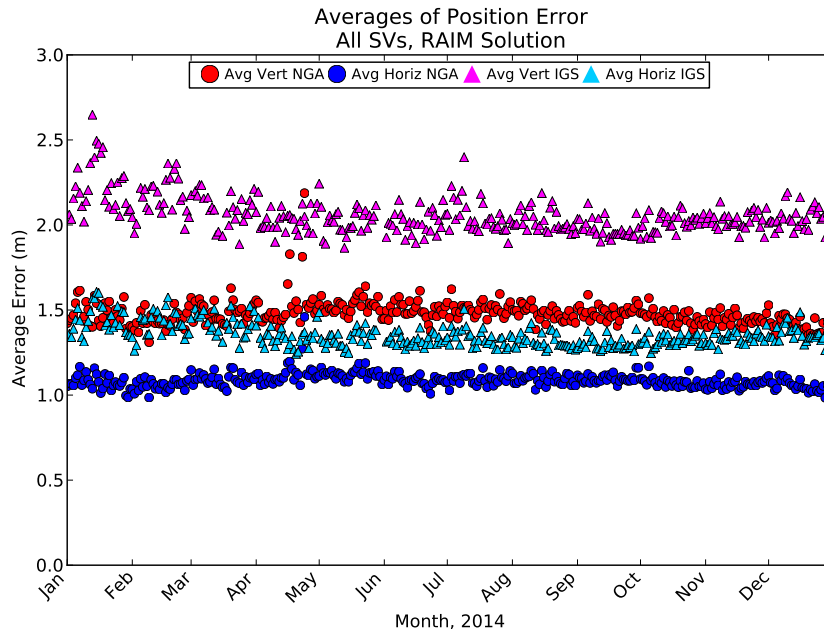


Figure 3.18: Pseudorange residuals for RAIM solution, enlarged to show variation in average residual.

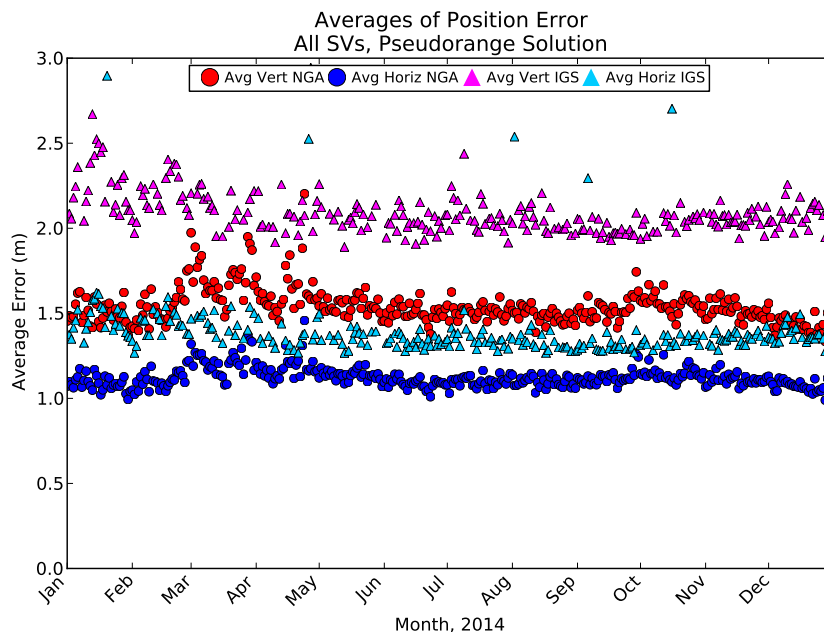


Figure 3.19: The non-edited pseudorange solution, enlarged to show variation in average residual.

contrast, the IGS data sets come from a variety of receivers and were prepared and submitted by a variety of organizations. These differences likely account for the greater variability in the results derived from the IGS data sets.

3.5.4.2 Results for Worst Site 95th Percentile

The edited, and the non-edited, 30 s position residuals were then processed (independently) to determine the worst site 95th percentile values. In this case, the 95th percentile was determined for each station in a given set, and the worst of these was used as the final 95th percentile value for that day. Figure 3.20 and Figure 3.21 show these values for the various processing options described in the previous section. The plots are followed by tables of the statistics for the average, median, maximum, and standard deviation of the daily worst site 95th percentile values. Some general observations on the results are included following the tables.

The statistics associated with the worst site 95th percentile values are provided in Table 3.17 through Table 3.20. There is one table each for the average, median, maximum, and standard deviation of the daily values across 2014. As before, the results are organized in this fashion to facilitate comparison of the same quantity across the various processing options. Precisions are chosen to be at the centimeter level, a choice based on:

- The magnitude of the standard deviation.
- The fact that the station positions are known only at the few-centimeter level.

Most of the observations from the daily averages hold true in the case of the results for the worst site 95th percentile case. However, there are a few additional observations.

- Comparison between processing options - The statistics for the RAIM solutions are slightly better than the statistics for the pseudorange solutions. However, the worst value in Table 3.17 (5.92 m for the vertical position maximum error) is well within the 95th percentile vertical error worst site requirement.
- Autonomous pseudorange vs. RAIM - Figure 3.21 contains a large number of out-of-family values for the solutions derived from the NGA data sets during late March through May. These came from several different stations, so it was not a station-specific effect. Given the RAIM solutions shown in Figure 3.20 do not share this feature, this appears to be another example which illustrates the importance of applying at least some minimal data editing.
- Comparison to threshold - The values for both average and maximum of the worst 95th percentile for both horizontal and vertical errors are well within the standard for both solution types. Compared to the thresholds of 17 m 95th percentile horizontal and 37 m 95th percentile vertical these results are outstanding.

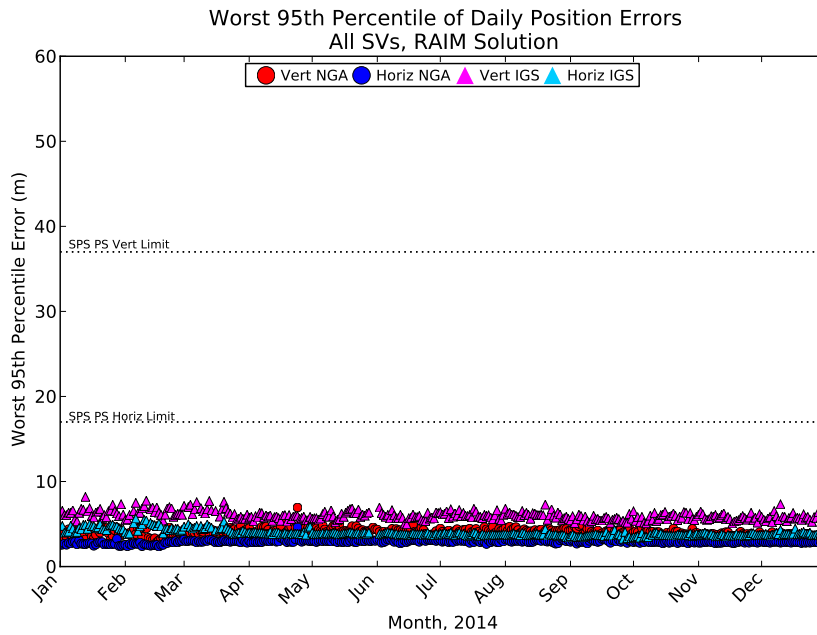


Figure 3.20: Worst site 95th percentile horizontal and vertical residuals for the RAIM Solution. Note that vertical and horizontal limits are not violated.

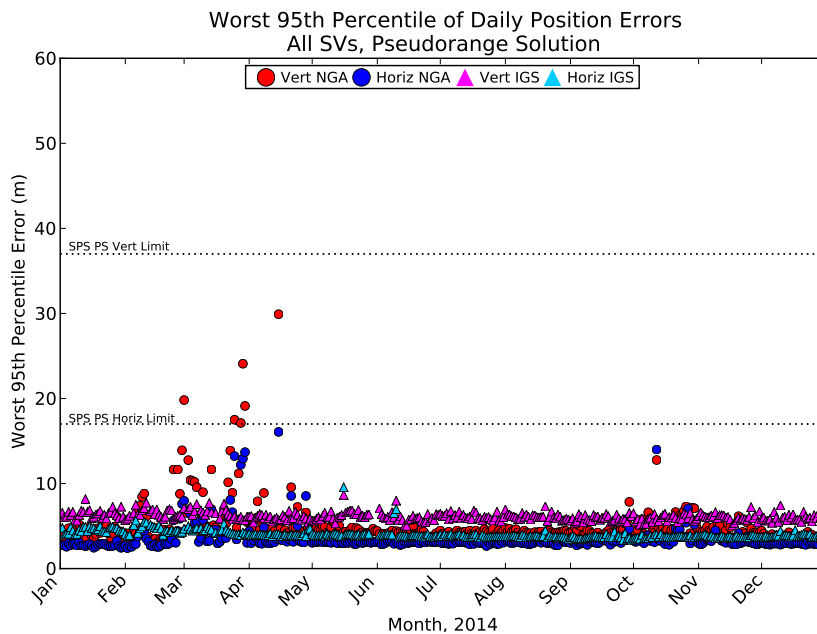


Figure 3.21: Worst site 95th percentile horizontal and vertical residuals. All SVs available, pseudorange solution with no data editing. Note that vertical and horizontal limits are not violated.

Table 3.17: Mean of Daily Worst Site 95th Percentile Position Errors for 2014

Quantity	Data Source	Position Residual Mean (m)	
		RAIM	No Editing
Horizontal	IGS Data	3.81	3.88
	NGA Data	2.92	3.52
Vertical	IGS Data	5.78	5.93
	NGA Data	4.05	5.08

Table 3.18: Median of Daily Worst Site 95th Percentile Position Errors for 2014

Quantity	Data Source	Position Residual Median (m)	
		RAIM	No Editing
Horizontal	IGS Data	3.83	3.88
	NGA Data	2.91	3.10
Vertical	IGS Data	5.90	6.05
	NGA Data	4.06	4.34

Table 3.19: Maximum of Daily Worst Site 95th Percentile Position Errors for 2014

Quantity	Data Source	Position Residual Maximum (m)	
		RAIM	No Editing
Horizontal	IGS Data	5.65	9.56
	NGA Data	4.65	16.07
Vertical	IGS Data	8.19	8.65
	NGA Data	6.94	29.91

Table 3.20: Standard Deviation of Daily Worst Site 95th Percentile Position Errors for 2014

Quantity	Data Source	Position Residual Std. Dev. (m)	
		RAIM	No Editing
Horizontal	IGS Data	0.93	1.00
	NGA Data	0.19	1.60
Vertical	IGS Data	1.30	1.32
	NGA Data	0.42	2.72

Chapter 4

Additional Results of Interest

4.1 Frequency of Different SV Health States

Several of the assertions require examination of the health information transmitted by each SV. We have found it useful to examine the rate of occurrence for all possible combinations of the six health bits transmitted in subframe 1.

Table 4.1 presents a summary of health bit usage in the ephemerides broadcast during 2014. Each row in the table presents a summary for a specific SV. The summary across all SVs are shown at the bottom. The table contains the count of number of times each unique health code was seen, the raw count of unique sets of subframe 1, 2, 3 collected during the year, and the percentage of sets of subframe 1, 2, 3 data that contained specific health codes.

Only two unique health settings were observed throughout 2014: binary 000000_2 (0x00) and binary 111111_2 (0x3F).

4.2 Age of Data

The Age of Data (AOD) represents the elapsed time between the observations that were used to create the broadcast navigation message and the time when the contents of subframes 1, 2, 3 are available to the user to estimate the position of a SV. The accuracy of GPS (at least for users that depend on the broadcast ephemeris) is indirectly tied to the AOD since the prediction accuracy degrades over time (see Section 3.1.1). This is especially true for the clock prediction. It has been recognized that reducing the AOD improves PVT solutions for autonomous users; however, there is an impact in terms of increased operations tempo at 2nd Space Operations Squadron.

Note that there is no need for a GPS receiver to refer to AOD in any position, velocity, or time computation other than the optional application of the navigation message correction table (NMCT). (See IS-GPS-200 Section 20.3.3.5.1.9 for a description of the

Table 4.1: Frequency of Health Codes

SVN	PRN	Count by Health Code		Total # SF 1, 2, 3 Collected	Percent of Time by Health Code		Operational Days for 2014	Avg # SF 1, 2, 3 per Operational Day
		0x3F	0x00		0x3F	0x00		
23	32	3	4755	4758	0.1	99.9	365	13.0
26	26	0	4754	4754	0.0	100.0	365	13.0
33	03	0	2871	2871	0.0	100.0	214	13.4
34	04	14	4763	4777	0.3	99.7	365	13.1
36	06	0	664	664	0.0	100.0	51	13.0
38	08	17	4118	4135	0.4	99.6	303	13.6
39	09	5	1883	1888	0.3	99.7	139	13.6
40	10	4	4899	4903	0.1	99.9	365	13.4
41	14	0	4766	4766	0.0	100.0	365	13.1
43	13	9	4756	4765	0.2	99.8	365	13.1
44	28	0	4826	4826	0.0	100.0	365	13.2
45	21	4	4762	4766	0.1	99.9	365	13.1
46	11	0	4770	4770	0.0	100.0	365	13.1
47	22	4	4797	4801	0.1	99.9	365	13.2
48	07	4	4762	4766	0.1	99.9	365	13.1
50	05	4	4761	4765	0.1	99.9	365	13.1
51	20	8	4755	4763	0.2	99.8	365	13.0
52	31	4	4763	4767	0.1	99.9	365	13.1
53	17	4	4771	4775	0.1	99.9	365	13.1
54	18	0	4766	4766	0.0	100.0	365	13.1
55	15	4	4760	4764	0.1	99.9	365	13.1
56	16	5	4755	4760	0.1	99.9	365	13.0
57	29	0	4765	4765	0.0	100.0	365	13.1
58	12	7	4758	4765	0.1	99.9	365	13.1
59	19	6	4757	4763	0.1	99.9	365	13.0
60	23	4	4751	4755	0.1	99.9	365	13.0
61	02	4	4755	4759	0.1	99.9	365	13.0
62	25	3	4769	4772	0.1	99.9	365	13.1
63	01	6	4769	4775	0.1	99.9	365	13.1
64	30	3	2814	2817	0.1	99.9	216	13.0
65	24	4	4825	4829	0.1	99.9	365	13.2
66	27	0	4764	4764	0.0	100.0	365	13.1
67	06	4	2666	2670	0.1	99.9	205	13.0
68	09	12	1375	1387	0.9	99.1	106	13.1
69	03	13	251	264	4.9	95.1	20	13.2
Total		160	145496	145656	0.1	99.9	365	399.1

NMCT.) It is computed here to validate that the operators are not modifying the operational tempo in order to maintain the URE accuracy described in Section 3.1.

The average AOD throughout 2014 is shown in the following table, along with values for the previous four years. The 2014 values for Block IIR, IIR-M and IIF SVs are nearly unchanged from 2012, while the average AOD for Block IIA SVs has recovered somewhat from a drop in 2012. The daily average AOD for the constellation and for each block is illustrated in the following figure. The AOD appears to be generally constant throughout 2014, which indicates that any variations in the URE results discussed earlier are not due to changes in operations tempo at 2 SOPS.

Table 4.2: Age of Data of the Navigation Message by SV Type

	Average Age of Data (hours)					
	2009	2010	2011	2012	2013	2014
Full Constellation	11.7	11.6	11.6	11.3	11.5	11.6
Block II/IIA	11.5	11.5	11.4	10.3	10.9	11.2
Block IIR/IIR-M	11.8	11.8	11.7	11.7	11.8	11.8
Block IIF	-	12.2	12.0	11.5	11.5	11.5

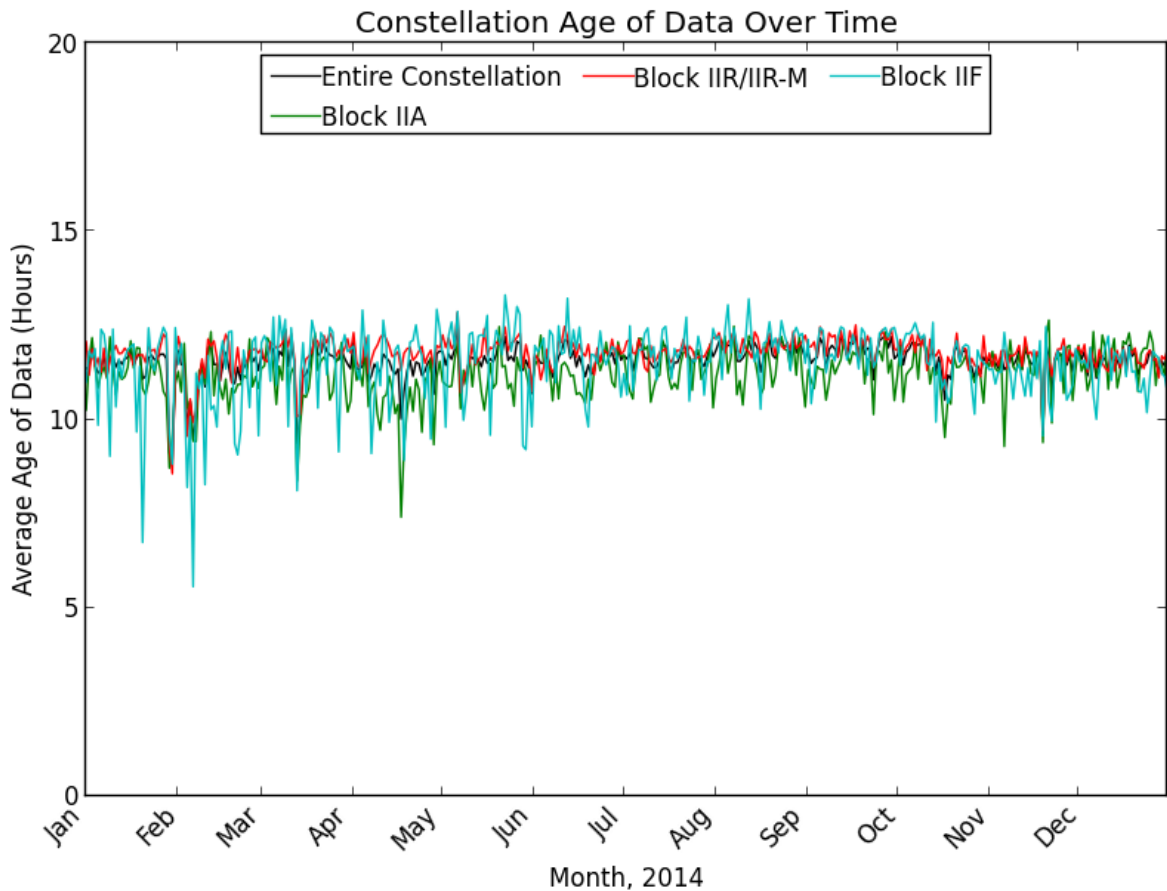


Figure 4.1: Constellation Age of Data for 2014

It is worth noting that the AOD for the Block II/IIA satellites is consistently slightly lower than that for the Block IIR/IIR-M and Block IIF satellites. This can be corroborated by reviewing the rightmost column on Table 4.1. This column shows the average number of unique sets of Subframe 1, 2, 3 data broadcast each day for each satellite. For the newer satellites, this value is typically 13.0 or 13.1. The number 13 comes about due to the fact that there would be 12 two-hour transmission periods in each day if one simply counts the number of two-hour periods in a day. However, when new navigation message data is uploaded, the cutover occurs within a two-hour interval, with the effect of adding a 13th unique set of navigation message data. Looking at the rightmost column of Table 4.1 to the lower SVN numbers, hence for older satellites, it can be seen that several of these satellites have slightly higher values for the average number of unique sets of Subframe 1, 2, 3 per day. These slightly higher values imply less time between uploads, and therefore slightly lower AOD values.

The AOD values (in both this section and in Section 3.1.1) were calculated by examination of the broadcast ephemeris and not by any information provided from the MCS. The method of calculation is described here to allow other organizations to independently repeat this analysis. As mentioned earlier, such an analysis is only relevant to a performance assessment such as this report. There is no operational reason that a GPS receiver needs to refer to AOD in any position, velocity, or time computation.

The AOD may be calculated by finding the upload times based on the t_{oe} offsets as defined in IS-GPS-200 Section 20.3.4.5 and then examining the t_{nmct} assuming.

- A complete set of the subframe 1, 2, 3 data broadcast by all SVs of interest is available throughout the time period of interest.
- The term t_{nmct} defined in IS-GPS-200 Section 20.3.3.4.4 represents the time of the Kalman state used to derive the corresponding navigation message.

Given these assumptions, the AOD at any point in time can be determined by

- work backward from the time of interest to finding the time when the most recent preceding upload was first broadcast,
- find the AOD offset (AODO) of the associated subframe 2,
- subtract the AODO from the t_{oe} (as described in IS-GPS-200 20.3.3.4.4) to determine the time of the Kalman state parameters, and
- calculate the difference between the time of interest and the Kalman state parameter time.

The search for the preceding upload is necessary because the AODO has a limited range and is not sufficiently large to maintain an accurate count for a complete upload cycle.

The results of this algorithm are generally consistent with the results provided by MCS analysis. The first assumption is fulfilled by the NGA MSN archive. The remaining assumptions were discussed with systems engineers supporting 2 SOPS and are believed to be valid with one possible exception.

That exception concerns the AODO value. The original motivation for the AODO value was to provide timing information for the Navigation Message Correction Table (NMCT). The AODO is defined in IS-GPS-200 Section 20.3.3.4.1 para. 6. The application of the AODO is described in IS-GPS-200 Section 20.3.3.4.4. Both of these definitions are in relation to use of the AODO as part of the NMCT process. IS-GPS-200 is unclear whether the AODO parameter will be set as described in 20.3.3.4.1 and 20.3.3.4.4 if the NMCT is not provided in the broadcast navigation message. The fact that AODO is only defined and described in terms of its relationship to NMCT may indicate that a decision to turn off NMCT would result in an undetermined state for the AODO value. Underscoring this concern, this approach cannot be used for PRN 32. Since PRN 32 cannot have a valid NMCT (IS-GPS-200 20.3.3.5.1.9), the AODO term is not reset with an upload but is always set to the “all ones” condition.

This analysis indicates that there are uses for the AODO parameter beyond the original application to NMCT timing. Therefore, it would be useful to maintain the AODO parameter even if the NMCT is not computed and broadcast.

4.3 User Range Accuracy Index Trends

Tables 4.3 and 4.4 present a summary of the analysis of the URA index values throughout 2014. The total number of navigation messages examined differs from the health summary in Section 4.1 because only URA index values corresponding to health settings of 0x00 are included in this analysis. Both the absolute count and the count as a percentage of the total are shown.

The vast majority of the values are 0, 1, or 2 (over 99.9%). Index values of 3 or 4 were very rare.

4.4 Extended Mode Operations

IS-GPS-200 defines Normal Operations as the period of time when subframe 1, 2, 3 data sets are transmitted by the SV for periods of two hours with a curve fit interval of four hours (IS-GPS-200 Section 20.3.4.4). This definition is taken to be the same as the definition of Normal Operations in SPSPS08 for the URE metrics. To determine if any SV operated in other than Normal Operations at any time in 2014, the broadcast ephemerides were examined to determine if any contained fit interval flags set to 1. (See IS-GPS-200 20.3.3.4.3.1 for definition of the fit interval flag.)

Table 4.3: Distribution of URA Index Values

SVN	PRN	URA Index					Total # SF 1, 2, 3 examined	Oper. Days for 2014	Avg # SF 1, 2, 3 per Oper. Day
		4	3	2	1	0			
23	32	1	3	3	294	4454	4755	366	13.0
26	26				478	4276	4754	365	13.0
33	03			144	805	1922	2871	214	13.4
34	04			3	357	4403	4763	365	13.0
36	06				39	625	664	51	13.0
38	08		2	87	1083	2946	4118	303	13.6
39	09			42	557	1284	1883	140	13.4
40	10			163	1535	3201	4899	366	13.4
41	14			148	852	3766	4766	365	13.1
43	13			1	217	4538	4756	365	13.0
44	28				917	3909	4826	365	13.2
45	21		4	2	112	4644	4762	366	13.0
46	11				370	4400	4770	365	13.1
47	22			238	1309	3250	4797	365	13.1
48	07	2	5	5	248	4502	4762	365	13.0
50	05				224	4537	4761	365	13.0
51	20			3	197	4555	4755	365	13.0
52	31			3	186	4574	4763	365	13.0
53	17			2	411	4358	4771	365	13.1
54	18				184	4582	4766	365	13.1
55	15			2	285	4473	4760	366	13.0
56	16			2	270	4483	4755	366	13.0
57	29			1	521	4243	4765	365	13.1
58	12			2	213	4543	4758	365	13.0
59	19	3	5	5	143	4601	4757	365	13.0
60	23	5	2	5	263	4476	4751	365	13.0
61	02			3	130	4622	4755	365	13.0
62	25			4	261	4504	4769	365	13.1
63	01				79	4690	4769	365	13.1
64	30			2	470	2342	2814	216	13.0
65	24		3	4	1074	3744	4825	365	13.2
66	27				181	4583	4764	365	13.1
67	06	1	1	5	172	2487	2666	205	13.0
68	09			3	232	1140	1375	106	13.0
69	03			10	45	196	251	20	12.6
Total		12	25	892	14714	129853	145496	365	398.6

Table 4.4: Distribution of URA Index Values (As a Percentage of All Collected). Values smaller than 0.1 are not shown. Constellation averages are weighted by the number of observations.

SVN	PRN	URA Index				
		4	3	2	1	0
23	32	0.0	0.1	0.1	6.2	93.7
26	26				10.1	89.9
33	03			5.0	28.0	66.9
34	04			0.1	7.5	92.4
36	06				5.9	94.1
38	08		0.0	2.1	26.3	71.5
39	09			2.2	29.6	68.2
40	10			3.3	31.3	65.3
41	14			3.1	17.9	79.0
43	13			0.0	4.6	95.4
44	28				19.0	81.0
45	21		0.1	0.0	2.4	97.5
46	11				7.8	92.2
47	22			5.0	27.3	67.8
48	07	0.0	0.1	0.1	5.2	94.5
50	05				4.7	95.3
51	20			0.1	4.1	95.8
52	31			0.1	3.9	96.0
53	17			0.0	8.6	91.3
54	18				3.9	96.1
55	15			0.0	6.0	94.0
56	16			0.0	5.7	94.3
57	29			0.0	10.9	89.0
58	12			0.0	4.5	95.5
59	19	0.1	0.1	0.1	3.0	96.7
60	23	0.1	0.0	0.1	5.5	94.2
61	02			0.1	2.7	97.2
62	25			0.1	5.5	94.4
63	01				1.7	98.3
64	30			0.1	16.7	83.2
65	24		0.1	0.1	22.3	77.6
66	27				3.8	96.2
67	06	0.0	0.0	0.2	6.5	93.3
68	09			0.2	16.9	82.9
69	03			4.0	17.9	78.1
Constellation Average		0.0	0.0	0.6	10.1	89.2

The analysis found a total of 18 examples of extended operations for satellites set healthy. The examples were distributed across 14 days. The average time of an occurrence was 50 minutes. The minimum duration was 120 seconds and the maximum duration was 2 hours 59 minutes. These results are summarized in Table 4.5.

Given the relative rarity of occurrence, the URE values for the periods summarized in Table 4.5 are included in the statistics presented in Section 3.1.1, even though a strict interpretation of the SPSPS08 would suggest that they be removed. However, the SVs involved were still set healthy and (presumably) being used by user equipment, it is appropriate to include these results to reflect performance seen by the users.

Examination of the ephemerides from past years reveals that 2014 is not an anomaly. Such periods have been found in all years checked (back to 2005), however, the rate of occurrence has been slowly declining and 2014 represents a new low.

Past discussions with the operators have revealed several reasons for these occurrences. Some are associated with Alternate MCS (AMCS) testing. When operations are transitioned from the MCS to the AMCS (and reverse) it is possible that SVs nearing the end of their daily cycle may experience a longer-than-normal upload cycle. Other occurrences may be caused by delays due to ground antenna maintenance or due to operator concentration on higher-priority issues with the constellation at the time.

Table 4.5: Summary of Occurrences of Extended Mode Operations

SVN	PRN	# of Occurrences		Duration (minutes)	
		Healthy	Unhealthy	Healthy	Unhealthy
23	32	1	0	25	0
26	26	1	0	87	0
33	03	1	0	26	0
34	04	1	0	72	0
41	14	2	0	169	0
43	13	1	0	170	0
45	21	1	0	117	0
48	07	2	0	29	0
51	20	1	0	2	0
52	31	1	0	10	0
53	17	1	0	71	0
56	16	1	0	7	0
57	29	1	0	82	0
61	02	1	0	7	0
62	25	1	0	2	0
64	30	1	0	15	0
Totals		18	0	900	0

Appendix A

URE as a Function of Age-of-Data

This appendix contains supporting information for the results presented in Section 3.1.2. The SIS RMS URE vs. AOD charts are presented for each GPS SV. The charts are organized by SV Block and by ascending SVN within each block.

These charts are based on the same set of 30 s Instantaneous RMS SIS URE values used in Section 3.1.1. For each SV, a period of 48 hours was divided into a set of 192 bins, each 15 minutes in duration. An additional bin was added for any AOD that appeared beyond 48 hours. All of the 30 s URE values for the year for a given SV were grouped according to AOD bin. The values in each bin were sorted and the 95th percentile and the maximum were determined. Once the analysis was complete, it was clear that most bins beyond the 26 hour mark contained too few points to be considered statistically relevant. Therefore, when the number of points in a bin falls below 10% of the number of points in most populated bin, the bin is not used for plotting purposes. The problem with bins with low counts is that, in our experience, the results tend to be dominated by one or two very good or very bad observations and this can lead to erroneous conclusions about behavior.

The figures on the following pages each show two curves. The blue curve represents the 95th Percentile SIS RMS URE vs. AOD (in hours). The green curve represents the number of data points that were available to form each URE estimate.

Note that for most SVs, the green curve has a well-defined horizontal plateau that begins near zero AOD, continues for roughly 24 hours, and then drops quickly toward zero. The location of the right-hand drop of the green curve toward zero provides an estimate of the typical upload period for the SV. In cases where the SV is uploaded more frequently, the shape of the green curve will vary reflecting that difference.

A.1 Notes

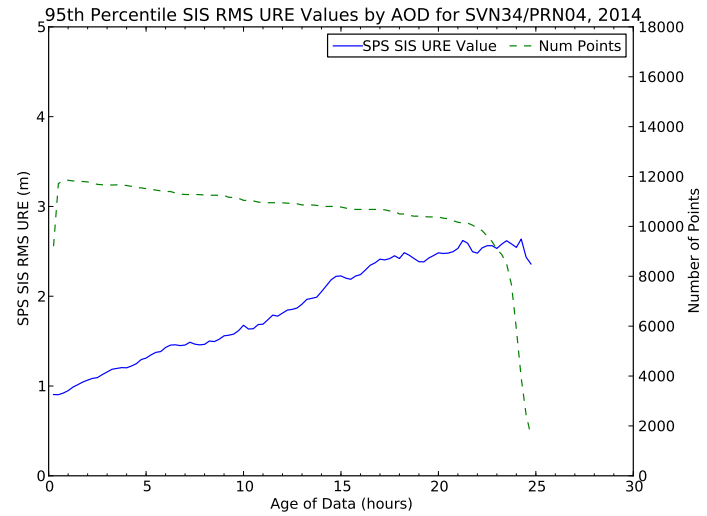
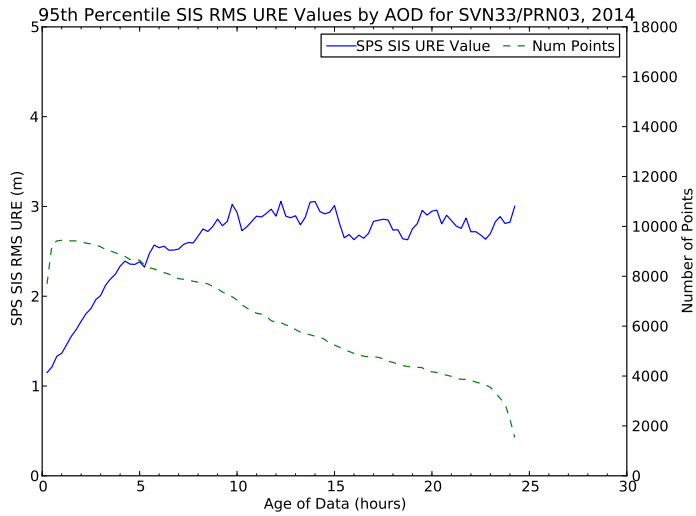
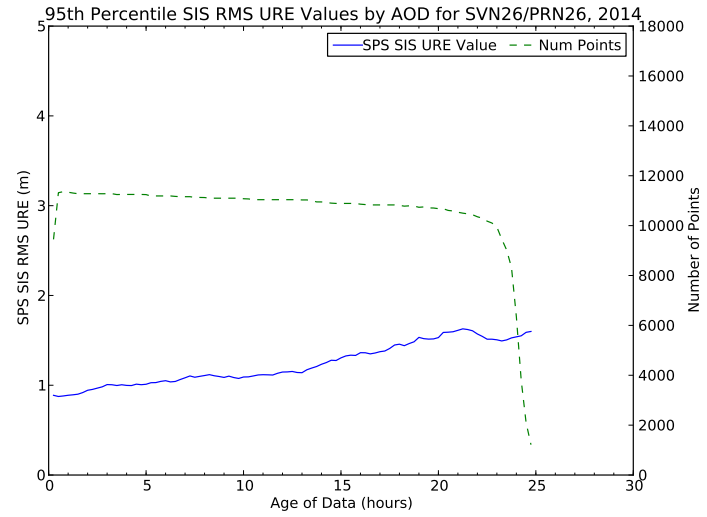
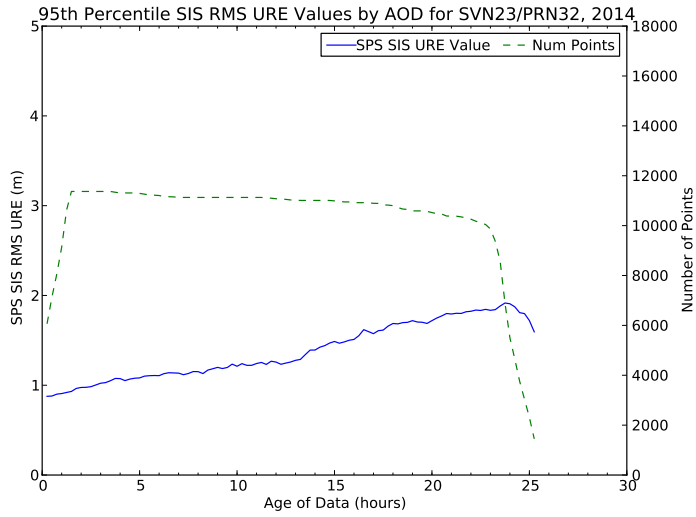
This section contains some notes on SV-specific behavior observed in the following charts.

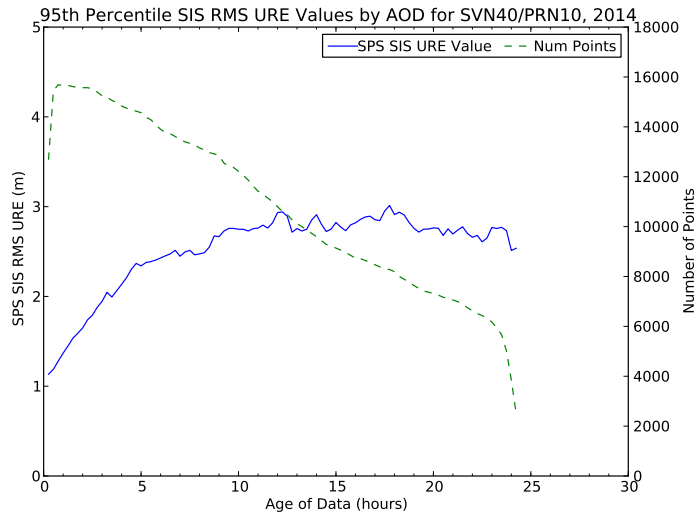
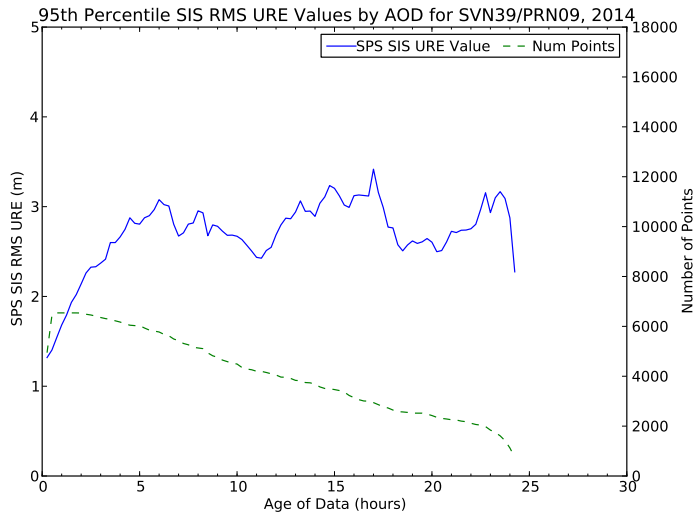
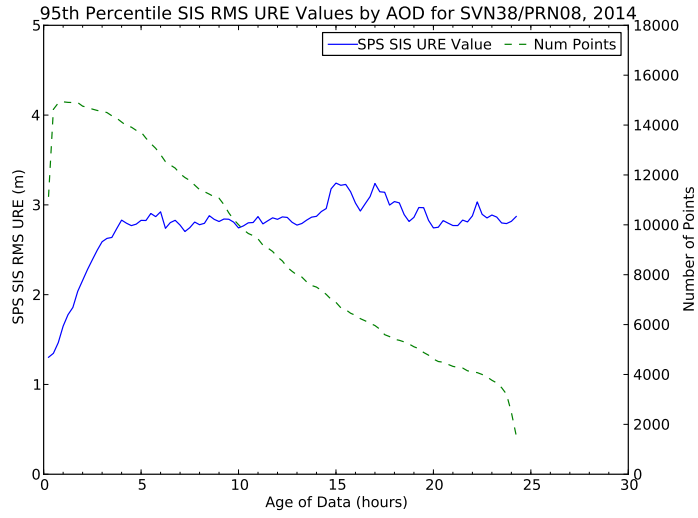
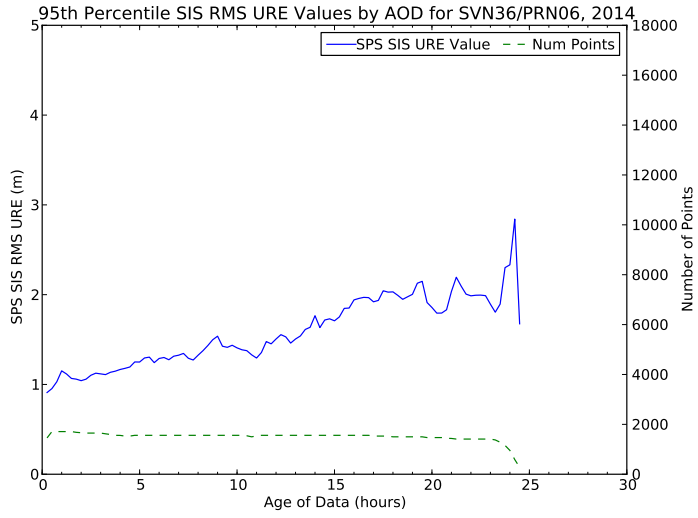
SVN 23/PRN 32: This SV presents a minor problem for this analysis. This problem is limited to the type of performance analysis presented in this report. There is no similar concern for a GPS receiver. The AOD values are based on the AODO field in subframe 2. The definition of the AODO field is tied to how AODO is used to determine the age of the data in the NMCT. Since PRN 32 can never be represented in the NMCT, the AODO field for PRN 32 is never reset to zero at a new upload, but remains at the “all ones” state. Therefore, the AOD for PRN 32 cannot be independently derived from the navigation message data. For the purposes of this plot, we looked at the AODO across the entire constellation and determined the annual average AODO was about 5153 seconds (~ 1.4 hours). We then used this “representative” value as the AODO for SVN 23.

SVN 38/PRN 08: This is the most obvious example of a SV that is being uploaded more frequently than normal. The fact that it is being uploaded more frequently is based on the shape of the dashed green curve which indicates the number of points in each AOD bin. The scale for this curve is on the right-hand vertical axis. The green curve does not exhibit the plateau seen in most plots, but instead has a fairly rapid, near-linear decrease in number of points with AOD after about 2.5 hours. If the SV were consistently being uploaded at a given interval, there would still be a plateau, only shorter than the typical plateau. For example, if an SV were being uploaded every 12 hours, one would expect a plateau from somewhere around an hour AOD out to 12 hours AOD. The near linear trend implies that the upload time for this SV is variable over a fairly large range. Similar effects, but less pronounced, may be seen in the plots for several of the Block IIA SVs.

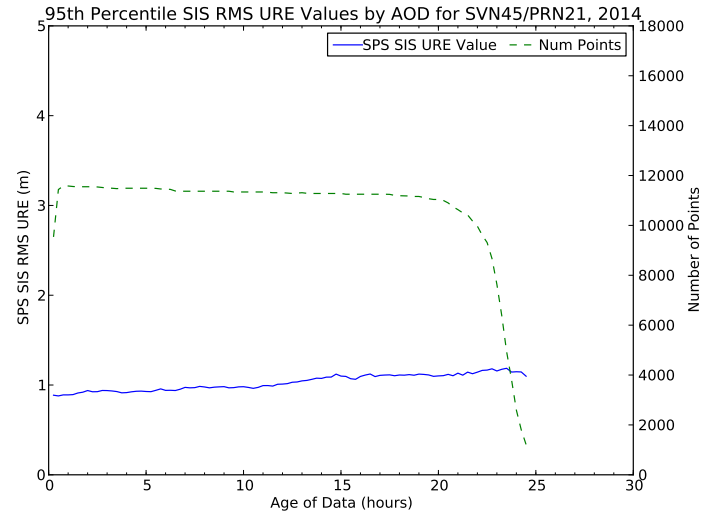
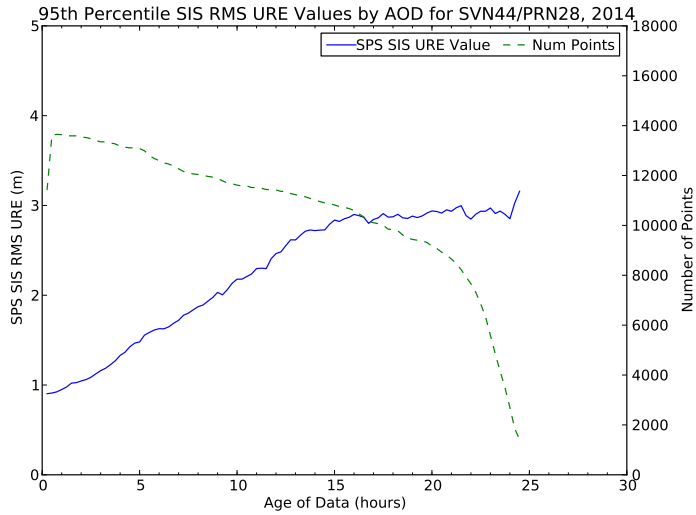
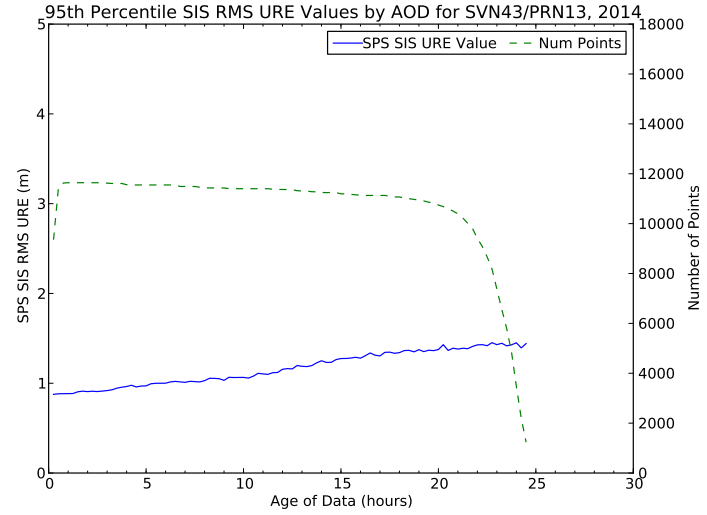
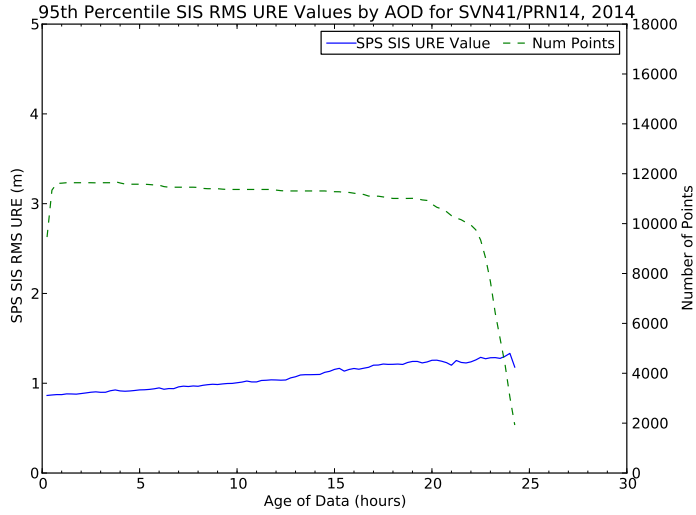
SVN 65/PRN 24: This Block IIF shows indications of occasional contingency uploads. This conclusion is based on the manner in which the SIS URE value line tends to flatten as it approaches the 3 m magnitude and the fact that the number of points starts to decline far earlier than the other Block IIF SVs. This is consistent with the higher 95th percentile URE shown in Table 3.1 and Figure 3.1. It is likely related to the fact that SVN 65/PRN 24 is the only Block IIF that is using a Cesium reference frequency.

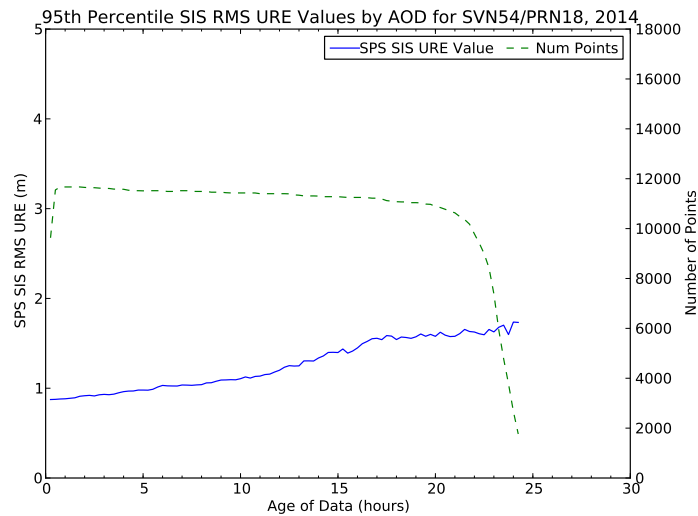
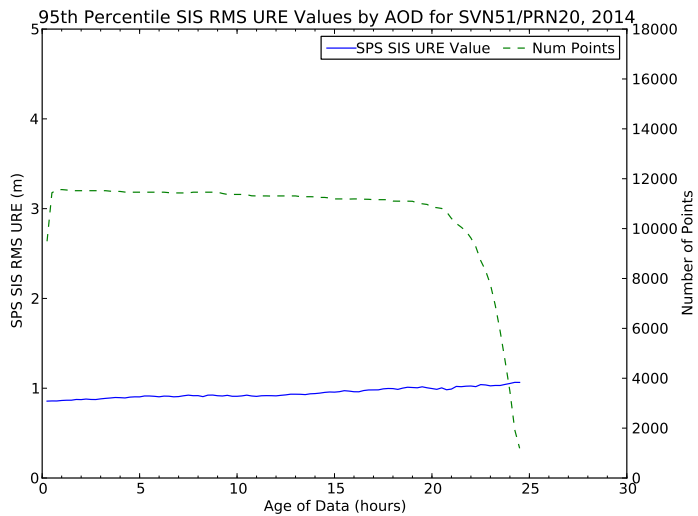
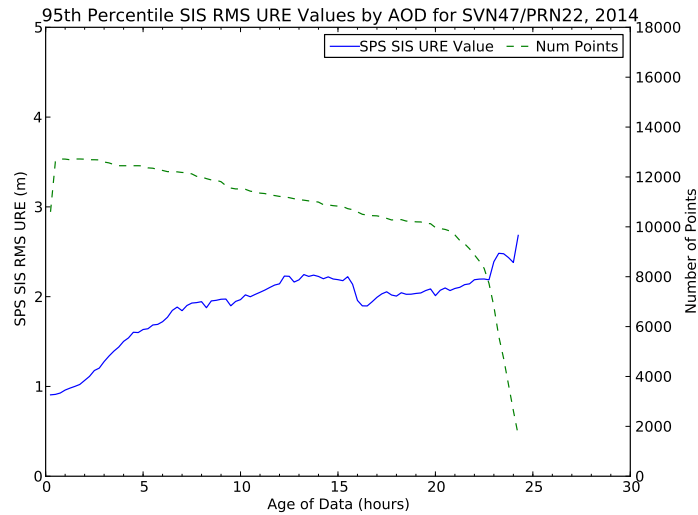
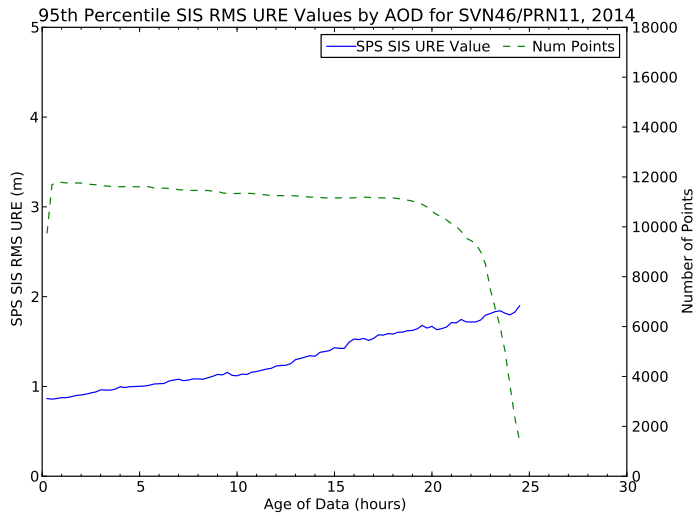
A.2 Block IIA SVs

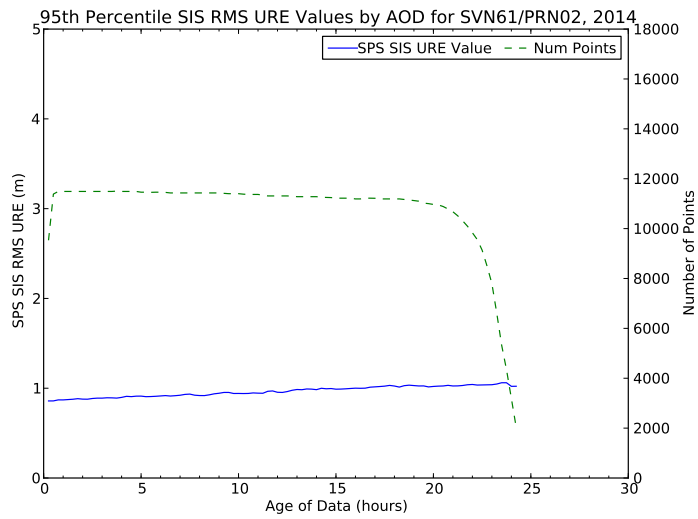
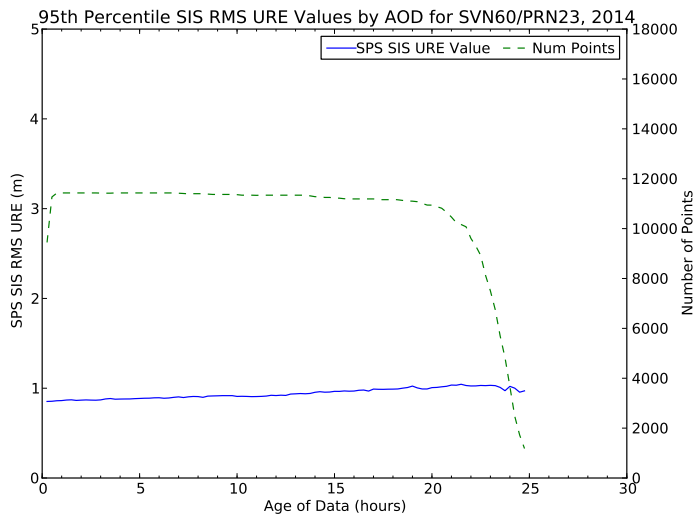
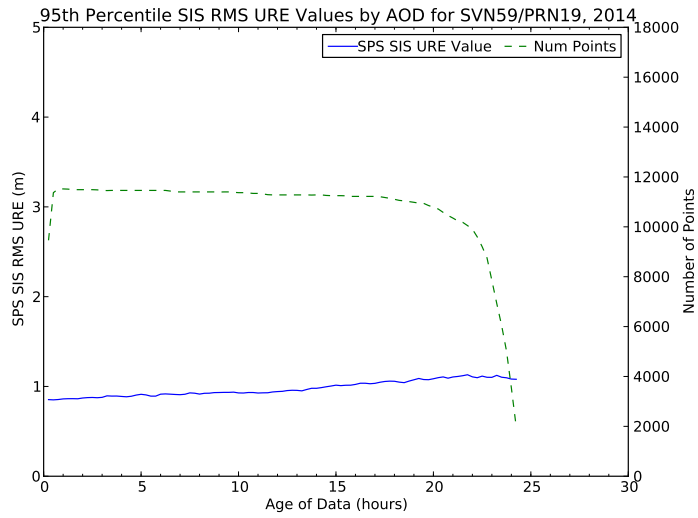
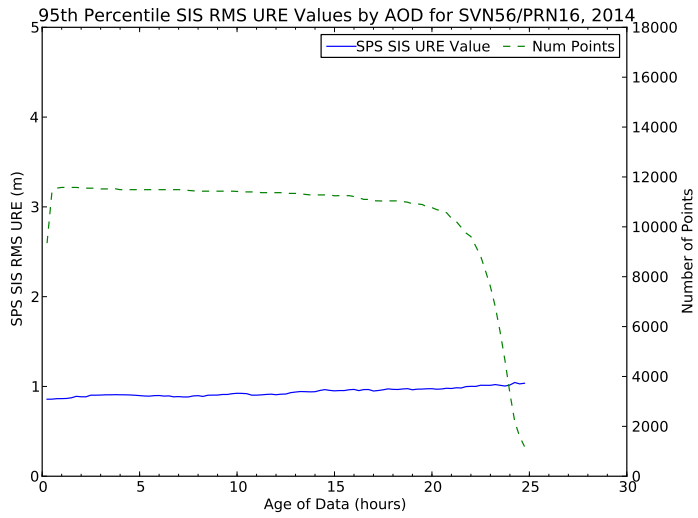




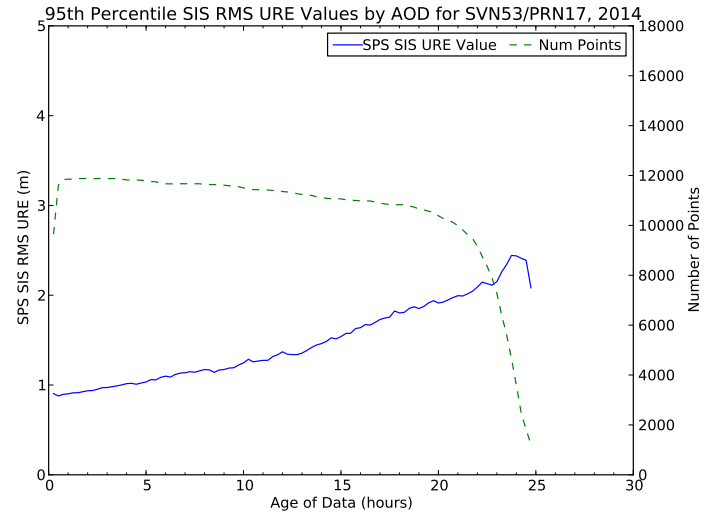
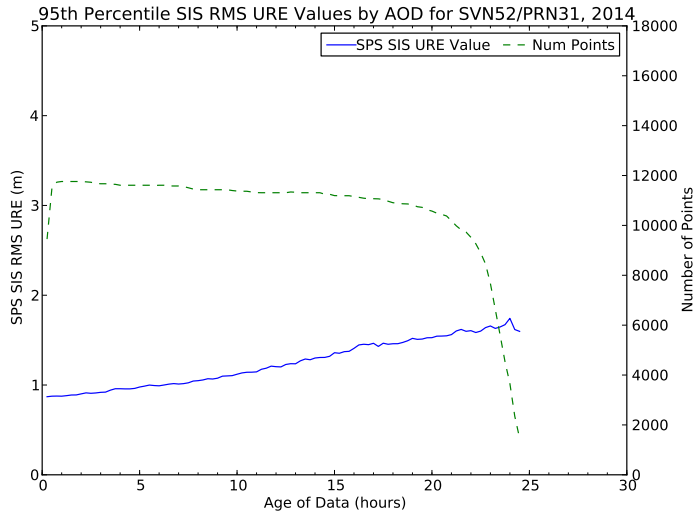
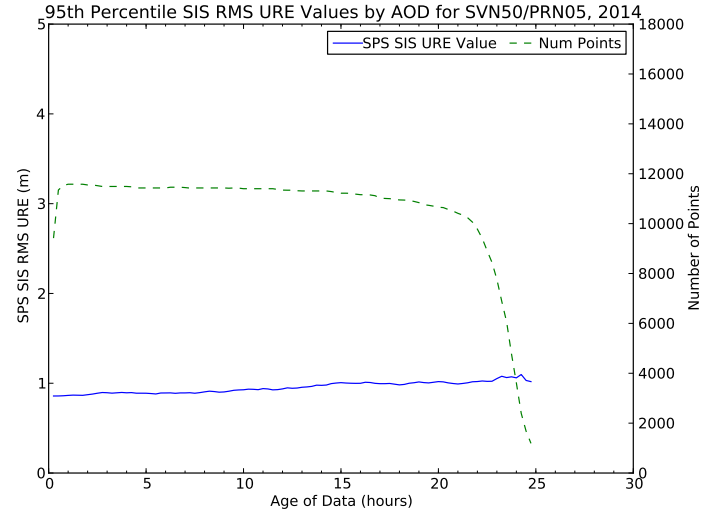
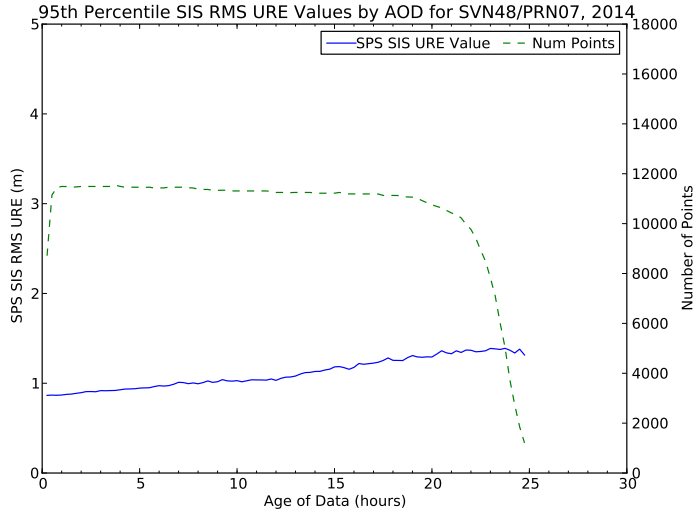
A.3 Block IIR SVs

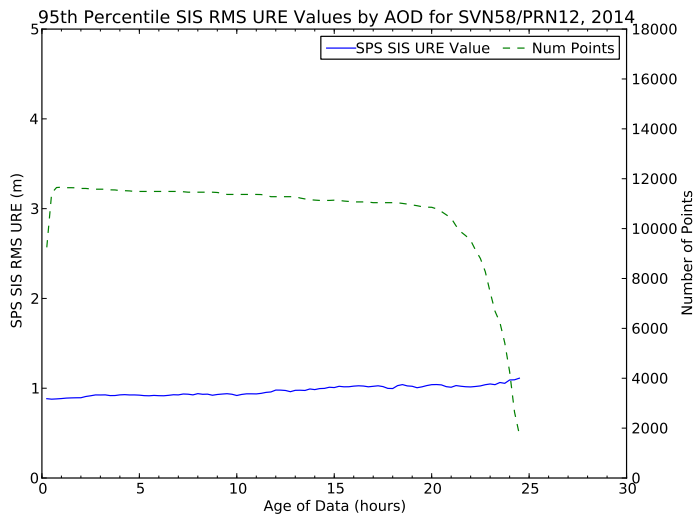
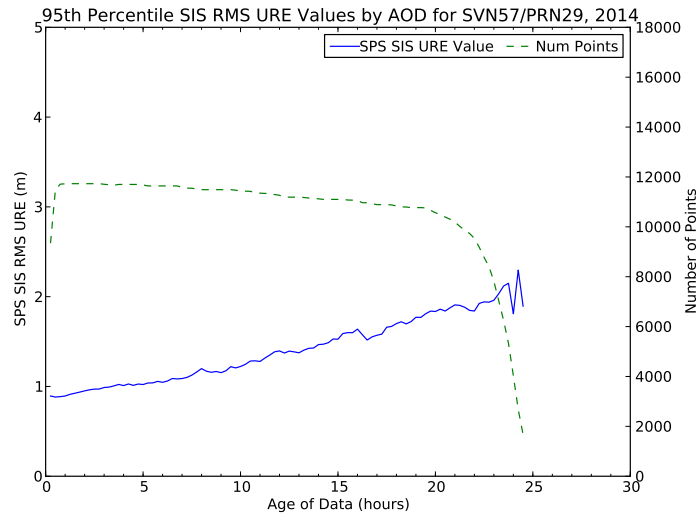
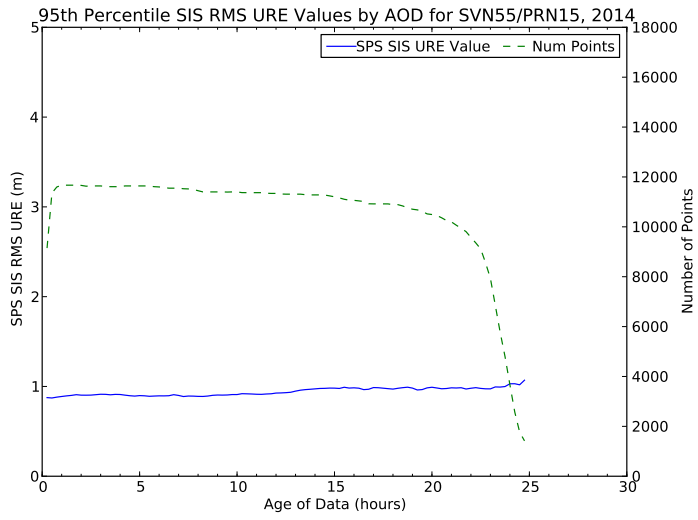




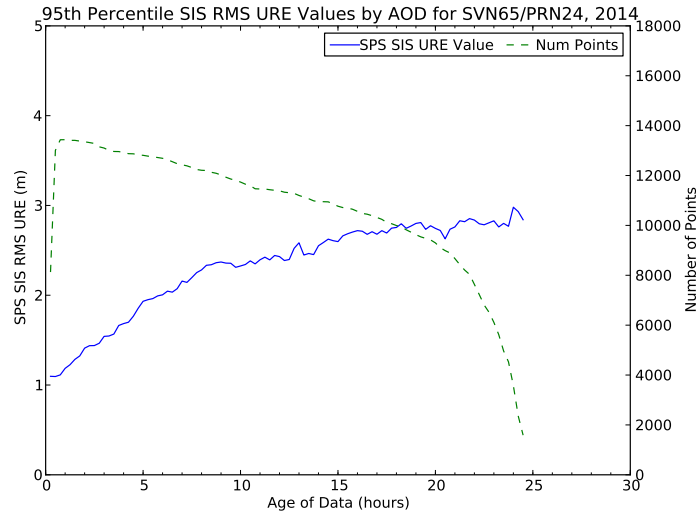
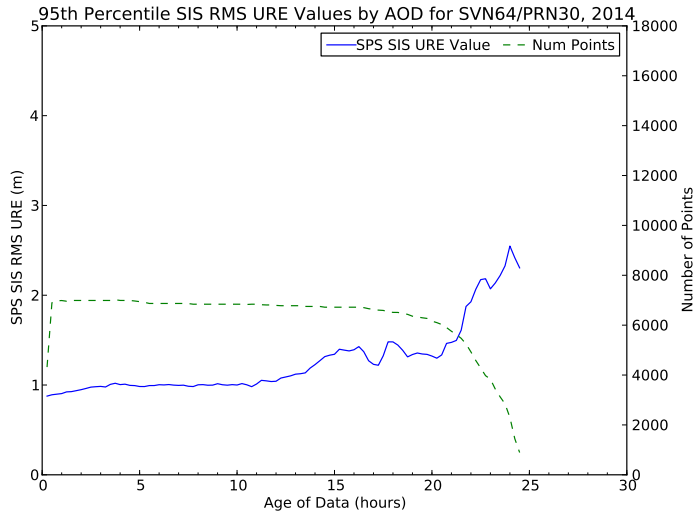
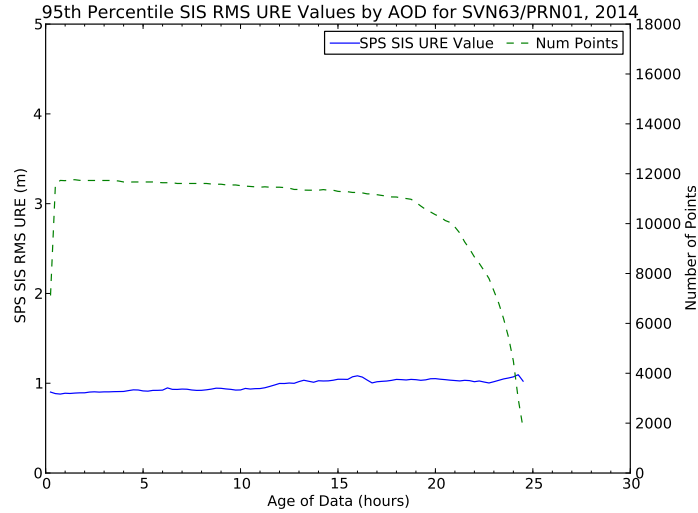
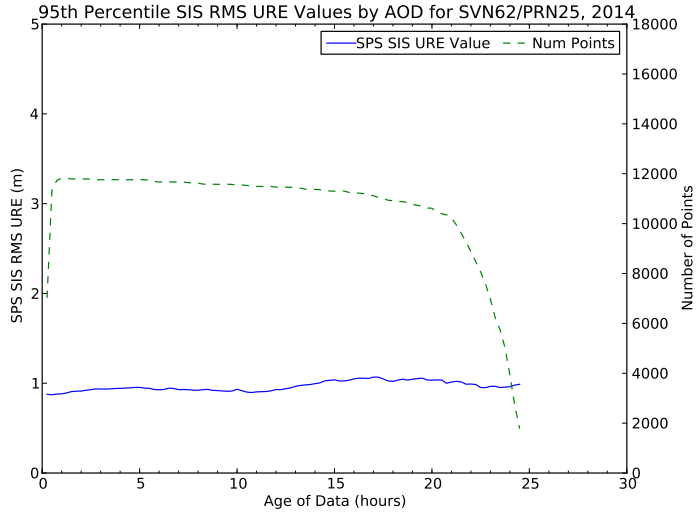


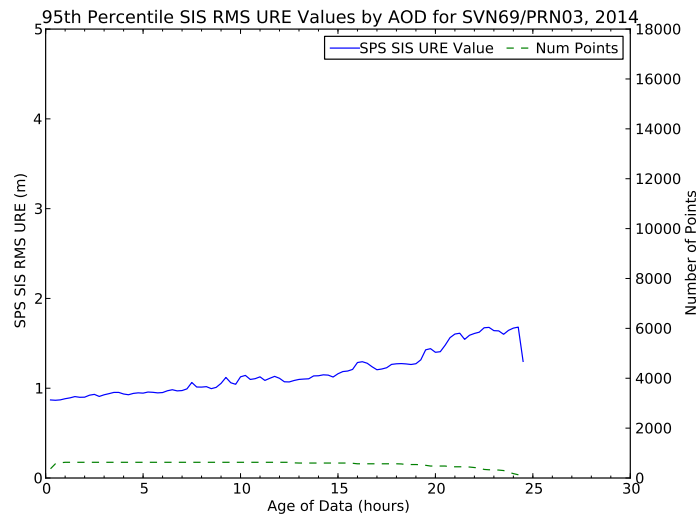
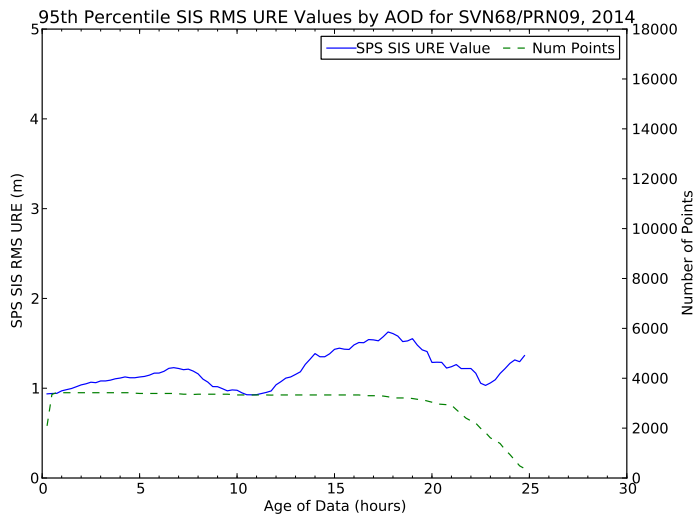
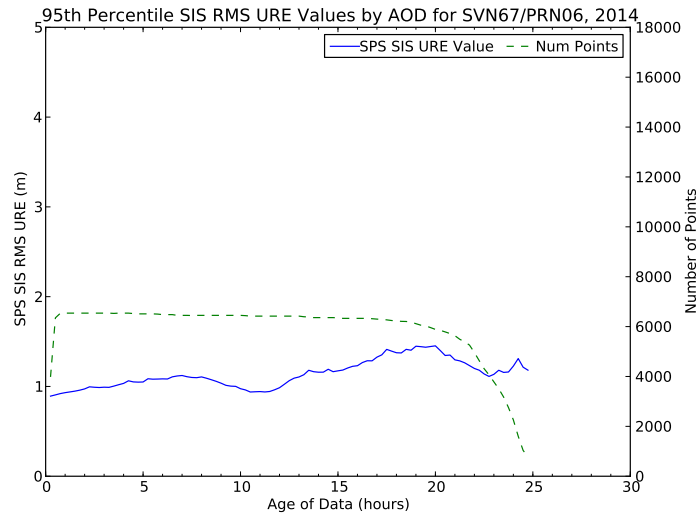
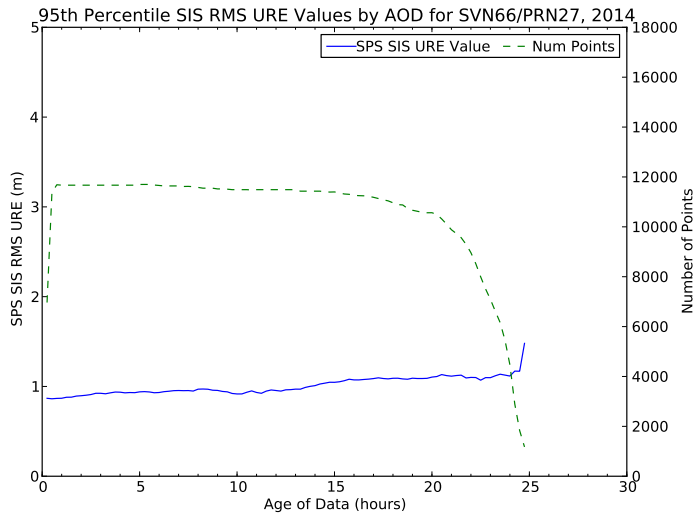
A.4 Block IIR-M SVs





A.5 Block IIF SVs





Appendix B

URE Analysis Implementation Details

B.1 Introduction

The User Range Error (URE) accuracy represents the accuracy of the broadcast navigation message. There are a number of error sources that affect the URE, including errors in broadcast ephemeris and timing errors.

Two approaches to URE analysis are provided in this report. The first approach uses separate statistical processes over space and time to arrive at the result. The second approach derives the result by a single statistical process but is more computationally demanding.

B.2 Clock and Position Values for Broadcast and Truth

The URE values in this report are derived by comparison of the space vehicle (SV) clock and position representations as computed from the broadcast Legacy Navigation (LNAV) message data (BCP) against the SV truth clock and position data (TCP) provided by a precise orbit calculated after the time of interest.

The broadcast LNAV message data used in the calculations were collected by the NGA MSN. These include the complete 300-bit subframes for nearly all unique sets of subframe 1, 2, 3 data and all the unique sets of subframe 4, 5 data. The broadcast LNAV messages provide a set of parameters for an equation which can be evaluated at any time for which the parameters are valid. Our process evaluates the parameters at either a 30 s or 5 min cadence (depending on the process).

The TCP values are computed from the archived National Geospatial-Intelligence Agency (NGA) products. The archived NGA products used in the calculations are the

antenna phase center (APC) precise ephemeris files available from the NGA public website [11]. The NGA products are provided in tabular SP3 format, with positions and clocks provided at a 5 min cadence. When TCP data are needed at a 5 min cadence, a simple table look-up is sufficient. When TCP data are needed at a 30 s cadence, a Lagrange interpolation scheme is used, in which the five points prior to and after the estimation time are used to estimate the SV position. Clock interpolation is handled via a linear interpolation since a multipoint Lagrange interpolation is not appropriate for clock dynamics.

B.3 95th Percentile Global Average As Per the SPS PS

The SPSPS08 specifications for URE suggest averaging across the service volume visible to a GPS SV at any specified point in time. The process is illustrated in Figure B.1.

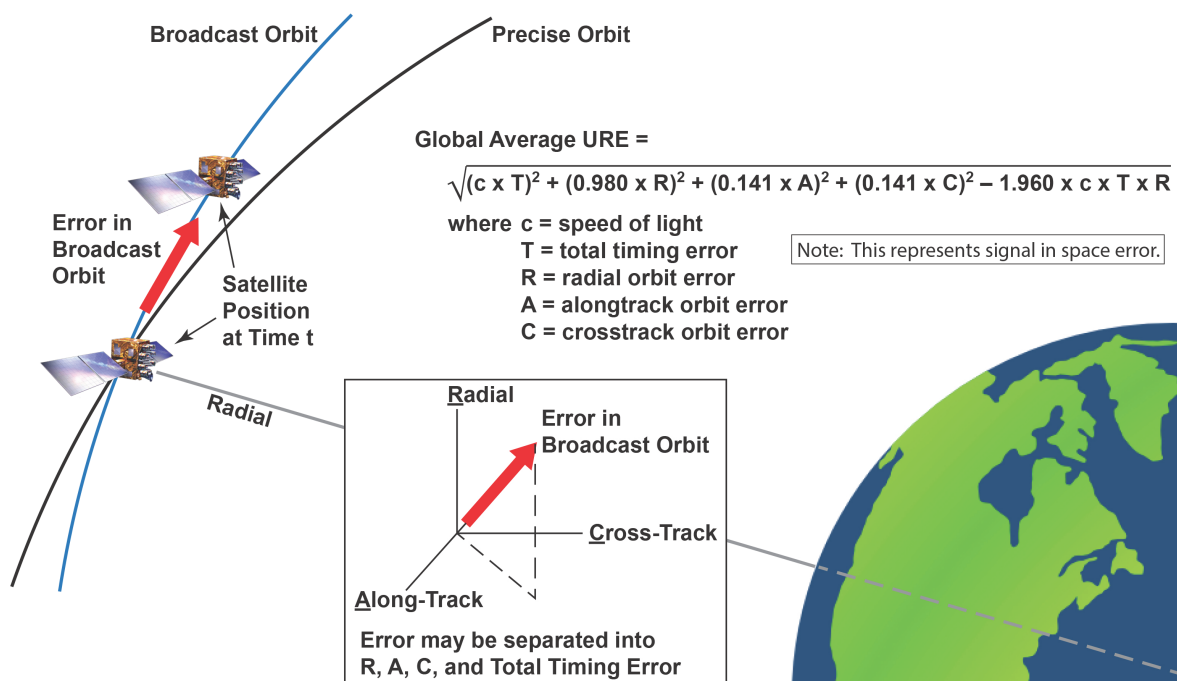


Figure B.1: Global Average URE as defined in SPS PS

The equation shown in Figure B.1 is equation A-1 of SPSPS08 Section A.4.11. This expression allows us to compute the URE accuracy from known errors.

For purposes of this report, the Instantaneous RMS SIS URE values were generated at 30 s intervals for all of 2014. The URE was formed by differencing the BCP and TCP to obtain the radial, along-track, cross-track, and time errors at each epoch. These errors were used as inputs to the SPSPS08 equation A-1.

After all the Instantaneous RMS SIS URE values were computed, values for periods when each SV was unhealthy or not broadcasting were discarded. The remaining values were then grouped by monthly period for each SV and sorted; the maximum and the 95th percentile values were identified for each SV, and this is the basis for Table 3.2. The monthly grouping corresponds closely to the 30 day period suggested in the SPSPS08 and PPSPS07 for URE Accuracy over all AODs while being more intuitive to the reader.

B.4 An Alternate Approach

The previous approach computes an SIS Instantaneous RMS URE (an average over space) at each time point over a month, then selects a 95th percentile value from that set. An alternate approach is to compute the SIS Instantaneous URE for a large number of locations at each time point and store those results. For each SV, this is done for a series of time points at a selected cadence, and the collection of SIS Instantaneous URE values at each time point are stored. When all the time points for a month have been computed, the absolute values of SIS Instantaneous URE values are gathered together in one monthly set. The 95th percentile value is selected from that set.

For this particular implementation, we selected an approximation of an equidistant grid with a spacing of roughly 550 km (five degrees of latitude on the surface of the Earth). This yields a set of 577 SIS Instantaneous URE values for each SV for each evaluation time. Figure B.2 illustrates this set of grid points for a particular SV-time shown as a projection onto the surface of the Earth.

We did this at a cadence of 5 min for each SV for all of 2014 and stored all 577 values for all time points. We then extracted sets of values corresponding to each month (approximately 5 million values per SV-month), took the absolute value of each, and selected the 95th percentile value as the result for the SV-month. This is the basis for Table 3.3.

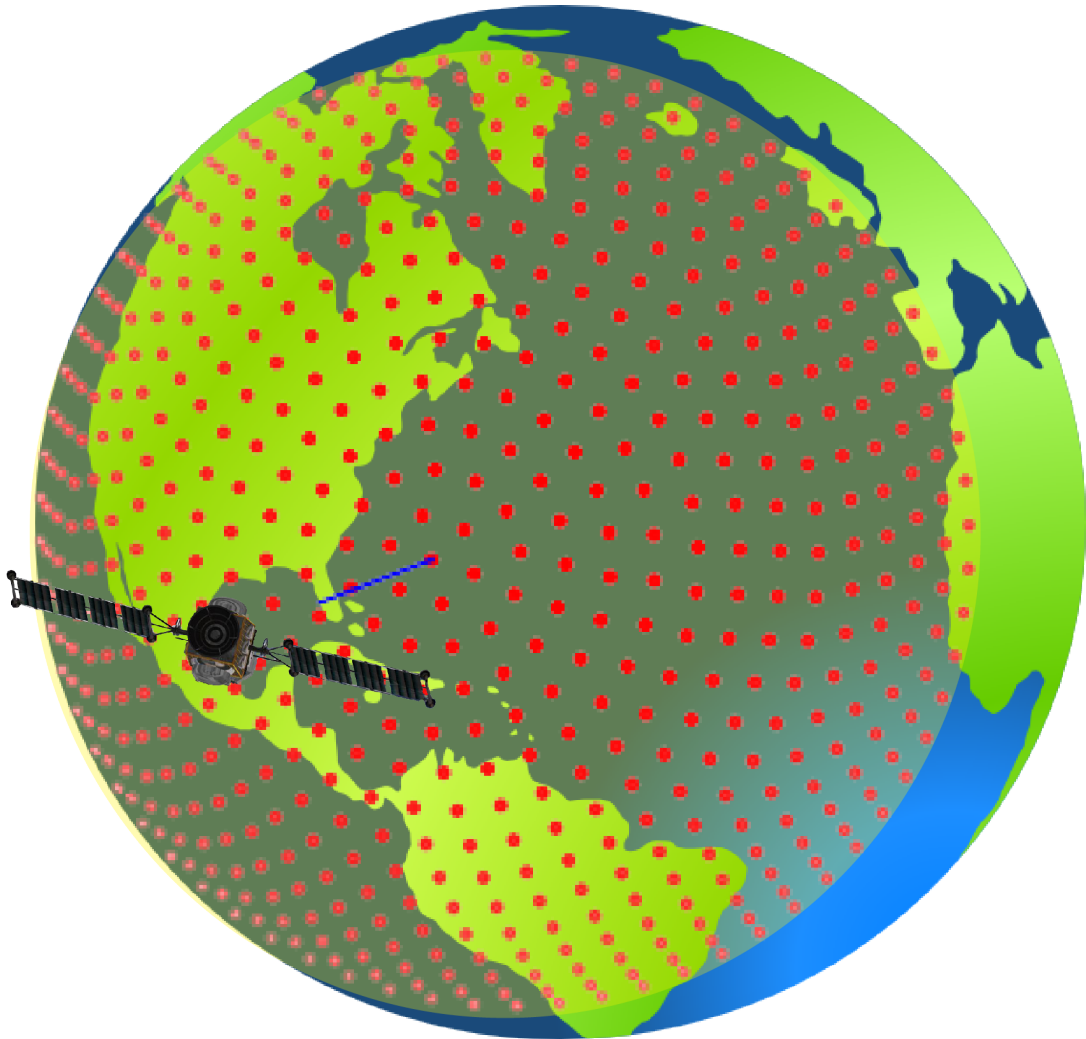


Figure B.2: Illustration of the 577 Point Grid

B.5 Limitations of URE Analysis

There are a number of subtleties in this approach to computing URE accuracies, and the following paragraphs detail some of these.

Selective Availability (SA) would be an additional significant difference between PPS and SPS results; however, SA was set to zero throughout this period [12].

The approaches described in B.2 - B.4 work well when the estimated URE accuracy is under the required thresholds, as it verifies that the system is operating as expected. However, experience has shown that when an actual problem arises, the use of this procedure, without other cross-check mechanisms, can create some issues and may lead to incorrect results. Consider the following two cases.

- In cases where an SV is removed from service for reasons that invalidate the broadcast ephemeris (such as a clock run-off) we need to compare the time at which the removal from service occurred with the time at which any of the URE accuracy bounds were exceeded to assess whether a violation of the SPS PS metrics occurred. However, because we have relied on the interpolation process to generate 30 s values, we cannot obtain an accurate estimate of the time at which the URE bound was exceeded. As a general rule, the UREs computed in our process should be reviewed when they are contained between two SP3 epochs, one of which contains a clock event.
- When a SV is set unhealthy or cannot be tracked, the precise ephemeris may provide misleading results. The analyst preparing the precise ephemeris has several options for handling discontinuities that occur during outages. Therefore, the URE values generated near such events may be incorrect. As a result, it is necessary to avoid accepting UREs into the statistical process under conditions in which the SV could not be tracked or was set unhealthy. This has been done for all the results presented here.

In all cases, when an apparent violation of the URE limits is encountered, we choose to reconcile the analysis described above with the behavior of ORDs formed from the data collected at NGA and IGS sites. Because the observational data used is collected at a 30 s cadence, we obtain a much higher resolution insight into the details of the actual event than we do with the interpolated PE.

Appendix C

SVN to PRN Mapping for 2014

Throughout the report, SVs have been referred to by both SVN and PRN. Keeping track of this relationship has become more challenging over the past few years as the number of operational SVs is typically very close to the number of available PRNs. As a result, the relationships have been changing several times throughout a year. Therefore it is useful to have a summary of the PRN to SVN mapping as a function of time. Figure C.1 presents that mapping for 2014. SVNs on the right vertical axis appear in the order in which they were assigned the PRN values in 2014. Start and end times of relationships are indicated by the dates along the upper horizontal axis.

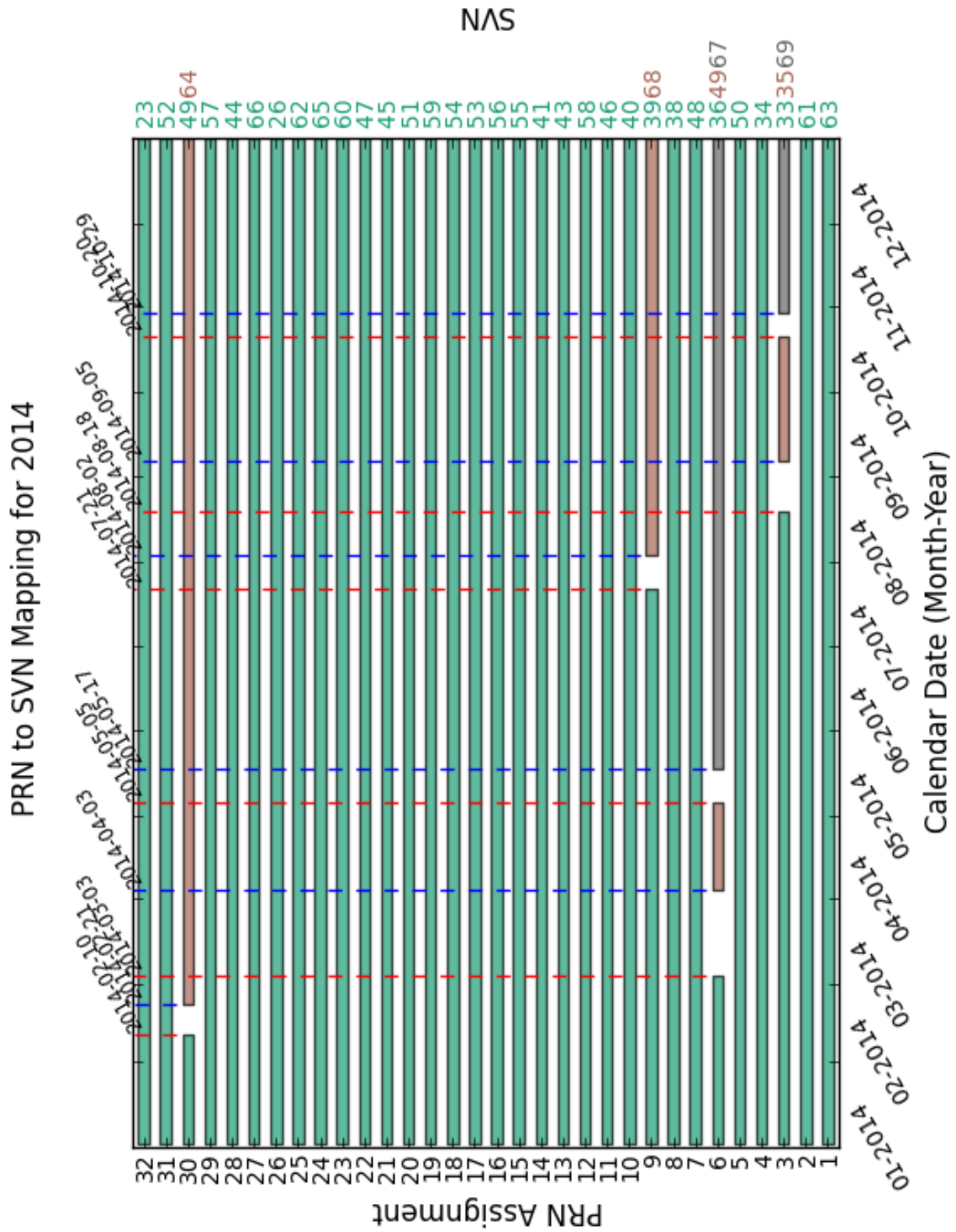


Figure C.1: PRN to SVN Mapping for 2014.

Appendix D

NANU Activity in 2014

Several sections in the report make use of NANUs. It is useful to have a time history of the relevant NANUs sorted by SVN. This makes it convenient to determine which NANU(s) should be examined if an anomaly is observed for a particular satellite at a particular time.

Figure D.1 presents a plot of the NANU activity in 2014. Green bars are scheduled outages and red bars represent unscheduled outages. Gray bars represent SVs that have been decommissioned. NANU numbers are indicated next to each bar. In the event there is more than one NANU for an outage, the last NANU number is displayed.

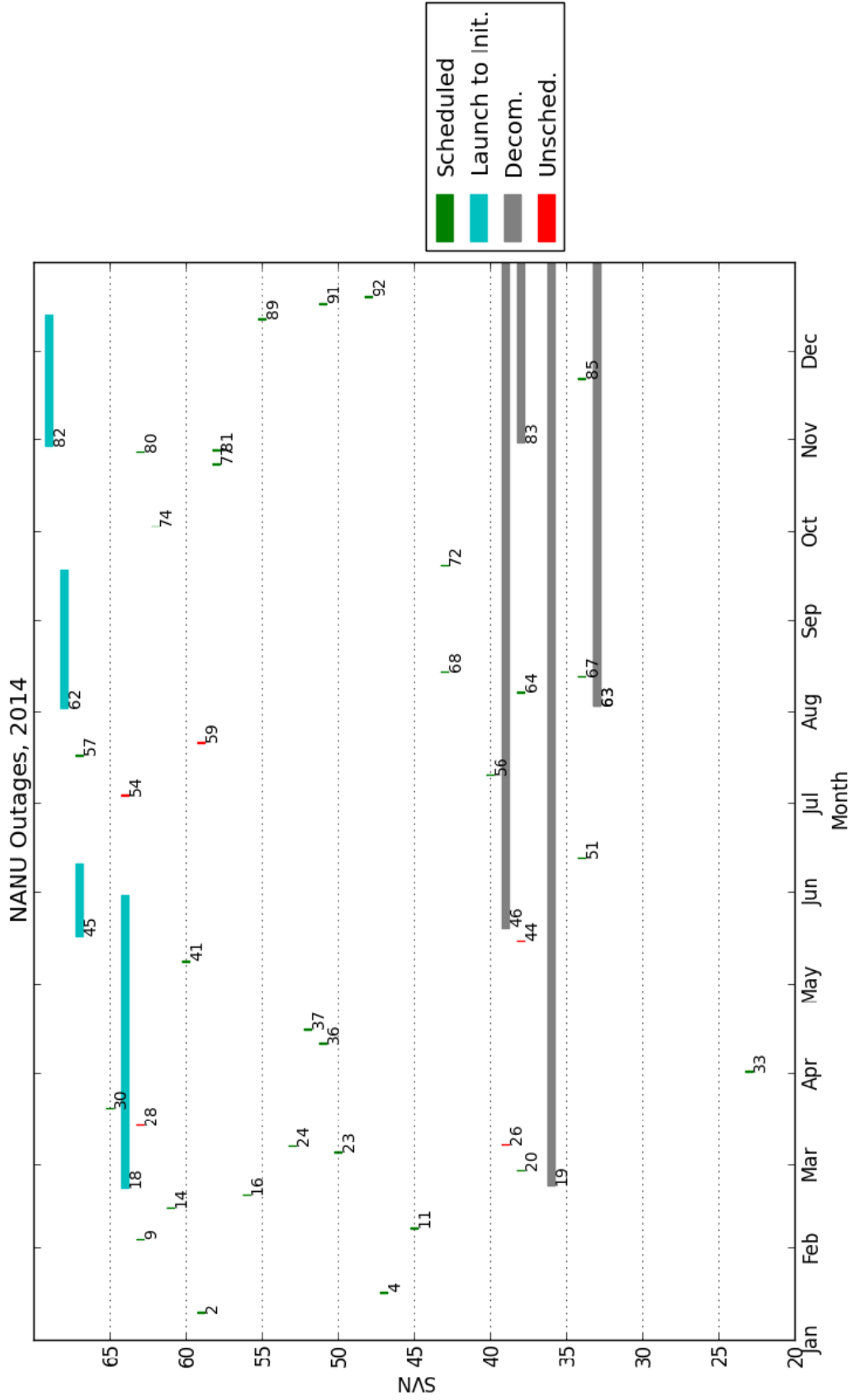


Figure D.1: Plot of NANU activity in 2014.

Appendix E

SVN to Plane-Slot Mapping for 2014

Several assertions in the PPS PS are related to the performance of the constellation as defined by the plane-slot arrangement specified in the performance standard. Evaluation of these assertions requires information on the plane-slot occupancy during the year.

The operational advisory (OA) provided by 2 SOPS to the United States Coast Guard (USCG) Navigation Center and defined in ICD-GPS-240 includes information on plane-slot assignments. However, the format of the OA does not permit it to clearly convey the status of expanded slots. (The format is limited to a letter representing the plane and a number representing the slot. There is no provision of the “fore/aft” designation.) The OA designations are also cluttered by use of numbers greater than the number of defined slots. These are “slots of convenience” defined by the operators, but have no fixed meaning in terms of position within the constellation. As a result, interpretation of the OA is challenging.

For the past several years, the plane-slot assignments have been provided to ARL:UT by Aerospace Corporation analysts supporting 2nd Space Operations Squadron (2 SOPS). The assignments are provided as a set of daily plane-slot relationships for the year.

Both of these sources are limited in that only a single satellite may be designated as being present in a slot at a given moment. In fact, as satellites are moved within the constellation, there exists occasional periods when more than one SV may be present within the defined boundaries of a slot. From the user’s point of view, if a satellite transmitting a healthy signal is present within the slot boundaries, the slot should be counted as occupied.

As part of the 2014 analysis, ARL:UT developed a process to independently assess the plane-slot relationships. In what follows, we present an initial independent verification of the plane-slot relationships. This was not present in previous reports.

Figure E.1 provides a graphical illustration of the plane-slot relationships throughout 2014. In some cases, multiple satellites fall within the slot definition for a period of time. Table E.1 provides the plane-slot relationships in a tabular form. The dates when satellites are judged to be present in a slot location are noted only when a change

occurs in the plane-slot during the year. This allows the reader to determine when multiple satellites occupied a slot.

Figure E.1 and Table E.1 both indicate that the B1 slot was considered to be an expanded slot throughout 2014 but only one of the two expanded slot locations was occupied. Slot B1F became vacant in March 2013 when SVN 35 was decommissioned and persisted until SVN 71 became available in April 2015. The ramifications for this are discussed further in Section 3.3 and Section 3.4.

Table E.1: Summary of SV-Slot Relationships for 2014

Plane-Slot	SVN	Start Date [†]	End Date [†]
A1	65		
A2	52		
A3	38	01/01/2014	05/26/2014
A3	64	05/31/2014	12/31/2014
A4	48		
B1A	56		
B1F	-		
B2	62		
B3	44		
B4	58		
C1	57		
C2	66		
C3	59		
C4	53		
D1	61		
D2A	63		
D2F	46		
D3	45		
D4	34	01/01/2014	06/10/2014
D4	67	06/11/2014	12/31/2014
E1	51	01/01/2014	12/16/2014
E1	69	12/12/2014	12/31/2014
E2	47		
E3	50		
E4	54		
F1	41		
F2A	55		
F2F	26	01/01/2014	12/31/2014
F2F	43	09/27/2014	12/31/2014
F3	43	01/01/2014	09/26/2014
F3	68	09/17/2014	12/31/2014
F4	60		

[†]If unspecified, the SV was the sole occupant of the slot for the entire year.

Time History of Satellite in Planes/Slots for 2014

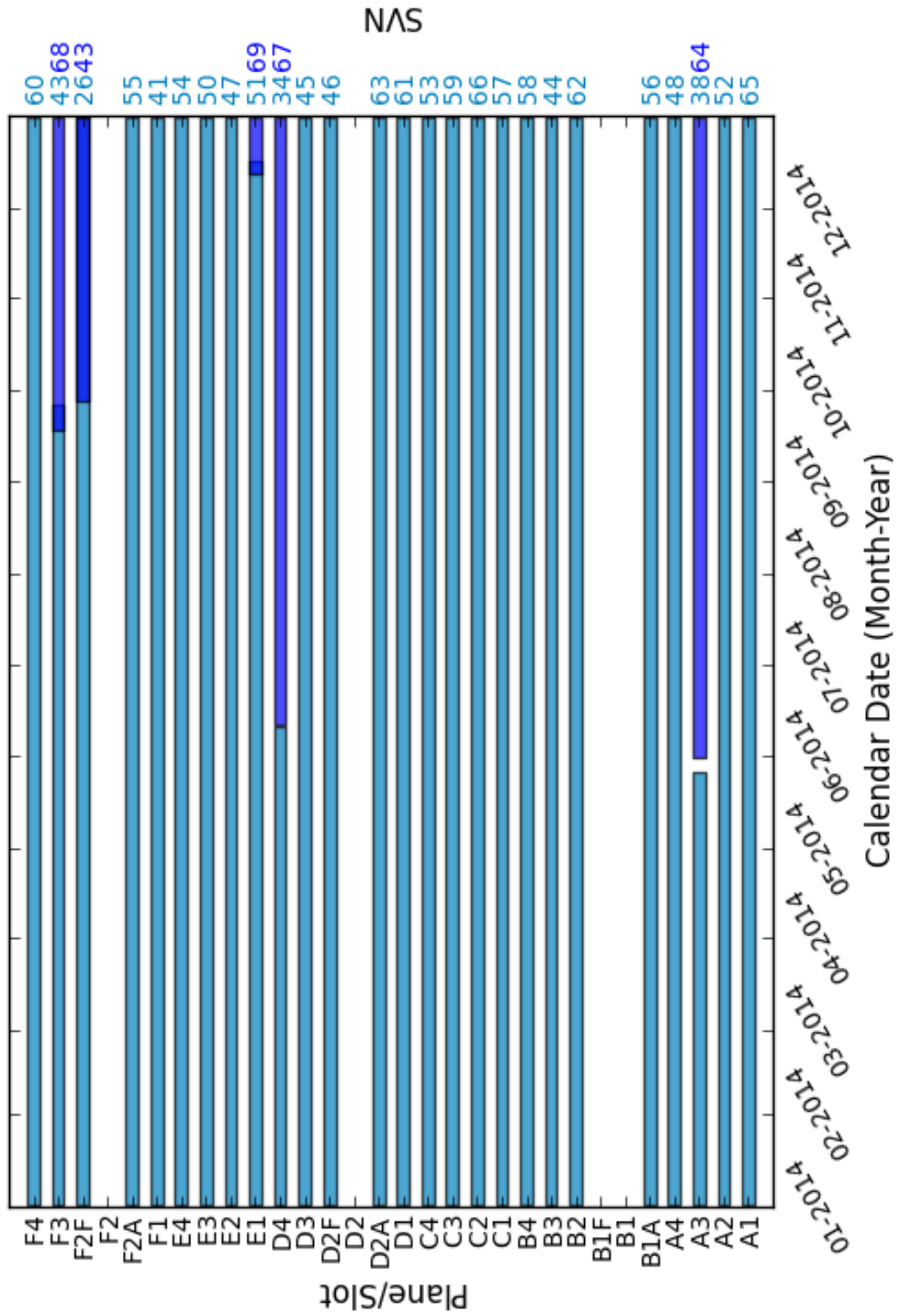


Figure E.1: Time History of Satellite Plane/Slots for 2014.

Appendix F

Translation of URE Statistics Between Signals

The URE process described in Appendix B is based on the data broadcast in subframes 1, 2, 3 of the navigation message and the NGA precise ephemeris. Both of these estimates of the satellite orbits and clock offsets are referenced to the dual frequency P(Y)-code signal. Therefore, the URE results are directly related to the PPS Dual-Frequency performance. This appendix explains how these results have been interpreted in order to apply to the SPS assertions.

The PPS Dual-Frequency results may be mapped to SPS equivalent results by considering the effects of both the group delay differential and the intersignal bias (ISB) between the P(Y)-Code and the C/A-Code on L1.

F.1 Group Delay Differential

As described in IS-GPS-200 Section 3.3.1.7, the group delay through the satellite transmission hardware is accounted for in the satellite clock offset. However, there remains a group delay differential effect that comes about due to the fact that the signals passing through the different frequency chains experience slightly different delays. An estimate of the group delay differential is transmitted to the users in the navigation message using the T_{GD} term in Subframe 1. Note that T_{GD} is not the group delay differential, but the group delay differential scaled to account for the difference between a dual-frequency observation and a single-frequency observation. This is described in IS-GPS-200 Section 20.3.3.3.2. This distinction will be relevant below when comparisons to other estimates are discussed.

IS-GPS-200 Section 3.3.1.7.2 states that the random plus non-random variations about the mean of the differential delay shall not exceed 3.0 nsec (95% probability). While this establishes an upper bound on the uncertainty, it does not represent actual performance. The quantization in the T_{GD} term is 0.5 nsec. Therefore, even with

perfect estimation, the floor on the uncertainty would be on the order of 0.25 nsec.

If one assumes that T_{GD} is correct and that the user equipment properly applies the correction, then the single-frequency results would be aligned with the dual-frequency results to within that quantization error. However, once the satellite is on orbit it is not possible to directly observe T_{GD} . Instead it must be estimated, and the estimates are subject to a variety of factors including receiver group delay differential effects and ionospheric dispersion. This uncertainty has the effect of inflating the PPS Dual-Frequency results when these results are interpreted in terms of the PPS Single-Frequency or SPS services. In fact, since the errors are not directly observable, the best that can be done is to examine the repeatability in the estimate or the agreement between independent estimates and consider these as proxies for the actual uncertainty.

Since 1999, the T_{GD} values have been estimated by Jet Propulsion Laboratory (JPL) and provided to 2 SOPS on a quarterly basis. Shortly before this process was instituted there was a study of the proposed estimation process and a comparison of the estimates to those independently developed by two other sources [13]. The day-to-day uncertainty in the JPL estimates appeared to be about 0.3 nsec and the RMS of the differences between the three processes (after removal of a bias) was between 0.2 nsec and 0.7 nsec.

The Center For Orbit Determination (CODE) at the University of Bern estimates the P1-P2 bias [14]. CODE provides a group delay differential estimate for each SV every month. CODE does not provide details on the estimation process, but it must include a constraint that the group differential delay averaged over the constellation is zero as all sets of monthly values for exhibit a zero mean.

A comparison of the CODE estimates and the T_{GD} values (scaled by to group differential delay values) shows a ~ 5 nsec bias between the estimates. This bias may be removed as we are comparing mean-removed vs non-mean removed values. After the bias across the constellation is removed, the level of agreement between the scaled T_{GD} values and the monthly CODE estimates is between 0.1 nsec and 0.8 nsec RMS. (Note: Results for SVN 49 appear to be out-of-family and have been excluded in this comparison)

Considering all these factors, for the purpose of this analysis the uncertainty in the T_{GD} is assumed to be 0.5 nsec RMS.

F.2 Intersignal Bias

The ISB represents the difference between two signals on the same frequency. This bias is due to differences in the signal generation chain coupled with dispersive effects in the transmitter due to the differing bandwidths of the signals. It is not possible to observe these effects directly. When examining the signal structure at the nanosecond level the chip edges are not instantaneous transitions with perfectly vertical edges but exhibit rise times that vary by signal. Therefore, measuring the biases requires assumptions

about the levels at which one decides a transition is in progress. These assumptions will vary between receivers.

There is no estimate of the ISB provided in the GPS legacy navigation message. However, CODE estimates the bias between the L1 P(Y)-code and the L1 C/A-code [14]. An estimate is provided for each SV every month. When this adjustment process was developed, these estimates were examined for each month in 2013. The monthly mean across all SVs is zero, indicating the estimation process is artificially enforcing a constraint. The RMS of the monthly values across the constellation is 1.2 nsec for each month. Since there is no estimate of the ISB, this RMS represents an estimate of the error C/A users experience due to the ISB.

F.3 Adjusting PPS Dual-Frequency Results for SPS

The PPS Dual-Frequency and SPS cases are based on a different combination and a different code. Therefore, the uncertainties in both T_{GD} and ISB must be considered. The PPS Dual-Frequency URE results are all stated as 95th% (2-sigma) values. This means that the RMS errors estimated in F.1 and F.2 must be multiplied by 1.96 (effectively 2, given that the amount of uncertainty in the values).

If it is assumed that these errors are uncorrelated, the total error may be estimated as

$$\begin{aligned} \text{Total error} &= \sqrt{((2 * T_{GD} \text{ uncertainty})^2 + (2 * \text{ISB uncertainty})^2)} \\ &= \sqrt{((2 * 0.5 \text{ nsec})^2 + (2 * 1.2 \text{ nsec})^2)} \\ &= \sqrt{(1 \text{ nsec}^2 + 5.76 \text{ nsec}^2)} \\ &= 2.6 \text{ nsec} \end{aligned} \tag{F.3.1}$$

Converted to equivalent range at the speed of light and given only a single significant digit is justified, the total error is about 0.8 m. This adjustment may then be combined with the PPS-Dual Frequency result in a root-sum-square manner.

Appendix G

Acronyms and Abbreviations

Table G.1: List of Acronyms and Abbreviations

2 SOPS	-	2 nd Space Operations Squadron
AMCS	-	Alternate Master Control Station
AOD	-	Age of Data
AODO	-	Age of Data Offset
ARL:UT	-	Applied Research Laboratories, The University of Texas at Austin
BCP	-	Broadcast Clock and Position
BE	-	Broadcast Ephemeris
CMPS	-	Civil Monitoring Performance Specification
CODE	-	Center For Orbit Determination
DECOM	-	Decommission
DOP	-	Dilution of Precision
ECEF	-	Earth-Centered, Earth-Fixed
FAA	-	Federal Aviation Administration
FCSTDV	-	Forecast Delta-V
FCSTEXTD	-	Forecast Extension
FCSTMX	-	Forecast Maintenance
FCSTRESCD	-	Forecast Rescheduled

FCSTUUFN	-	Forecast Unusable Until Further Notice
GNSS	-	Global Navigation Satellite System
GPS	-	Global Positioning System
GPSTK	-	GPS Toolkit
HDOP	-	Horizontal Dilution Of Precision
IGS	-	International GNSS Service
IODC	-	Issue of Data, Clock
IODE	-	Issue of Data, Ephemeris
ISB	-	Intersignal Bias
JPL	-	Jet Propulsion Laboratory
LSB	-	Least Significant Bit
MCS	-	Master Control Station
MSB	-	Most Significant Bit
MSI	-	Misleading Signal Information
MSN	-	Monitor Station Network
NANU	-	Notice Advisory to Navstar Users
NAV	-	Navigation Message
NGA	-	National Geospatial-Intelligence Agency
NMCT	-	Navigation Message Correction Table
NTE	-	Not to Exceed
OA	-	Operational Advisory
ORD	-	Observed Range Deviation
PDOP	-	Position Dilution of Precision
PE	-	Precise Ephemeris
PRN	-	Pseudo-Random Noise
PVT	-	Position, Velocity, and Time
RAIM	-	Receiver Autonomous Integrity Monitoring
RINEX	-	Receiver Independent Exchange Format

RMS	-	Root Mean Square
SA	-	Selective Availability
SINEX	-	Station Independent Exchange Format
SIS	-	Signal-in-Space
SMC/GP	-	Global Positioning Systems Directorate
SNR	-	Signal to Noise Ratio
SP3	-	Standard Product 3
SPS	-	Standard Positioning Service
SPS PS(SPPSPS08)	-	2008 Standard Positioning Service Performance Standard
SV	-	Space Vehicle
SVN	-	Space Vehicle Number
TCP	-	Truth Clock and Position
T _{GD}	-	Group Delay
UNUNOREF	-	Unusable with No Reference
UNUSUFN	-	Unusable Until Further Notice
URA	-	User Range Accuracy
URAE	-	User Range Acceleration Error
URE	-	User Range Error
URRE	-	User Range Rate Error
USCG	-	United States Coast Guard
USNO	-	U.S. Naval Observatory
WGS 84	-	World Geodetic System 1984
ZAOD	-	Zero Age of Data

Bibliography

- [1] U.S. Department of Defense. Standard Positioning Service Performance Standard, 4th Edition, 2008.
- [2] U.S. Department of Defense. Navstar GPS Space Segment/Navigation User Interfaces, IS-GPS-200, Revision G, September 2012.
- [3] John M. Dow, R.E. Neilan, and C. Rizos. The International GNSS Service in a changing landscape of Global Navigation Satellite Systems. *Journal of Geodesy*, 2009.
- [4] B. Renfro, D. Munton, and R. Mach. Around the World for 26 Years - A Brief History of the NGA Monitor Station Network. In *Proceedings of the Institute of Navigation International Technical Meeting*, Newport Beach, CA, 2012.
- [5] U.S. Naval Observatory. Block II Satellite Information. <ftp://tycho.usno.navy.mil/pub/gps/gpstd.txt>, January 2011.
- [6] W. Gurtner and L. Estey. RINEX: The Receiver Independent Exchange Format Version 2.11, 2006.
- [7] U.S. Department of Defense. Navstar GPS Control Segment to User Support Community Interfaces, ICD-GPS-240, Revision A, January 2010.
- [8] U.S. Department of Transportation. Global Positioning System (GPS) Civil Monitoring Performance Specification, DOT-VNTSC-FAA-09-08, April 2009.
- [9] B. Tolman et al. The GPS Toolkit - Open Source GPS Software. In *Proceedings of the 17th International Technical Meeting of the Satellite Division of the Institute of Navigation (ION GNSS 2004)*, Long Beach, CA, 2004.
- [10] NIMA Technical Report TR8350.2. Department of Defense World Geodetic System 1984, Its Definition and Relationships With Local Geodetic Systems, July 1997.
- [11] National Geospatial-Intelligence Agency. NGA Antenna Phase Center Precise Ephemeris products. <http://earth-info.nga.mil/GandG/sathtml/ephemeris.html>.
- [12] The White House, Office of the Press Secretary. Statement by the President Regarding the United States' Decision to Stop Degrading Global Positioning System Accuracy, May 2000.

[13] Colleen H. Yinger, William A. Feess, Ray Di Esposti, The Aerospace Corporation, Andy Chasko, Barbara Cosentino, Dave Syse, Holloman Air Force Base, Brian Wilson, Jet Propulsion Laboratory, Maj. Barbara Wheaton, and SMC/CZUT. GPS Satellite Interfrequency Biases, June 1999.

[14] Data Set for 2013. <ftp://ftp.unibe.ch/aiub/CODE/2013>, 2013.